Catalysis Today 147 (2009) 1–59

Contents lists available at ScienceDirect

Catalysis Today

journal homepage: www.elsevier.com/locate/cattod

Decontamination and disinfection of water by solar photocatalysis: Recent overview and trends

S. Malato [a,*], P. Fernández-Ibáñez [a], M.I. Maldonado [a], J. Blanco [a], W. Gernjak [b]

[a] Plataforma Solar de Almería (CIEMAT), Carretera Senés, Km 4, 04200 Tabernas (Almería), Spain
[b] The University of Queensland, Advanced Water Management Centre (AWMC), Qld 4072, Australia

ARTICLE INFO

Article history:
Available online 3 August 2009

Keywords:
Heterogeneous photocatalysis
Photo-Fenton
Solar disinfection
Solar water treatment

ABSTRACT

In recent years, there has been a tremendous amount of research and development in the area of photocatalysis (heterogeneous and homogeneous), a process included in a special class of oxidation techniques defined as Advanced Oxidation Processes (AOPs), all characterized by the same chemical feature, production of $^{\bullet}OH$ radicals. This paper reviews the use of sunlight to produce the $^{\bullet}OH$ radicals by TiO_2 photocatalysis and photo-Fenton process. The reacting systems necessary for performing solar photocatalysis are described. The paper also summarizes most of the research carried out related to solar photocatalytic degradation of water contaminants, and how it could significantly contribute to the treatment of persistent toxic compounds. It outlines how to enhance the process efficiency by integration with biotreatment. Various solar reactors for photocatalytic water treatment mainly based on non-concentrating collectors built during the last few years are also described in detail in this review, as well as the use of the solar photocatalytic processes to inactivate microorganisms present in water, placing special emphasis on experimental systems made to optimize this disinfection technique.

Contents

* Corresponding author. Tel.: +34 950387940; fax: +34 950365015.
E-mail address: sixto.malato@psa.es (S. Malato).

0920-5861/$ – see front matter © 2009 Elsevier B.V. All rights reserved.
doi:10.1016/j.cattod.2009.06.018

1. Introduction

One of the most pervasive problems affecting people throughout the world is inadequate access to clean water and sanitation. Problems with water are expected to grow worse in the coming decades, with water scarcity occurring globally, even in regions currently considered water-rich. Addressing these problems calls out for a tremendous amount of research to be conducted to identify robust new methods of purifying water at lower cost and with less energy, while at the same time minimizing the use of chemicals and impact on the environment. The many problems worldwide associated with the lack of clean, fresh water are well known: 1.2 billion people lack access to safe drinking water, 2.6 billion have little or no sanitation, millions of people die annually – 3900 children a day – from diseases transmitted through unsafe water or human excreta. In both developing and industrialized nations, a growing number of contaminants are entering water supplies from human activity: from traditional compounds such as heavy metals to emerging micropollutants such as endocrine disrupters and nitrosoamines [1–3]. Increasingly, public health

and environmental concerns drive efforts to decontaminate waters previously considered clean. More effective, lower-cost, robust methods to disinfect and decontaminate waters from source to point-of-use are needed, without further stressing the environment or endangering human health by the treatment itself.

Conventional methods of water disinfection and decontamination can address many of these problems. However, these treatment methods are often chemically, energetically and operationally intensive, focused on large systems, and thus require considerable infusion of capital, engineering expertise and infrastructure, all of which precludes their use in much of the world. Furthermore, intensive chemical treatments (such as those involving ammonia, chlorine compounds, hydrochloric acid, sodium hydroxide, ozone, permanganate, alum and ferric salts, coagulation and filtration aids, anti-scalants, corrosion control chemicals, and ion exchange resins and regenerants) and residuals resulting from treatment (sludge, brines, toxic waste) can add to the problems of contamination and salting of freshwater sources.

Advanced Oxidation Processes (AOPs) may be used for decontamination of water containing organic pollutants, classified as bio-recalcitrant, and/or for disinfection removing current and emerging pathogens. These methods rely on the formation of highly reactive chemical species which degrade even the most recalcitrant molecules into biodegradable compounds. Although there are different reacting systems (http://www.jaots.net/), all of them are characterized by the same chemical feature: production of hydroxyl radicals (•OH), which are able to oxidize and mineralize almost any organic molecule, yielding CO_2 and inorganic ions. Rate constants (k_{OH}, $r = k_{OH}$ [•OH] C) for most reactions involving hydroxyl radicals in aqueous solution are usually on the order of 10^6 to $10^9\ M^{-1}\ s^{-1}$. They are also characterized by their not-selective attack, which is a useful attribute for wastewater treatment and solution of pollution problems. The versatility of the AOPs is also enhanced by the fact there are different ways of producing hydroxyl radicals, facilitating compliance with the specific treatment requirements. Methods based on UV, H_2O_2/UV, O_3/UV and H_2O_2/O_3/UV combinations use photolysis of H_2O_2 and ozone to produce the hydroxyl radicals. Other methods, like heterogeneous photocatalysis and homogeneous photo-Fenton, are based on the use of a wide-band gap semiconductor and addition of H_2O_2 to dissolved iron salts, respectively, and irradiation with UV–vis light [4,5]. Both processes are of special interest since sunlight can be used for them.

The overarching goal for the future of reclamation and reuse of water is to capture water directly from non-traditional sources such as industrial or municipal wastewaters and restore it to potable quality. Municipal wastewaters are commonly treated by activated sludge systems that use suspended microbes to remove organics and nutrients, and large sedimentation tanks to separate the solid and liquid fractions. This level of treatment produces wastewater effluent suitable for discharge to surface waters or for restricted irrigation and some industrial applications. Current wastewater reuse systems use a conventional activated sludge process, followed by a microfiltration pretreatment of the secondary effluent, which has high quantities of suspended and dissolved solids. The effluent water still partially contains dissolved species and colloidal substances that act to foul the membranes of the subsequent Reverse Osmosis (RO) system used as a final barrier to contaminants in the product water. Employing a 'tight' ultrafiltration membrane in the Membrane Bio Reactors (MBRs) lets through fewer dissolved solids than does microfiltration, allowing the RO system to operate with significantly less fouling. Futuristic direct reuse systems envisioned [6] involve only two steps: a single-stage MBR with an immersed nanofiltration membrane (obviating the need for an RO stage), followed by a photocatalytic reactor to provide an absolute barrier to pathogens and to destroy low molecular-weight organic contaminants that may pass the nanofiltration barrier.

Industrial wastewater is often polluted by toxic or nonbiodegradable organic compounds. Alternatives to the conventional activated sludge treatment need to be employed. Among these, chemical oxidative treatments, and especially, Advanced Oxidation Processes (AOPs), are well known for their capacity for oxidizing and mineralizing almost any organic contaminant [7]. Nevertheless, technical applications are still scarce. As the process costs may be considered the main obstacle to their commercial application, several promising cost-cutting approaches have been proposed, such as integration of AOPs as part of a treatment train. In the typical basic process design approach an AOP pretreats nonbiodegradable or toxic wastewater, and once biodegradability has been achieved, the effluent is transferred to a cheaper biological treatment. The key is to minimize residence time and reagent consumption in the more expensive AOP stage by applying an optimized coupling strategy. Other proposed cost-cutting measures are the use of renewable energy sources, i.e., sunlight as the irradiation source for running the AOP.

The publications regarding the photocatalytic process rose continuously over the last years surpassing meanwhile a total number of more than 1000 peer-reviewed publications per year. Though such a simple search does not necessarily include every single article correctly, it still serves to prove the general trend of an increasing interest of the scientific community. Fig. 1 shows the evolution of these publication activities. Fig. 1 also illustrates that much of the literature takes into account the possibility of driving the process with solar radiation. This fact is due to that a priori the photocatalytic process seems to be the most apt of all AOPs to be driven by sunlight. In this monograph we highlight some of the science and technology being developed to improve the solar photocatalytic disinfection and decontamination of water, as well as efforts to increase water supplies through the safe reuse of wastewater and adequate treatment of industrial wastewater.

2. Solar heterogeneous photocatalysis

2.1. Introduction

The heterogeneous solar photocatalytic detoxification process consists of making use of the near-ultraviolet (UV) band of the solar spectrum (wavelength shorter than 400 nm), to photo-excite a semiconductor catalyst in contact with water and in the presence

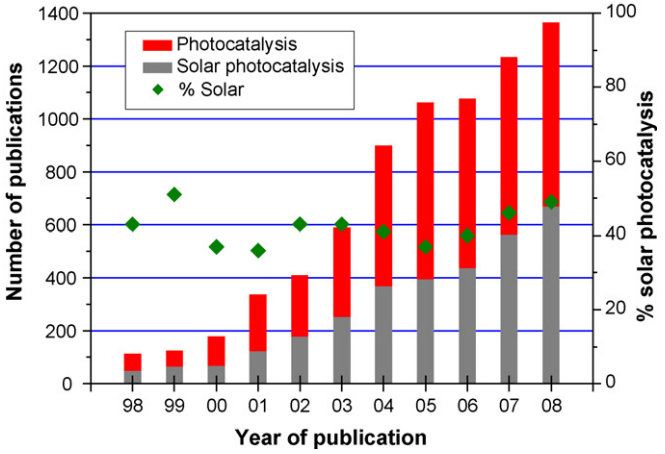

Fig. 1. Publication treating photocatalysis and the share treating solar-driven photocatalysis (source: http://www.scopus.com, 2009, search terms "photocatalysis" and "solar" within these results).

of oxygen. Some semiconductor catalyst can absorb above 400 nm (Fe_2O_3, CdS, etc.). Thus, other photons than those having wavelengths below 400 nm could be used under certain circumstances, as explained below. Oxidizing species (hydroxyl radicals, •OH, produced due to the photogenerated holes), which attack oxidizable contaminants, are generated producing a progressive break-up of molecules yielding CO_2, H_2O and diluted inorganic acids. The most important features of this process making it applicable to the treatment of contaminated aqueous effluents are:

- The process takes place at ambient temperature and without overpressure.
- Oxidation of the substances into CO_2 and other inorganic species is complete.
- The oxygen necessary for the reaction can be directly obtained from atmosphere.
- The catalyst is cheap, innocuous and can be reused.
- The catalyst can be attached to different types of inert matrices.
- The energy for photo-exciting the catalyst can be obtained from the Sun.

The basic principles of this method are well established [8] and are briefly summarized in the following sentences. Semiconductors (e.g., TiO_2, ZnO, Fe_2O_3, CdS and ZnS) can act as sensitizers for light-induced redox processes due to their electronic structure which is characterized by a filled valence band and an empty conduction band. Absorption of a photon of energy greater than the bandgap energy leads to the formation of an electron/hole pair. In the absence of suitable scavengers, the stored energy is dissipated within a few nanoseconds by recombination. If a suitable scavenger or surface defect state is available to trap the electron or hole, recombination is prevented and subsequent redox reactions may occur. The valence band holes are powerful oxidants (+1.0 to +3.5 V vs. NHE depending on the semiconductor and pH), while the conduction band electrons are good reductants (+0.5 to −1.5 V vs. NHE) [9]. Most organic photodegradation reactions utilize the oxidizing power of the holes either directly or indirectly; however, to prevent a build-up of charge one must also provide a reducible species to react with the electrons. In semiconductor electrodes only one species, either the hole or electron, is available for reaction due to band bending, while the complementary reaction takes place in the counter electrode. However, in very small semiconductor particle suspensions both species are present on the surface. Therefore, careful consideration of both the oxidative and the reductive paths is required.

Fig. 2 shows a drawing which is frequently used to illustrate photocatalytic processes. It consists of a superposition of the energy bands of a generic semiconductor (valence band VB, conduction band CB) and the geometrical image of a particle. Absorption of a photon with an energy $h\nu$ greater or equal to the bandgap energy E_g generally leads to the formation of an electron/hole pair in the semiconductor particle. These charge carriers subsequently either recombine and dissipate the input energy as heat, get trapped in metastable surface states, or react with electron donors and acceptors adsorbed on the surface or bound within the electrical double layer. Simultaneously, in the presence of a fluid (water) a spontaneous adsorption occurs (water and pollutant) and according to the redox potential of each adsorbate, an electron transfer proceeds towards acceptor molecules, whereas a positive hole is transferred to a donor molecule. Each ion formed subsequently reacts to form the intermediates and final products. Since the photonic excitation of the catalyst appears as the initial step of the activation of the whole catalytic system, being necessary that the photon has enough energy to be absorbed by the catalyst, not by the reactants. Subsequently, the activation of the process goes trough the excitation of the solid but not through that of the reactants. It is well known that O_2 and water are essential for photooxidation. There is no degradation in the absence of either, except some simple organic molecules, e.g., oxalate and formic acid, that can be oxidised to CO_2 by direct electrochemical oxidation where the electrons are passed on to an alternative electron acceptor, such as metal ions in solution [10]. Furthermore, the oxidative species formed (in particular the hydroxyl radicals) react with the majority of organic substances (pollutants). For example, in aromatic compounds, the aromatic part is hydroxylated and successive steps in oxidation/addition lead to ring opening. The resulting aldehydes and carboxylic acids are decarboxylated and finally produce CO_2. However, the important issue governing the efficiency of photocatalytic oxidative degradation is minimizing electron–hole recombination by maximizing the rate of interfacial electron transfer to capture the photogenerated electron and/or hole. This issue is discussed in more detail later.

Whenever different semiconductor materials have been tested under comparable conditions for the degradation of the same compounds, TiO_2 has generally been demonstrated to be the most active (Fig. 3). TiO_2's strong resistance to chemical breakdown and photocorrosion, its safety and low cost, limit the choice of convenient alternatives. This semiconductor is of special interest, since it can use natural (solar) UV because it has an appropriate energetic separation between its valence and conduction bands (see Fig. 3) which can be surpassed by the energy content of a solar photon ($390\ nm > \lambda > 300\ nm$). The artificial generation of photons required for photocatalyst activation is the most important source of costs during the operating of photocatalytic waste water treatment plants. This suggests using the sun as an economically and ecologically sensible light source. With a typical UV-flux near the surface of the earth of 20–30 W m^{-2} the sun puts 0.2–0.3 mol photons m^{-2} h^{-1} in the 300–400 nm range at the

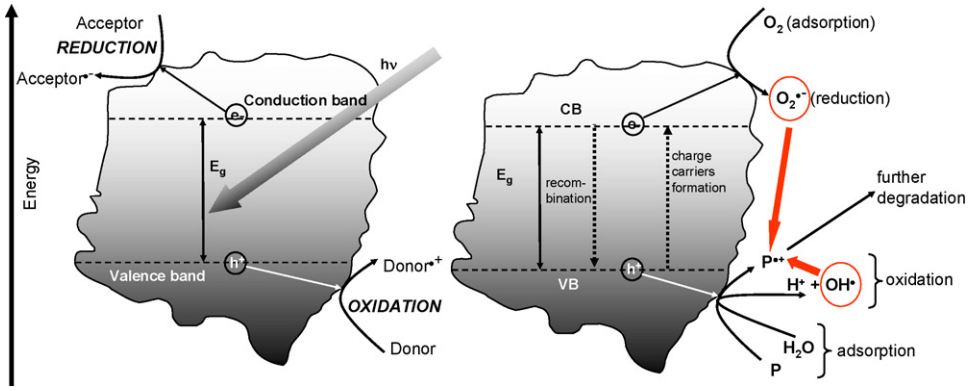

Fig. 2. Energy band diagram and fate of electrons and holes in a semiconductor particle in the presence of water containing a pollutant (*P*).

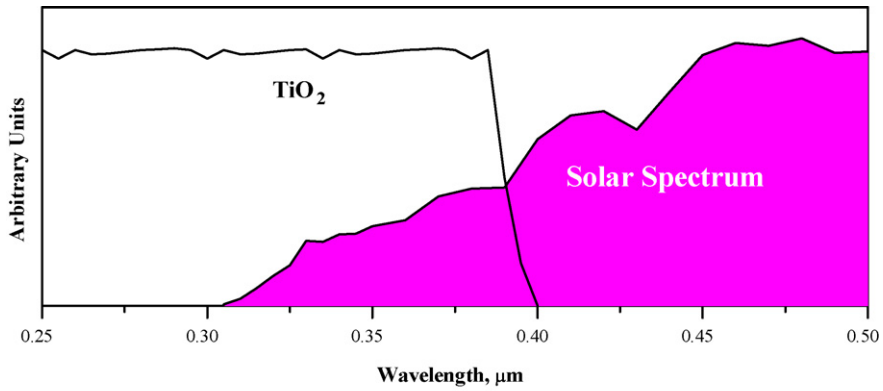

Semiconductor	VB (V vs. NHE ± 0.1 V)	CB (V vs. NHE ± 0.1)	E_g (eV)	Band gap wavelength (nm)
TiO_2	+3.1	-0.1	3.0	380
SnO_2	+4.1	+0.3	3.9	318
ZnO	+3.0	-0.2	2.8	440
ZnS	+1.4	-2.3	3.7	336
WO_3	+3.0	+0.2	2.8	443
CdS	+2.1	-0.4	2.5	497
CdSe	+1.6	-0.1	1.7	730
GaAs	+1.0	-0.4	1.4	887
GaP	+2.2	-1.0	2.3	540

Fig. 3. Band position (water at pH 1) for some common semiconductor photocatalyst: VB (valence band), CB (conduction band), E_g (band-gap energy). TiO_2 absorption spectrum compared with solar spectrum is also shown.

process' disposal. Although there are many different sources of TiO_2, Degussa P25 TiO_2 has effectively become a standard [11] because it has (i) a reasonably well defined nature (i.e., typically a 70:30 anatase:rutile mixture, non-porous, BET surface area $55 \pm 15\ m^2\ g^{-1}$, average particle size 30 nm) and (ii) a substantially higher photocatalytic activity than most other readily available (commercial) TiO_2. Other semiconductor particles, e.g., CdS or GaP absorb larger fractions of the solar spectrum and can form chemically activated surface–bond intermediates, but unfortunately, these photocatalysts are degraded during the repeated catalytic cycles involved in heterogeneous photocatalysis producing final toxic products.

2.2. Fundamental parameters

The rate and efficiency of a photocatalytic reaction depends on a number of factors which govern the kinetics of photocatalysis such as initial concentration of reactant, solar UV radiation, mass of catalyst, pH, temperature, radiant flux and concentration of oxygen.

2.2.1. Initial concentration of reactant

In the photomineralization of organic pollutants sensitized by TiO_2, it has been traditionally reported that the initial rate of disappearance of the pollutant (X) fits a Langmuir–Hinshelwood (L–H) kinetic scheme. According to the L–H model (Eq. (2.1)), the reaction rate (r) is proportional to the fraction of surface covered by the substrate (θ_x), k_r the reaction rate constant, C the concentration of species X, and K is the reactant adsorption constant:

$$r = -\frac{dC}{dt} = k_r\theta_x = \frac{k_r KC}{1 + KC} \tag{2.1}$$

As oxidation proceeds, less and less of the surface of the TiO_2 particles is covered as the contaminant is decomposed. Evidently, at total decomposition, the rate of degradation is zero and a decreased photocatalytic rate is to be expected with increasing illumination time. Most authors agree that, with minor variations, the expression for the rate of photomineralization of organic substrates with irradiated TiO_2 follows the L–H law (quantitative description of the gas–solid reactions between two adsorbed reactants that take place on the interface of the two systems) for the same saturation-type kinetic behaviour in any of the four possible situations: (i) the reaction takes place between two adsorbed substances; (ii) the reaction occurs between a radical in the solution and the adsorbed substrate; (iii) the reaction takes place between the radical linked to the surface and the substrate in the solution; and (iv) the reaction occurs with both species in solution. In all cases, the expression is similar to the L–H model. From kinetic studies only, it is therefore not possible to find out whether the process takes place on surface or in solution.

Traditionally, K is taken to represent the Langmuir absorption constant of the species X on the surface of TiO_2, and k_r is a proportionality constant which provides a measure of the intrinsic reactivity of the photoactivated surface with X. It is found that k is proportional to Φ_e^n, where Φ_e is the rate of effective (able to form electron/hole pairs) light absorption and n is a power term which is less than 1 or 1, at high or low light intensities, respectively. In Section 2.2.6 the effect of Φ on the reaction rate is discussed in more detail. 20 years ago different researchers have measured dark Langmuir adsorption isotherms for TiO_2 for a variety of different organic pollutants and found them to be significantly smaller than the values of K obtained from plots $1/r$, vs. $1/C$. It appears likely that the value of K derived from a kinetic study is not directly equivalent to the Langmuir adsorption coefficient for X on TiO_2 in the dark as adsorption–desorption phenomena are different in the dark in comparison to those under illumination.

Although the L–H isotherm has been rather useful in modeling the process, it is generally agreed that both rate constants and orders are only "apparent" [12–14]. They serve to describe the rate of degradation, and may be used for reactor optimization, but they have no physical meaning, and may not be used to identify surface processes. Thus, while not a useful tool for describing the active species involved in oxidation, engineers and solar designers seem to have a common understanding of the usefulness of the unmodified L–H model.

Graphics similar to those depicted in Fig. 4 may be obtained from the experimental data. The effect of the initial concentration on the degradation rate is shown in Fig. 4, where, due to the saturation produced on the semiconductor surface as the concentration of the

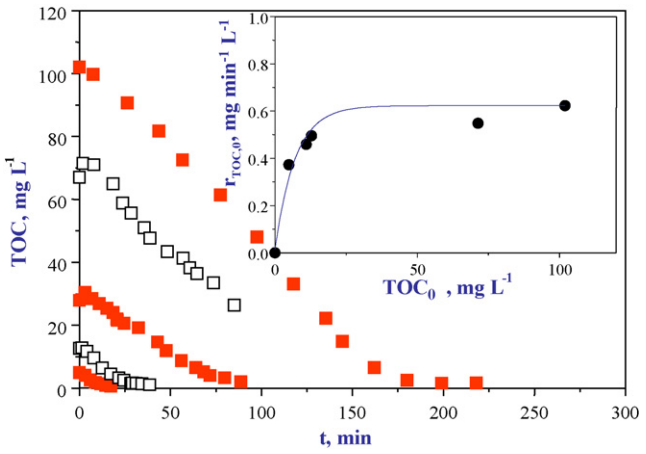

Fig. 4. Effect of the initial concentration on the degradation rate using TOC as key parameter.

reactant increases, it reaches a point at which the rate becomes steady. An understanding of the reaction rates and how the reaction rate is influenced by different parameters is important for the design and optimization of an industrial system. The L–H reaction rate constants are useful for comparing the reaction rate under different experimental conditions. Once the reaction constants k_r and K have been evaluated, the disappearance of reactant can be estimated if all other factors are held constant. Due to this, a series of tests at different initial substrate concentrations has to be performed to demonstrate whether the experimental results could be adjusted with this model. The concentration range has to be wide enough to allow correct fit of the L–H linearization. This means, from the lowest concentration at which the initial rate could be determined until the limit where the relationship between initial reaction and initial concentration remains constant (see Fig. 4). Since hydroxyl radicals react non-selectively, numerous intermediates are formed en-route to complete mineralization at different concentrations. Because of this, very often tests are carried out using Total Organic Carbon (TOC) as key parameter (instead of concentration of parent compound, C), because the photocatalytic treatment must destroy not only the initial contaminant, but any other organic compound as well. The results shown in Fig. 4 are examples of experiments carried out with a real wastewater. It is possible to see that mineralization, once begun, maintains the same slope until at least 60–70% of the initial TOC has been degraded.

As the reaction is not expected to follow simple models like first or zero-order kinetics, overall reaction rate constants cannot be calculated. The complexity of the results, of course, is caused by the fact that the *TOC* is a sum parameter often including a lot of products that undergo manifold reactions. One parameter is proposed in order to obtain a practical point of comparison for various experiments: the maximum gradient of the degradation curve, which is the slope of the tangent at the inflection point ($r_{TOC,0}$). It has the unit of a zero-order rate constant and therefore appears to be easy to handle. Furthermore this gradient can be roughly considered as the initial rate of the mineralization reaction, because it is preceded by a period of nearly constant *TOC* level. This parameter $r_{TOC,0}$ is referred to as "maximum rate". In the graphic insert in Fig. 4, it may be observed that the initial rate is steady from 20–30 mg of TOC per liter. At this concentration, saturation occurs and the reaction rate becomes constant. It could be concluded from this discussion that the photocatalytic treatment is more efficient when working at the saturation level, where reaction rate becomes constant.

As commented before, although the L–H model is not a perfect explanation of the mechanism of the photocatalytic process, its usefulness is generally accepted, since the behaviour of the reaction rate vs. reactant concentration can very often be adjusted to a mathematical expression with it. In the case of using *TOC* (as an alternative to C) instead of using the L–H model ($r = kKC/(1 + KC)$) directly, the use of a well-known model [15] is better for fitting experimental data in solar photocatalytic plants, by an approximate kinetic solution of the general photocatalytic kinetic system, which has the analytical form of an L–H equation. With these considerations, the rate of TOC disappearance is given by Eq. (2.2) (analogous to L–H model but without its original significance, being β_1, β_2 and β_3 empirical):

$$r_{TOC,0} = \frac{\beta_1 [TOC]}{\beta_2 + \beta_3 [TOC]} \tag{2.2}$$

The experimental results shown in Fig. 4 could be used to calculate the constants (β_i). By inversion of Eq. (2.2) these constants can be calculated from the intercept and the slope of the line of fit (Eq. (2.3)), which is shown in the inset in Fig. 4:

$$\frac{1}{r_{TOC}} = \frac{\beta_3}{\beta_1} + \frac{\beta_2}{\beta_1}\frac{1}{[TOC]}; \qquad \frac{\beta_3}{\beta_1} = 1.67\ \text{min L mg}^{-1}; \qquad \frac{\beta_2}{\beta_1} = 5.07\ \text{min} \tag{2.3}$$

Using these values, experimental results could be fitted with Eq. (2.4). This equation allows TOC degradation to be predicted as a function of initial TOC and treatment time, and the reverse, treatment time necessary to reach a specific degree of mineralization. Therefore, useful design equations may be obtained with a L–H type model, in spite of not fitting the heterogeneous photocatalytic reaction mechanism. For now these equations must be obtained at pilot plant size, however, they will be useful for larger plants if the same type of collector is used:

$$\frac{1}{\beta_1}\left\{\beta_2 \ln\left(\frac{[TOC]_{0x}}{[TOC]}\right) + \beta_3([TOC]_0 - [TOC])\right\} = t \tag{2.4}$$

Nevertheless, solar UV radiation data (TiO_2 absorption spectrum overlaps with the solar UV spectrum at earth surface) collected during pilot plant experimentation and for the final plant location must be available for dimensioning adequately the treatment plant, as Solar UV is an essential parameter for the correct evaluation of data obtained in a specific solar photocatalytic plant.

2.2.2. Solar UV radiation

The kinetic constants of photocatalytic processes can be obtained by plotting substrate concentration as a function of three different variables: time, incident radiation inside the reactor and photonic flux absorbed by the catalyst. Depending on the procedure, the complexity of obtaining these constants, as well as their applicability, varies. When the photonic flux absorbed by the catalyst is used as an independent variable, extrapolation of the results is better. However, many parameters (incident photons passing through the reactor without interacting with the catalyst, directions of light scattering, size distribution of the TiO_2 particles suspended in the liquid, etc.) must be known for this, making it almost impractical in large size solar photoreactors [16,17].

Use of the experimental time as the calculation unit could give rise to misinterpretation of results, because the reactor consists of illuminated and non-illuminated elements. Large experimental reactors require much instrumentation and the reactor must also be as versatile as possible, substantially increasing the non-illuminated volume. With use of residence time, that is, the time the water has been exposed to the radiation, the conclusions would be erroneous, too. This is because when time is the independent variable, the differences in the incident radiation in the reactor during an experiment are not taken into account.

A simple way is to introduce a standardized illumination time. 30 W m^{-2} can be considered a standard global UV irradiance ($I^{\circ}_{G,UV}$) under clear skies in sunny countries. The measurement of broadband UV radiation can be considered the most appropriate spectral range to standardize photocatalytic results. The intensity of the solar spectrum is dependent on the wavelength; nevertheless, to characterize solar irradiation or the power input into a solar collector usually figures are employed, which describe the irradiance power within a defined spectral range. These numbers are commonly obtained by broadband measurements, contrarily to spectral intensity measurements. The first type of measurement is performed with so-called broadband radiometers, the second one with spectroradiometers. The measurement of global UV irradiance at the same orientation than solar photocatalytic reactors is considered the most appropriate way to describe the solar power input to the solar collector [17]. The choice of the measurement position of the radiometer is obvious and global radiation measurement is more adequate than direct radiation measurement, because of the nature of the type of solar collectors used nowadays (see Section 2.3.2), which are able to utilize global radiation. The choice of the UV spectral range for radiometers used in photocatalysis has two principal reasons; first, UV radiometers adjust themselves in their spectral range best to the active radiation of the TiO_2 photocatalysis ($\lambda < 400$ nm) and they are also the option widely available on the market (compared with visible or infrared radiometers) for photo-Fenton process ($\lambda < 580$ nm), and second, scientists working on at lab scale with artificial lamps often choose the same spectral range to evaluate experimental results. Consequently, comparison of results is greatly simplified.

Consequently, under constant global UV irradiance Eq. (2.5) yields an expression for the normalised irradiation time $t_{30\,W}$. Yet, Eq. (2.6) has to be used under real conditions, because, as stated, solar irradiance is never constant, being $t_{30\,W} = 0$ the moment when illumination was started:

$$t_{30\,W} = t\frac{I_{G,UV}}{I^{\circ}_{G,UV}} \tag{2.5}$$

$$t_{30\,W} = \frac{1}{I^{\circ}_{G,UV}}\int_0^t I_{G,UV}(t)dt \tag{2.6}$$

One step beyond follows the suggestion to incorporate the specifications of the solar hardware as well. This makes comparison of the experimental performance of different solar collectors possible. The best concept to compare different technical solutions would be, naturally, the treatment cost in the absence of other compelling criteria (e.g., compliance with legal discharge limits). Yet, assessment of treatment costs is difficult and in most cases not very accurate. Hence, IUPAC recommended comparing solar systems based on the collector area (A) necessary to achieve a certain goal in a unit time [19]. To this end Q, the accumulated UV energy incident on the collector surface per litre waste water, is calculated by Eq. (2.7), being V_{tot} the volume of water treated until certain level of polishing between $t = 0$ and each time, t. Finally, with Eq. (2.8) the collector area per mass as defined by IUPAC can be calculated, where Δc is the concentration difference regarding the analytical target parameter (concentration of contaminant, *TOC*, *COD*, etc.) between start and end of the treatment:

$$Q = \frac{A}{V_{tot}}\int_0^t I_{G,UV}(t)dt \tag{2.7}$$

$$A = \frac{Q}{I^{\circ}_{G,UV}\Delta c} \tag{2.8}$$

Fig. 5 shows the improvement obtained using this equation to calculate the reaction rate in a 2-day photocatalytic degradation experiment with a model compound. Obviously, UV power changes during the day and clouds, during the first day, make this variation still more noticeable, but with Eq. (2.7), the data for both days can still be combined and compared with other photocatalytic experiments. Therefore, both $t_{30\,W}$ and Q could be used for determining the kinetic constants of photocatalytic processes (Section 2.2.1) as function of the final goal.

2.2.3. Mass of catalyst

TiO_2 is often used as suspension and the rate of photomineralization is generally found to increase with catalyst concentration towards a limiting value at high TiO_2 concentration. This limit depends on the geometry and working conditions of the

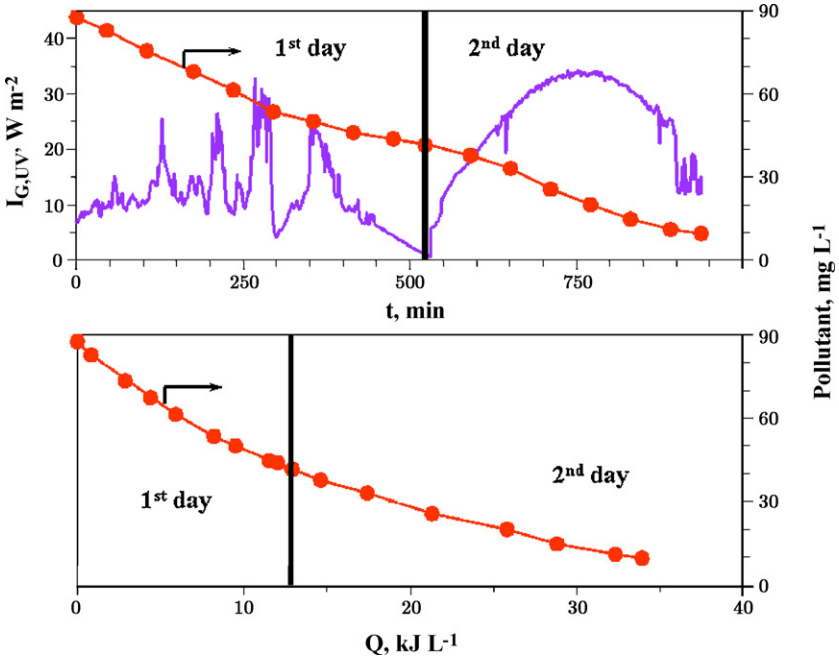

Fig. 5. Example of solar degradation experiments depicted vs. t (up) and vs. Q (down). Solar UV irradiance throughout the experiment is also shown.

photoreactor and is for a definite amount of TiO_2 in which all the particles, i.e., all the surface exposed, are totally illuminated. When catalyst concentration is very high, after travelling a certain distance on an optical path, turbidity impedes further penetration of light in the reactor. In any given application, this optimum catalyst mass has to be found in order to avoid excess catalyst and ensure total absorption of efficient photons [16,20].

There are a number of studies in the literature on the influence of catalyst concentration on process efficiency. The results are very different, but from all of them it may be deduced that radiation incident on the reactor and path length inside the reactor are fundamental in determining the optimum catalyst concentration. In the case of solar photoreactors where the path length is several centimeters long, the appropriate catalyst concentration is several hundreds of milligrams per liter. In this case, it is very clear that the highest rate (i.e., lowest collector are per mass, see Eq. (2.8)) is attained at lower catalyst concentrations when the photoreactor diameter is increased. As one important factor related to the photoreactor design is its diameter, it seems obvious that uniform flow must be maintained at all times in the reactor, since non-uniform flows causes non-uniform residence times that can lower efficiency compared to the ideal. In the case of the heterogeneous process with TiO_2 in suspension, sedimentation and deposition of the catalyst along the hydraulic circuit must also be avoided, so that turbulent flow in the reactor must be guaranteed [21]. Turbulent flow makes pressure loss an important parameter that can condition design, especially in the case of an industrial plant with long reactor tube lengths. For these reasons diameters of less than 20–25 mm are not feasible. On the other hand, diameters over 50–60 mm are not considered practical. Furthermore, every photoreactor design must guarantee that all the useful incoming photons are used and do not escape without having intercepted a particle in the reactor.

Although TiO_2 suspensions absorb solar photons with less than 390–400 nm wavelengths, there is also a strong light scattering effect due to particles. Both effects must be considered in determining the optimum catalyst load as a function of optical path length in the photoreactor. Fig. 6 shows the combination of both effects and the resulting Extinction Coefficient of TiO_2 (ε). Note that this parameter has been calculated (see Eq. (2.9)) as surface/mass because TiO_2 is suspended in water (not dissolved). In Eq. (2.9) A is light absorption, l is path length and c is substance concentration (kg/L for particle suspension, mol/L for a homogenous phase). The Extinction Coefficient of TiO_2 shown in Fig. 6 (inset) was calculated by combining the scattering and absorption coefficients developed by Cassano and Alfano [16]. Therefore, it is not really an "Extinction Coefficient", but a parameter obtained from the scattering and absorption coefficients, so this notation is used only to simplify interpretation:

$$A = \varepsilon l c \tag{2.9}$$

Wavelengths where the catalyst does not absorb light are better for determining the optimum catalyst concentration as a function of light-path length. Under these conditions, measurement of photon losses is only affected by turbidity and it is easier to evaluate the effect of the photoreactor diameter. In Fig. 6, where these results are shown for different tube diameters, it may be seen how larger photoreactor diameters result in a lower optimum catalyst concentration, and vice versa.

2.2.4. pH

The pH of the aqueous solution significantly affects TiO_2, including the charge on the particles, the size of the aggregates it forms, and the positions of the conductance and valence bands. It is somewhat surprising, therefore, that the rate of photocatalytic mineralization is not usually found to be strongly dependent upon pH between values ranging from 4 to 10. To work outside these values is not logical due to environmental and economical reasons, if the wastewater pH would need to be adjusted. Often, the pH of industrial wastewater can be very acidic or basic. In this case, the effect of pH on TiO_2 photocatalytic efficiency should be taken into account as the process could be enhanced varying the pH by simple/cheap methods as for example mixing different streams.

The pH at which the surface of an oxide is uncharged is defined as the Zero Point Charge (pH_{zpc}), which for TiO_2 depends on the production method ($4.5 < pH_{zpc} < \sim 7$). Above and below this value, the catalyst is negatively or positively charged according to:

$$-TiOH_2^+ \leftrightarrow TiOH + H^+ \tag{2.10}$$

$$-TiOH \leftrightarrow TiO^- + H^+ \tag{2.11}$$

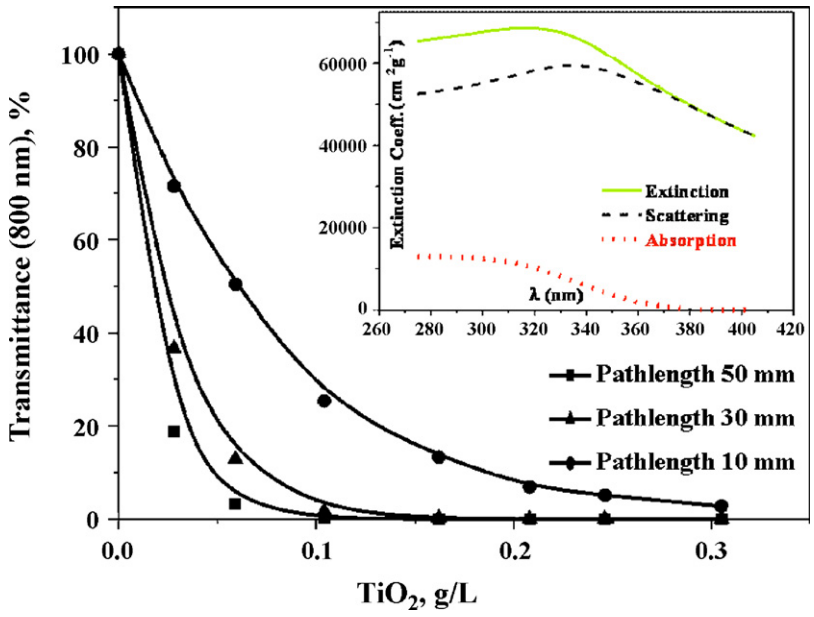

Fig. 6. Transmittance and extinction coefficient (inset) of TiO_2 Degussa P-25, at pH 6, suspension in water.

The equilibrium constants of these reactions [22] are $pK_{TiOH_2^+} = 2.4$ and $pK_{TiOH} = 8.0$, the abundance of all the species as a function of pH been $-TiOH \geq 80\%$ when $3 < pH < 10$; $-TiO^- \geq 20\%$ if $pH > 10$; $-TiOH_2^+ \geq 20\%$ when $pH < 3$. In many cases, a very important feature of photocatalysis is not taken into account when it is to be used for decontamination of water, is that during the reaction, a multitude of intermediate products are produced that may behave differently depending on the pH of the solution. To use only the rate of decomposition of the original substrate could yield an erroneous pH as the best for contaminant degradation. Therefore, a detailed analysis of the pH conditions should include not only the initial substrate, but also the rest of the compounds produced during the process. Measurement of an overall parameter as *TOC* (or *COD*, or toxicity, or biodegradability, etc.) should be used for choosing the optimum pH, or at least to determine the effect of pH on the behaviour of the chosen key parameter.

The size of the aggregates formed by TiO_2 particles is also affected by pH. Mean particle-size measurements (an example is presented in Fig. 7) have been found to be constant at pH far from 7. 300 nm sizes increase to 2–4 μm when dispersion reaches pH_{zpc}. The zero surface charge yields zero electrostatic surface potential that cannot produce the interactive rejection necessary to separate the particles within the liquid. This induces a phenomenon of aggregation and TiO_2 clusters become larger. The large mean size in suspension at pH close to 7 becomes much smaller at pH far from 7. This effect is clearly related to the capability of the suspension for transmitting and/or absorbing light. Furthermore, larger clusters sediment more quickly than small particles, thus the agitation necessary to maintain good catalyst uniformity must be more vigorous. Therefore, pH close to Zero Point Charge should be avoided in order to not promote TiO_2 particles aggregation. It is necessary to remark that pH usually drops due to carboxylic acids (degradation products from larger molecules prior to mineralization) and inorganic acids release (HCl, H_2SO_4, HNO_3, etc., are produced from contaminants containing chlorine, sulphur, nitrogen, etc.) during degradation of organic compounds. This spontaneous pH drop provoked by the photocatalytic process itself should be taken into account when pH studies are performed.

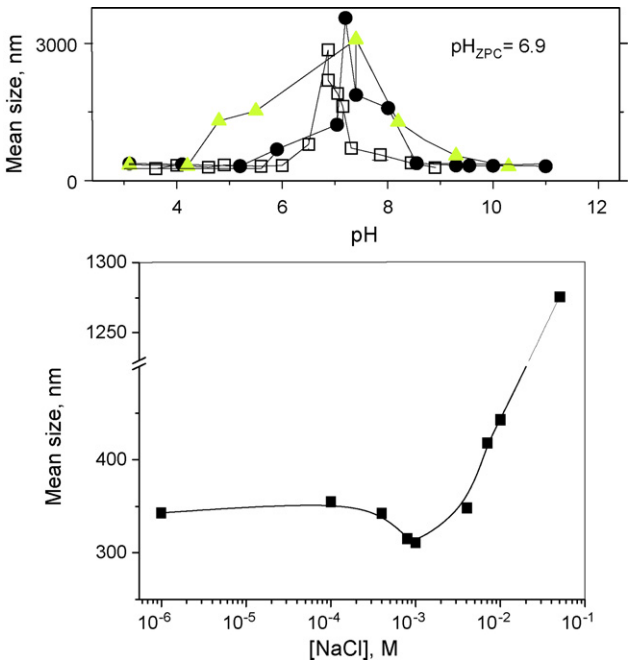

Fig. 7. P25–TiO_2 mean particle size vs. pH (up): [NaCl] = 0 (□), [NaCl] = 10^{-3} M (●), [NaCl] = 5×10^{-3} M (▲) and vs. NaCl concentration at pH 4 (down).

The mean size measurements at NaCl concentrations of 0, 1 and 5 mM show a bell curve (see Fig. 7) the width of which increases as electrolyte concentration rises. This indicates that the presence of salts usually diminishes the colloidal stability, probably due to a screening effect of the particle surface charge, double layer compression and surface charge neutralisation, which makes the potential on the diffuse layer lower and the clusters larger. Ions induce a strong change in the mean size of the TiO_2 clusters.

In contrast, these variations in particle size could be an advantage for separating the catalyst from water (by sedimentation and/or filtration) at completion of photocatalytic treatments. Mean cluster size at pH 7 around pH_{zpc} demonstrates a clear aggregation process over time. However, in conditions of colloidal stability the mean size is around 330 nm (pH far from the pH_{zpc}) remaining nearly constant over time. At such pH a slight difference in size may be observed up to a certain time. Fig. 7 shows the effect of electrolyte (NaCl) concentration at pH 4. At this pH the suspension is stable if no electrolyte is added. A very sudden increase in mean size was found when electrolyte concentration was increased to 10^{-2} M. This would explain sedimentation of large clusters as confirmed by the evolution of mean size.

The above characterisation and colloid properties can be applied for enhancement of a cheap/easy sedimentation of the TiO_2 catalyst used in photocatalytic degradation. Photocatalytically treated wastewater is most commonly acid pH (due to the generation of inorganic acids from the heterogeneous content in organic contaminants). Two alternative procedures could be established to induce aggregation and fast sedimentation: change in pH of suspensions to the pH_{zpc} and addition of an electrolyte. The first option is the most suitable process in water treatment, since the other produces high concentrations of salts that cannot be disposed of into the environment and increases the cost. Anyway, very often both procedures could be applied at the same time as wastewaters usually contain large quantities of dissolved ions as chloride, sulphate, etc. Furthermore, the pH of the suspensions after TiO_2 sedimentation by charge neutralization is within the permitted disposal range for treated water. Aggregation of the particles may be visually observed and the weight of the clusters formed makes them settle very fast [23]. The induced sedimentation takes a short time (an easy task to be operated during the night in the case of solar photocatalysis) to reduce the concentration of particles in suspension to less than 3% of the initial concentration. This small remaining fraction of catalyst can easily be recovered by microfiltration.

2.2.5. Temperature

Because of the photonic activation, the photocatalytic systems do not require heating and are operating at room temperature. The true activation energy is nil, whereas the apparent activation energy is often very small (a few kJ/mol) in the medium temperature range (between 20 and 80 °C). However, at very low temperatures (below 0 °C) the apparent activation energy increases. The desorption of the final product becomes the rate limiting step and trends to the heat of adsorption of the product. On the other hand, when temperature increases above 80 °C and approaching to the boiling point of water, the exothermic adsorption of reactants becomes disfavoured and tends to become the rate limiting step. Correspondingly, the activity decreases and the apparent activation energy becomes negative. As a consequence, the optimum temperature is generally comprised between 20 and 80 °C. This absence of heating is attractive for photocatalytic reactions carried out in aqueous media and in particular for photocatalytic water purification. There is no need to waste energy in heating water which possesses a high heat capacity [20]. It is also necessary to take into account that the solubility of oxygen decreases with increasing temperature, affecting therefore to the

kinetics described in Section 2.2.7. Temperature does become a factor in photocatalytic disinfection and as such is commented in Section 5.

This behaviour can be easily explained within the frame of the Langmuir–Hinshelwood mechanism described above. The decrease in temperature favours adsorption, which is a spontaneous exothermic phenomenon, θ_x approaches to unity and KC becomes $\gg 1$. The lowering in T also favours the adsorption (K_P) of the final reaction products, inhibiting the reaction as the term $K_P C_P$ appears in the denominator of Eq. (2.1). Above 80 °C the adsorption of reactants is disfavoured and KC becomes $\ll 1$, being $r = k_{ap}C$.

2.2.6. Radiant flux

Since 1990 there has been a clarification of the kind of solar technology which should be involved in photocatalysis. The question was if it is necessary to concentrate the radiation for the photocatalysis technology and if a non-concentrating collector can be as efficient as concentrating ones. Initially it was thought that concentrating collectors were the ideal alternative and in fact, the first large pilot plants operated were using them. However, their high cost and the fact that they can only operate with direct solar radiation (this implies their location in highly irradiated areas with few cloud cover) led to consider static non-concentrating collectors as an alternative. The reason of using one-sun systems for water treatment is firmly based on two factors: first the high percentage of UV photons in the diffuse component of solar radiation (see Fig. 8) and second the low order dependence of rates on light intensity.

Fig. 8 presents degradation tests comparing a non-concentrating collector (CPC see Section 2.3) and a two axis parabolic-trough concentrating collector. Both systems were operated in parallel at Plataforma Solar de Almería (Spain), at the same catalyst concentration (200 mg L^{-1} Degussa P-25), at the same dichloroacetic acid initial concentration (5 mM) and performing one test around the 15th of each month during 1 year. The tests were performed on perfect sunny days to permit the parabolic through to be in operation all day from sunrise to sunset. The ratio encountered between both systems working in analogous conditions for degradation is higher than 5 in favour of the CPC, and this ratio would be even higher considering cloudy periods. Taking into consideration that diffuse UV radiation component is so important and the low quantum efficiency of concentrating collectors, the ratio encountered was rather consistent. These results and other similar obtained by different authors have focused the development of photoreactors for solar photocatalysis on non-concentrating collectors, avoiding nowadays the use of earlier designs of solar collectors developed for solar thermal applications. Section 2.3 explains these constraints in more detail.

It has been shown, for all types of photocatalytic reactions, that the rate of reaction is proportional to the radiant flux (Φ). This confirms the photo-induced nature of the activation of the catalytic process, with the participation of photo-induced electrical charge (electrons and holes) to the reaction mechanism. However, above a certain value the reaction rate becomes proportional to $\Phi^{0.5}$. This modification does not seem to happen at well-established radiation intensity, as different researchers obtain different results. It is presumable that the experimental conditions affect significantly, but it has been stated that with a typical Solar UV-flux of 20–30 W m^{-2} (0.2–0.3 mol photons m^{-2} h^{-1} in the 300–400 nm) the concentration of sunlight (R_C) on the photoreactor using specific solar concentrating collectors ($R_C = A/2\pi r$, being A the collector aperture width and r the reactor tube radius) is not convenient as reaction rate is usually proportional to $\Phi^{0.5}$. A practical appraisal to this statement is that more than 50 W (<400 nm) per square meter of photoreactor (being tubular or flat-plate) will produce a loss of photonic efficiency. Most authors [25–28] impute the transition of $r = f(\Phi)$ to $r = f(\Phi^{1/2})$, to the excess of photogenerated species (e^-, h^+ and $^\bullet$OH). A very simple explanation could be the following (based on the first stages of the process). The first stages considered are: (i) formation of electron/hole pairs (Eq. (2.12)), (ii) recombination of the pairs (Eq. (2.13)) and (iii) oxidation of a reactant R (Eq. (2.14)):

$$TiO_2 + h\nu \xrightarrow{k_f} e^- + h^+ \tag{2.12}$$

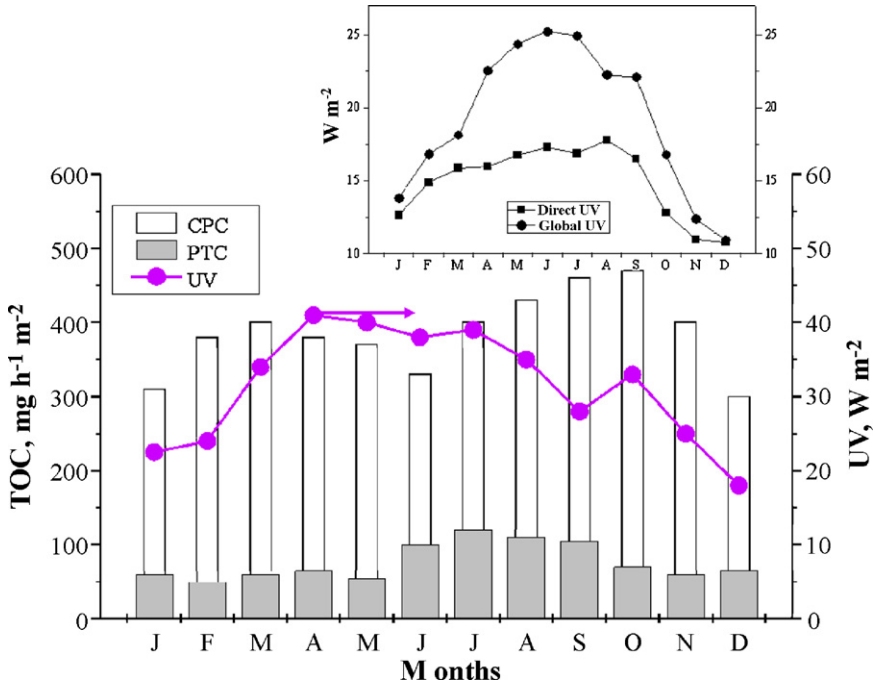

Fig. 8. TOC disappearance reaction rate for a concentrating (PTC) and a non-concentrating (CPC) collector system [24]. The mean value of global UV radiation during the experimental periods is also shown. Average UV direct and UV global (direct + diffuse) irradiance for each month of the year at Plataforma Solar de Almería is shown in the inset.

$$e^- + h^+ \xrightarrow{k_R} \text{energy} \quad (2.13)$$

$$h^+(\text{or } {}^\bullet\text{OH}) + R \xrightarrow{k_0} R_1 \quad (2.14)$$

In an n-type semiconductor such as titania, the photo-induced holes are much less numerous than electrons (photo-induced electrons plus n-electrons): $[h^+] \ll [e^-]$. Therefore holes are the limiting active species. At any instant, one has:

$$r = k_0[h]R \quad (2.15)$$

$$\frac{d[h]}{dt} = k_f\Phi - k_R[e][h] - k_0[h]R = 0 \quad (2.16)$$

In the case of high Φ, the instantaneous concentration of e^- and h^+ could be the same and thus $[h^+]\,[e^-] = [h^+]^2$, being also $k_R[h]^2 \gg k_0[h]R$:

$$k_f\Phi = k_R[h]^2 + k_0[h]R \quad (2.17)$$

When Φ is very high, a large number of holes and electrons are generated and therefore $k_R[h]^2 \gg k_0[h]R$. As the reaction rate depends on the amount of hydroxyl radicals present, and these are generated in the holes (see Fig. 2), then r is proportional to $\Phi^{0.5}$ when Φ is high. Under these conditions, the quantum yield diminishes because the rate of electron–hole formation becomes greater than the photocatalytic rate, which favours the electron–hole recombination. In the same manner, when Φ is small, $k_R[h]^2 \ll k_0[h]R$ and reaction rate is directly proportional to the light flux:

$$\text{At high } \Phi; \qquad k_f\Phi \approx k_R[h]^2 \rightarrow [h] \approx k_{ap}\Phi^{0.5} \quad (2.18)$$

$$\text{At low } \Phi; \qquad k_f\Phi \approx k_0[h]R \rightarrow [h] \approx k'_{ap}\Phi \quad (2.19)$$

$$r = k_0k_{ap}\Phi^{0.5}R; \qquad r \propto \Phi^{0.5} \quad (2.20)$$

$$r = k'_{ap}\Phi R; \qquad r \propto \Phi \quad (2.21)$$

At much higher radiation intensities, another transition from $r = f(\Phi^{0.5})$ to $r = f(\Phi^0)$ is produced. At this moment, the photocatalytic reaction leaves its dependence on the received radiation, to depend only on the mass transfer within the reaction. So, the rate is constant although the radiation increases. This effect can be due to different causes, as can be the lack of electrons scavengers (i.e., O_2), or organic molecules in the proximity of TiO_2 surface and/or excess of products occupying active centers of the catalyst, etc. In practical applications these phenomena are observed more frequently when working with supported catalyst, and/or at low agitation level. This implies low catalyst surface in contact with the liquid and smaller turbulence. Thus, the contact of reactants with the catalyst and the diffusion of products from the proximity of the catalyst to the liquid are not favoured.

These effects may be appreciably attenuated if some products that reduce the importance of the electron/hole recombination are added. When the electrons are trapped, recombination of e^-/h^+ is impeded. Either way, addition of electron trapping substances (oxidants) can improve the efficiency of the process at high illumination intensities. Moreover, this type of compounds can increase the quantum yield even at low irradiation levels due to their strong oxidizing character. The use of inorganic peroxides has been demonstrated to enhance the rate of degradation of different organic contaminants remarkably because they trap the photo-generated electrons more efficiently than O_2. Another advantage related to the use of peroxides comes up when solar energy is the photon source. The increase of the photocatalytic reaction rate with these additives would decrease photoreactor dimensions proportionally and dramatically decrease overall costs. All these are discussed in more detail in Section 3.2.

2.2.7. Concentration of oxygen

In semiconductor photocatalysis for water purification, the pollutants are usually organic and, therefore, the overall process can be summarized by Eq. (2.22). Given the reaction stoichiometry of this equation, there is no photomineralization unless O_2 is present. The literature provides a consensus regarding the influence of oxygen. Oxygen is necessary for complete mineralization and does not seem to be competitive with other reactives during the adsorption on TiO_2 since oxidation takes place at a different location from where reduction occurs (see Fig. 2). The concentration of oxygen also affects the reaction rate but it seems that the difference between using air ($p_{O_2} = 0.21$ bar) or pure oxygen ($p_{O_2} = 1$ bar) is not drastic. In an industrial plant it would be purely a matter of economy of design. It has been reported that the rate of oxidation was independent of oxygen concentrations below air saturation values, suggesting also that the mass transfer of oxygen to the surface could be rate limiting:

$$\text{organic pollutant} + O_2 \underset{\text{ultrabandgap energy}}{\overset{\text{semi conductor}}{\longrightarrow}} CO_2 + H_2O + \text{mineral acids} \quad (2.22)$$

Due to its availability in water adsorbed oxygen often serves as the electron acceptor in semiconductor photocatalysis. Rate equations have been derived assuming a Langmuir adsorption of oxygen onto the titanium dioxide surface. The role of oxygen may not only be that of an electron acceptor. Oxygen for instance may be involved in the formation of other oxidative species (superoxide, hydrogen peroxide, hydroxyl radicals), in the prevention of reduction reactions, in the stabilisation of radical intermediates, mineralization, and direct photocatalytic reactions:

$$r = -\frac{dC}{dt} = \frac{k_rKC}{1 + KC}\frac{K_{O_2}C_{O_2}}{1 + K_{O_2}C_{O_2}} = \frac{k_{ap}KC}{1 + KC} \quad (2.23)$$

It is generally assumed that oxygen adsorbs on titania from the liquid phase, where it is dissolved following Henry's law. If the oxygen is regularly supplied, it can be assumed that its coverage at the surface of titania is constant and can be integrated into the apparent rate constant (k_{ap}). In most kinetic studies, the observed variation of the rate of photomineralization as a function of concentration of oxygen is described very well by Eq. (2.23). Thus, a double reciprocal plot of the data yields a straight line and from the ratio of the intercept to the gradient of the straight line a value of K_{O_2} can be obtained. Fig. 9 illustrates plots of r vs. $\%O_2$ and $1/r$, vs. $1/\%O_2$, as example of a kinetic study of the photodegradation of a contaminant by TiO_2 photocatalysis. Thus, increasing the oxygen concentration in aqueous solution from air saturated (21% O_2) to O_2 saturated (100% O_2) conditions, will typically increase the rate by only a small quantity (Table 1).

2.3. Solar photocatalysis hardware

2.3.1. Specific hardware for solar photocatalysis

The specific hardware needed for solar photocatalytic applications have much in common with those used for thermal applications. As a result, both reactors and photocatalytic systems have followed conventional solar thermal collector designs, such as parabolic troughs and non-concentrating collectors. At this point, their designs begin to diverge, since: (i) the fluid must be exposed to ultraviolet solar radiation, and, therefore, the absorber must be UV-transparent, and (ii) temperature does not play a significant role in the photocatalytic process, so no insulation is required.

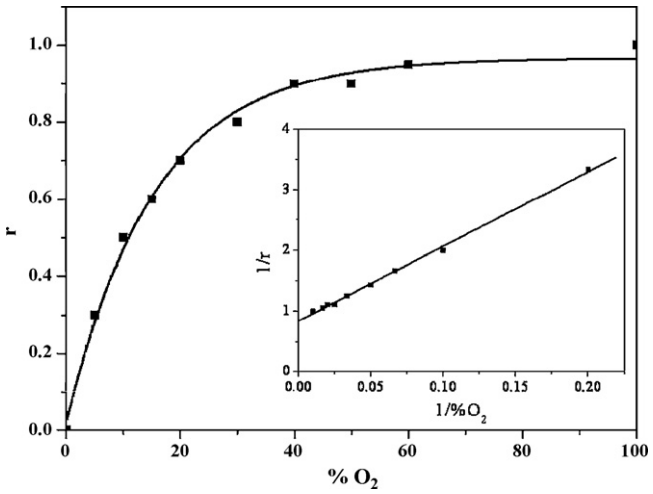

Fig. 9. Plots of initial relative rate (r) vs. concentration of oxygen (%O_2) and $1/r$ vs. $1/\%O_2$.

For many of the solar detoxification system components [18], the equipment is identical to that used for other types of water treatment and construction materials are commercially available. Most piping may be made of polyethylene or polypropylene, avoiding the use of metallic or composite materials that could be degraded by the oxidant conditions of the process. Neither must materials be reactive, interfering with the photocatalytic process. All materials used must be inert to degradation by UV solar light in order to be compatible with the minimum required lifetime of the system (10 years).

Photocatalytic reactors must transmit UV light efficiently because of the process requirements. In some cases, when the vapor pressure of contaminants in water is sufficiently low, a closed system could not be required and then a transmissive UV containment material could be avoided. All pipes, reactor and connection devices must be strong enough to withstand the necessary water-flow pressure. Typical parameters are 2–4 bar for nominal system pressure drop and a maximum of 5–7 bar.

With regard to the reflecting/concentrating materials, aluminum is the best option due to its low cost and high reflectivity in the solar UV spectrum on earth surface. The photocatalytic reactor must contain the catalyst and be transparent to UV radiation providing good mass transfer of the contaminant from the fluid stream to an illuminated photocatalyst surface with minimal pressure drop across the system. The reflectivity (reflected radiation/incident radiation) between 300 and 400 nm of traditional silver-coated mirrors is very low and aluminum-coated mirrors is the best option in this case. Aluminum is the only metal surface that is highly reflective throughout the ultraviolet spectrum. Reflectivities range from 92.3% at 280 nm to 92.5% at 385 nm. Comparable values for silver are 25.2% and 92.8%, respectively. A fresh deposited aluminum surface is fragile and needs to be protected from weathering and abrasion, but the conventional glass cover used for silver-backed mirrors has the drawback of significantly filtering UV light (an effect that is doubled as the light reflects back through the glass). The thin oxide layer that forms naturally on aluminum is not sufficient to protect it in outdoor environments. Under such exposure conditions, the oxide layer continues to grow and UV reflectance drops off dramatically. The surfaces currently available that best fit these requirements are: (i) electropolished anodized aluminum and (ii) organic plastic films with an aluminum coating.

Adequate flow distribution inside the reactor must be assured, as non-uniform distribution leads to non-uniform residence times inside the reactor, resulting in decreased performance compared to an ideal-flow situation. If the catalyst is used in suspension (slurry in the case of TiO_2), the Reynolds number (Re) must always be over 4000 in order to guarantee turbulent flow. This is critical in avoiding catalyst settlement. Another important design issue is that internal reactor materials must not react with either the catalyst or the pollutants to be treated or their by-products. The choice of materials that are both transmissive to UV light and resistant to its destructive effects is limited. Also the reactor must be able to withstand summer temperatures of around 60–70 °C in order to guarantee that there will be no damage. Finally, low pH resistance is needed since the production of inorganic acids as reaction by-products is quite normal (e.g., the destruction of chlorinated hydrocarbons leads to the production of HCl). Common materials that meet these requirements are fluoropolymers, acrylic polymers and several types of glass. Quartz has excellent UV transmission as well as good temperature and chemical resistance, but high cost makes it completely unfeasible for photocatalytic applications. Fluoropolymers are a good choice of plastic for photoreactors due to their good UV transmittance, excellent ultraviolet stability and chemical inertness. One of their greatest disadvantages is that, in order to achieve a desired minimum pressure rating, the wall thickness of a fluoropolymer tube has to be increased, which in turn will lower its UV transmittance. Acrylics could also potentially be used but they are very brittle. Other low cost polymeric materials are significantly more susceptible to be attacked by $^{\bullet}OH$ radicals.

Glass is another alternative for photoreactors. Standard glass, used as protective surface, is not satisfactory because it absorbs

Table 1
Summary of factors which govern the kinetics of photocatalysis and their effect on the rate of the photocatalytic reaction. Optimum range for each of them is also included.

Parameter	Main effect	Optimum range
Initial concentration of reactant	Langmuir–Hinshelwood (L–H) kinetic or adapted for TOC $r = -(dC/dt) = k_r\theta_x = ((k_rKC)/(1 + KC))$ $r_{TOC,0} = [\beta_1[TOC]_0]/[\beta_2 + \beta_3[TOC]_0]$	$C > C(r_{max})$ or TOC > TOC(r_{max})
Mass of catalyst	$\uparrow[TiO_2]$ $\uparrow r$; until a maximum	Optical path length of the photoreactor 25–50 mm; $[TiO_2] = 200–500$ mg L^{-1}.
pH	Influence adsorption Influence particle aggregation	Avoid pH_{zpc}
Temperature	$\uparrow T$. Volatilisation of contaminants and/or water. Adsorption of contaminants disfavoured $\downarrow T$. Desorption of the final product disfavoured	20 °C < T < 80 °C
Radiant flux	$r \propto \Phi^{0.5}$ (high flux) $r \propto \Phi$ (low flux)	≤50 W m^{-2} in the 300–400 nm
Concentration of oxygen	$\uparrow[O_2]$ $\uparrow r$; until a maximum	$\geq p_{O_2} = 0.21$ atm

part of the UV radiation that reaches it, due to its iron content. Borosilicate glass has good transmissive properties in the solar range with a cut-off of about 285 nm [29]. Therefore, such a low-iron-content glass would seem to be the most adequate. Therefore, as both fluoropolymers and glass are valid photoreactor materials, cost becomes an important issue. In large volumes, glass piping could be more expensive than fluoropolymer tubing, but from the perspective of performance, the choice is the material that has the best combination of tensile strength and UV transmittance. On this basis, if a large field is being designed, large collector area means also a considerable number of reactors and, as consequence, high system pressure rating. Thus, fluoropolymer tubes are not the best choice of material since high-pressure is linearly related to thickness and could result in higher cost. A detailed analysis is recommended for any specific design.

2.3.2. Concentrating or non-concentrating collectors

To ensure efficient conversion of incident photons to charge carriers, the appropriate design of a solar reactor is of utmost importance (see Fig. 10). It has been stated that light concentrating systems, such as parabolic-trough reactors, do not necessarily exhibit advantages over non-light concentrating systems [30]. It is well known that in the wavelength range of the solar spectrum that can be used for the excitation of TiO_2, the diffuse and direct portion of the solar radiation reaching the surface of the earth are almost equal [31], as it is also shown in Fig. 10. This means that a light concentrating system cannot employ much more than half of the solar radiation available for catalyst activation.

The original solar photoreactor designs [32] for photochemical applications were based on line-focus parabolic-trough concentrators (PTCs). In part, this was a logical extension of the historical emphasis on trough units for solar thermal applications. Furthermore, PTC technology was relatively mature and existing hardware could be easily modified for photochemical processes. The parabolic-trough collector consists of a structure that supports a reflective concentrating parabolic surface. This structure has one or two motors controlled by a solar tracking system on one or two axes respectively that keep the collector aperture plane perpendicular to the solar rays. In this situation, all the solar radiation available on the aperture plane is reflected and concentrated on the absorber tube that is located at the geometric focal line of the parabolic trough. Parabolic-trough collectors make efficient use of direct solar radiation and, as an additional advantage, the thermal energy collected from the concentrated radiation could simultaneously be used for other applications. The reactor is small, while receiving a large amount of energy per volume unit. The flow is turbulent and volatile compounds do not evaporate, making handling and control of the liquid to be treated simple and cheap. The main disadvantages (also commented in detail in Section 2.2.6) are that the collectors (i) use only direct radiation (as concentrators collect $1/R_C$ of diffuse radiation), (ii) are expensive and (iii) have low optical and quantum efficiencies.

One-sun (non-concentrating) collectors have no moving parts or solar tracking devices. They do not concentrate radiation, so efficiency is not reduced by factors associated with concentration and solar tracking. As there is no concentrating system (with its inherent reflectivity), the optical efficiency is higher than for PTCs. Manufacturing costs are cheaper because their components are simpler, which also means easy, low-cost maintenance. They are able to utilize the diffuse as well as the direct portion of the solar UV-A. An extensive effort in the design of small non-tracking collectors has resulted in the testing of several different non-concentrating solar reactors [30,33]. Although one-sun collector designs possess important advantages, the design of a robust one-sun photoreactor is not trivial, due to the need for weather-resistant and chemically inert ultraviolet-transmitting reactors. In addition, non-concentrating systems require significantly more photoreactor area than concentrating photoreactors and, as a consequence, full-scale systems (normally composed of hundreds of square meters of collectors) must be designed to withstand the operating pressures anticipated for fluid circulation through a large field. In uncovered, non-concentrating systems exposed to the ambient, reactants and catalyst could become contaminated. Very often the chemical inertness of the materials used (to resist corrosion caused by outdoor operation and exposure to solar irradiation) for constructing the non-concentrating collector would be difficult to guarantee.

To design a solar collector for photocatalytic purposes, there is a group of constraints for performing the optimization: (1) the collection of UV radiation, (2) working temperatures as close as possible to ambient temperature in order to avoid the loss of volatile organic compounds, (3) quantum efficiency decreases with light intensity, (4) concentrators collect $1/R_C$ of the available diffuse radiation. As a result of these considerations, the concentration for detoxification applications would be $R_C = 1$. Finally, its construction must be economical and should be efficient, with a low pressure drop. As a consequence, the use of tubular photoreactors has a decisive advantage because of the inherent structural efficiency of tubing. Tubing is also available in a large variety of materials and sizes and is a natural choice for a pressurized fluid system. As already mentioned there is a category of low concentration collectors, called Compound Parabolic Concentrators (CPCs), that are used in thermal applications. For thermal applications they are an interesting option, between parabolic concentrators and static flat systems, since they combine characteristics of each: they concentrate solar radiation, but they conserve the properties of the flat plate collectors, being static and collecting diffuse radiation. Thus they also constitute a good option for solar photochemical applications [34]. CPCs are static collectors with a reflective surface designed to be ideal in the sense of Non-Imaging Optics and can be designed for any given reactor shape. When the absorber has another shape the more precise way of describing them would be CPC type collectors. CPCs were invented in the 60s [35] to achieve solar concentration with static devices, since they were able to concentrate on the receiver all the radiation that arrives within the collector's "angle of acceptance". They do so illuminating the complete perimeter of the receiver, rather than

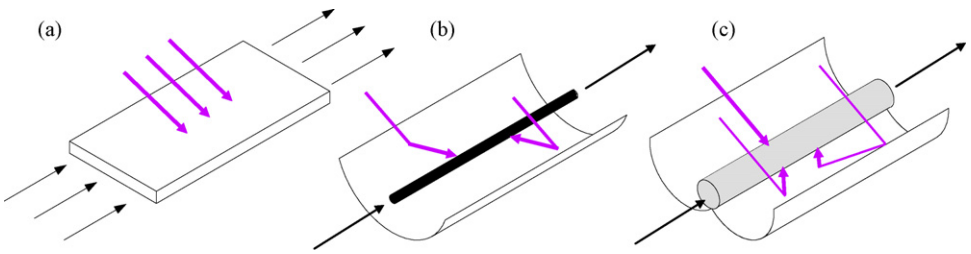

Fig. 10. Design concepts for solar water photocatalytic reactors: (a) non-concentrating (one-sun reactor), (b) concentrating (parabolic trough), and (c) compound parabolic collector.

just the "front" of it, as in conventional flat plates. These concentrating devices have ideal optics, thus maintaining both the advantages of the PTC and static systems. The concentration factor (R_C) of a two dimensional CPC collector is given by Eq. (2.24):

$$R_{C,CPC} = \frac{1}{\sin\theta_a} = \frac{A}{2\pi r} \quad (2.24)$$

The normal values for the semi-angle of acceptance (θ_a), for photocatalytic applications, are between 60 and 90°. This wide angle of acceptance allows the receiver to collect both direct and a large part of the diffuse light ($1/R_C$ of it), with the additional advantage of decreasing errors of both the reflective surface and receiver tube alignment, which become important for achieving a low cost photoreactor. A special case is the one in which $\theta_a = 90°$, whereby $R_C = 1$ (non-concentrating solar system). When this occurs, all the UV radiation that reaches the aperture area of the CPC (direct and diffuse) can be collected and redirected to the reactor. If the CPC is designed for an acceptance angle of +90° to −90°, all incident solar diffuse radiation can be collected (Fig. 11). The light reflected by the CPC is distributed all around the tubular receiver so that almost the entire circumference of the receiver tube is illuminated and the light incident on the photoreactor is the same that would be impinging on a flat plate. CPCs have the advantages of both technologies (PTCs and non-concentrating collectors) and none of the disadvantages so they seem to be the best option for photocatalytic processes based on the use of solar radiation. They can make highly efficient use of both direct and diffuse solar radiation, without the need for solar tracking. There is no evaporation of possible volatile compounds and water does not heat up. They have high optical efficiency, since they make use of almost all the available radiation, and high quantum efficiency, as they do not receive a concentrated flow of photons. Flow also can be easily maintained turbulent inside the tube reactor.

2.3.3. Photocatalyst issues

TiO_2 is the most often used photocatalyst due to its considerable activity, high stability, non-environmental impact and low cost. In water photocatalytic processes, the TiO_2 catalyst is generally applied in the form of powder suspended in slurry. The inconvenience of this kind of approach at large scale is the catalyst-recovering step from the solution at the end of operation. This problem can be solved immobilizing the catalyst on an inert surface, such as glass, quartz, concrete or ceramics [36–38]. This configuration for wastewater treatment has its advantages and disadvantages. Due to the fact that fixation determines mass transfer limitations of pollutants to the surface of the catalyst and also a loss of photocatalytic activity, slurry reactor systems excel the fixed ones with respect to photocatalytic degradation efficiency. The accessibility of the catalytic surface to photons and pollutants significantly influences the degradation rate, being less efficient the fixed ones. In designing fixed bed reactors, one must address uniform distribution of light and mass transfer, which is usually a not trivial.

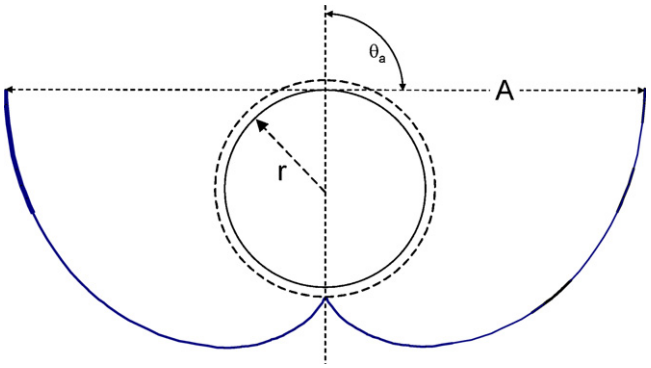

Fig. 11. Schematic drawing of CPC with a semi-angle of acceptance of 90°.

In the case of solar photocatalysis, as the catalyst must be exposed to sunlight and in contact with the pollutant, the support must be configured to efficiently route the pollutant to the illuminated zone and, at the same time, maintain a high flow rate in the water to ensure good mixing without significantly increasing system pressure, which means more power for pumping, and thereby higher operating costs. Also, the same criteria discussed for photoreactor materials must be kept in mind and applied when choosing a support. Several important performance requirements are directly related to the process used for catalyst fixation, such as the durability of the coating, catalyst activity, lifetime, possible fouling of immobilized TiO_2, etc. Studies performed to date have not yet identified a fixed-catalyst system that performs as efficiently as slurry systems. In slurry/suspended systems, compared to an unsupported catalyst, immobilization of TiO_2 results in a reduction in performance. An important direct consequence of this fact is the necessity of increasing the size of necessary solar collector field if similar efficiencies want to be obtained, making the overall system clearly less cost efficient and competitive than slurry systems. In addition to the above, a key question is how long supported catalysts will last in a real stream of water; a short period of activity would mean frequent replacement and, consequently, an important rise in the overall system cost. To the contrary of fixed catalyst configurations, slurry configurations have the advantage of higher throughputs, a low pressure-drop through the reactor and excellent fluid-to-catalyst mass transfer.

However, as said, for slurry reactors, mainly for the continuous ones, the TiO_2 particles have to be separated from the treated water at the exit from the detoxification process. Thus, for the development of the photocatalytic technology, the solid–liquid separation is an extremely important issue. The best possible recovery of TiO_2 particles must be ensured in order to prevent a decrease of the catalyst concentration in the reactor system and to avoid the wash out of TiO_2 particles causing a non-acceptable secondary pollution related to the possible toxicity of nanoparticles [39,40]. The production process of TiO_2 catalysts generates very fine powders. P25 Degussa has an average primary particle size of about 20 nm even if in aqueous media the particles form aggregates more than 10 times bigger (see Fig. 7). In this range of particle size, solid–liquid separation is influenced by interfacial effects of the aggregates rather than by the size of the primary particles. The classical solid–liquid separation processes, such as sedimentation, flotation and membrane filtration may find, in principle, application in the separation of TiO_2 particles from a liquid if the controlling parameters are optimized. From a practical point of view, however, the sedimentation of TiO_2 after pH adjustment or the coagulation with flocculants like basic aluminium chloride is not satisfactory because the sedimentation takes very long, lasting hours, and the supernatant needs to be filtered after the sedimentation step.

As commented in Section 2.2.4 the best choice is change in pH of suspensions to the pH_{zpc}. Furthermore, the pH of the suspensions after TiO_2 sedimentation by charge neutralization is within the permitted disposal range for treated water. The small remaining fraction of catalyst can easily be recovered by membrane microfiltration. Application of the above concepts and sedimentation of a TiO_2 suspension after the solar water photocatalytic process can be described as follows. When the photocatalysis treatment is completed, the suspensions are stored in a settling tank where they undergo sedimentation after pH adjustment. Aggregation of the particles may be visually observed and the weight of the clusters formed makes them settle very fast. In

comparison with spontaneous sedimentation, induced sedimentation takes a shorter time (less than 5 h) to reduce the earliest concentration of particles in suspension to less than 3% of the initial concentration. Fig. 12 shows the evolution of absorbance (800 nm, therefore only turbidity of the suspension is measured) of a 0.3 g L^{-1} suspension during a sedimentation. After 5 storage hours almost all the particles remained in the bottom of the tank. The last data (1 complete day) shows a nearly negligible catalyst concentration (8 mg L^{-1}). This small remaining fraction of catalyst can easily be recovered by microfiltration (Fig. 12 inset). As it is shown in the inset of Fig. 12, no catalysts remained in the outlet stream of microfiltration process, as the absence of the specific UV absorption spectrum of TiO_2 (see TiO_2 absorption spectrum in Fig. 3).

Membrane filtration of TiO_2 offers advantages and disadvantages [41]. It is purely a physical separation process, which does not involve a phase change or interphase mass transfer, and may be used as a single step for the complete recovery of TiO_2 particles from liquids. The major problems, when membrane separation is applied to powder photocatalyst recovery, are the great membrane flux decline and the rapid membrane fouling. In the field of membrane separation, microfiltration is a solid–liquid separation process useful when colloids and fine particles in the 0.1–5 μm range are involved. In comparison with ultrafiltration, microfiltration offers the further advantages of needing relatively low transmembrane pressure for operation (usually <300 kPa) and of providing a relatively high filtration rate with a consequent reduction of equipment and operating costs. The microfiltration separation process allows the TiO_2 be easily separated, recovered and reused; more significantly, it is efficient to maintain high flux of membranes.

An approach to immobilize photocatalytic powders is to combine a slurry with membrane filtration; in this system, membranes are used as a separating layer to retain the catalyst. A drawback of membrane reactors is that the use of photocatalytic powders determines that the reactants must diffuse to the catalyst surface before photocatalytic reactions can occur. This diffusion process is relatively slow and so it is likely to be a rate-determining step, especially for the case where reactants at low concentrations must be degraded. In order to solve this problem, a recent strategy was to utilize photocatalytic membranes with pores of several nano-meters in which the photocatalyst is capable not only of performing selective permeation of organics but also of producing an oxidized permeate stream. In this configuration, oxidation by $HO^{\bullet}$ radicals occurs both on the external surface of membrane and inside the pores, while reactants are permeating in a one-pass flow.

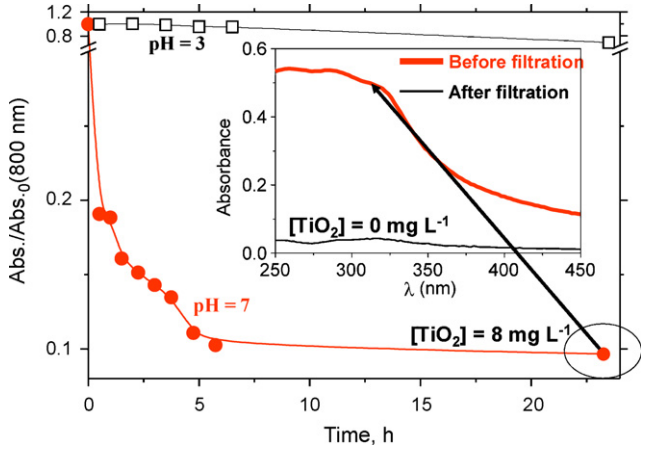

Fig. 12. Absorbance of P-25 catalyst suspension (300 mg L^{-1}) during sedimentation. In the inset is shown absorbance spectra of the water after sedimentation process (TiO_2 = 8 mg L^{-1}) and after microfiltration (TiO_2 = 0 mg L^{-1}).

The main advantage of membrane photoreactors is that this configuration allows one to minimize the mass transfer resistances between the bulk of the fluid and the semiconductor surface.

A review work from Ollis [42] explores the coupling between photocatalysis (PC) and microfiltration (MF), ultrafiltration (UF) and reverse osmosis (RO). Four configurations are discussed: (1) PC + MF for catalyst slurry recycle, (2) PC + UF for catalyst slurry and reactant recycle, (3) immobilized PC and UF/RO for reactant recycle, and (4) immobilized PC on UF/RO membrane for membrane self-cleaning. The simplest configuration is the use of a membrane filtration modulus in a recirculation loop with the conventional photoreactor. Another possibility is introducing the membrane system inside the photoreactor, being the permeate the outlet of the system. Finally, the third approach is transforming a membrane modulus into a photoreactor by including the light source into the feed chamber. The two first configurations are more indicate for the use of catalyst suspensions, whereas the latter is more likely to be applied when the catalytic material is directly immobilized onto the membrane. The main problems related with the use of photocatalytic reactors arise with the great decrease in the permeate flux produce by membrane fouling. According to Mozia et al. [43], a way of reducing this fouling is the substitution of pressure driven microfiltration and nanofiltration membranes by the use of distillation membranes. Although the literature review is encouraging with respect to plausibility, the shortage of examples indicates a need for substantial effort to fully exploit the suggested possibilities for process development.

2.4. Target contaminants and applications

In general, the types of contaminants that have been degraded include a large number of organics. Until now, the absence of total mineralization has been observed only in s-triazine herbicides, for which the final product obtained was essentially 1,3,5-triazine-2,4,6, trihydroxy (cyanuric acid), which is, fortunately, nontoxic. Special attention has recently been given to the so-called "emerging contaminants", mostly unregulated compounds that may be candidates for future regulation depending on research on their potential effects on health and monitoring data regarding their occurrence. Particularly relevant examples of such emerging compounds are those which do not need to persist in the environment to cause a negative effect, because their high transformation/removal rates can be compensated by their continuous introduction into the environment [44]. The solar photocatalytic degradation of these new environmental contaminants (pharmaceuticals, antibiotics, analgesics, steroids, hormones, MTBE, cyanotoxins, etc.; and their hydrolysis/photolysis reaction intermediates) many of them until recently unknown, is the focus of much research [45].

In photocatalysis, transformation of the parent organic compound is desirable in order to eliminate its toxicity and persistence, but the principal objective is to mineralize all pollutants. For chlorinated molecules, Cl^- ions are easily released in the solution and are the first of the ions appearing during the photocatalytic degradation. This could be interesting in a process, where photocatalysis would be associated with a biological treatment (see Section 4.5.3) which is generally not efficient for chlorinated compounds. Nitrogen-containing molecules are mineralized mostly into NO_3^- and NH_4^+. Ammonium ions are relatively stable, and the proportion depends mainly on the oxidation stage of organic nitrogen and irradiation time [46]. By comparing the sequence of appearance, NH_4^+ appears as the primary product with respect to NO_3^- in the case of amine compounds. The nitrogen atoms in the amino-groups can lead to NH_4^+ ions by successive attacks by hydrogen-containing species. The total amount of nitrogen-containing ions present in the

solution at the end of the experiments is usually lower than that expected from stoichiometry indicating that N-containing species remain adsorbed in the photocatalyst surface or most probably, that significant quantities of N_2 and/or NH_3 have been produced and transferred to the gas-phase. The formation of N_2 in azo bounds can be accounted for by the same processes responsible for NH_4^+ formation [47]. When nitrogen is present in the −3 state as in amino groups or in pyrazoline ring, it spontaneously evolves as NH_4^+ cations with the same oxidation degree, before being subsequently and slowly oxidized into nitrate. In the azo bonds each nitrogen atom is in its +1 oxidation degree. This oxidation degree favours the evolution of gaseous dinitrogen by the two step reduction process expressed in Eqs. (2.27)–(28). N_2 evolution constitutes the ideal case for a decontamination reaction involving totally innocuous nitrogen-containing final product:

$$R - NH_2 + H^\bullet \rightarrow R^\bullet + NH_3 \quad (2.25)$$

$$NH_3 + H^+ \rightarrow NH_4^+ \quad (2.26)$$

$$R - N = N - R' + H^\bullet \rightarrow R - N = N^\bullet + R'H \quad (2.27)$$

$$R - N = N^\bullet \rightarrow R^\bullet + N{\equiv}N \quad (2.28)$$

Organophosphorous contaminants produce phosphate ions. However, in the pH range used (usually >4), phosphate ions remain adsorbed on TiO_2. This strong adsorption somewhat inhibits the reaction rate, though it is still acceptable. In photo-Fenton, phosphate sequestrates iron forming the corresponding non-soluble salt and retarding the reaction rate. Therefore, more iron is necessary when water containing phosphates is treated by photo-Fenton. Contaminants containing sulfur atoms are mineralized into sulphate ions. The release of SO_4^{2-} can be accounted by an initial attack by a photo-induced $^\bullet$OH radical. In all the studies the formation of SO_4^{2-} was always observed and in most cases its stoichiometric formation was found in the final steps of the photoreaction when organic intermediates were still present. Initial rate was high indicating that SO_4^{2-} ions are initial products, directly resulting from the initial attack on the sulfonyl group. Non-stoichiometric formation of sulphate ions is usually explained by a strong adsorption on the photocatalyst surface. This strong adsorption could partially inhibit the reaction rate which, however, remains acceptable. Sulphate, chloride and phosphate ions, especially at concentrations greater than 1 mM can reduce the rate due to the competitive adsorption at the photoactivated reaction sites.

The effectiveness of degradation is not demonstrated only because the entire initial compound is decomposed. Reactants and products might be lost (evaporation, adsorption on reactor components, etc.) which introduces uncertainty in results. The mineralization rate is determined by monitoring inorganic compounds, such as CO_2, Cl^-, SO_4^{2-}, NO_3^-, PO_4^{3-}, etc. When organics decompose, a stoichiometric increase in the concentration of inorganic anions is produced in the water treated and very often an increase in the concentration of hydrogen ions (decrease in pH). For this reason, the analysis of these two products of the reaction is of interest for the final mass balance. However, the decrease in pH is not a very reliable parameter of this balance because it is influenced by other processes which take place in the medium: the effect of the TiO_2 suspension, the formation of CO_2 and intermediates, etc.

Treatment of industrial wastewater seems to be one of the most promising fields of application of solar photocatalysis. There is no general rule at all, each case being completely different [48]. Consequently, preliminary research is always required to assess potential pollutant treatments and optimize the best option for any specific problem, on a nearly case-by-case basis. In general, the types of compounds which have been degraded include alkanes, haloalkanes, aliphatic alcohols, carboxylic acids, alkenes, aromatics, haloaromatics, polymers, surfactants, herbicides, pesticides and dyes. Eq. (2.29) generally holds true for an organic compound of general formula $C_nH_mO_p$:

$$C_nH_mO_p + \left(\frac{m-2p}{4} + n\right)O_2 \rightarrow nCO_2 + \frac{m}{2}H_2O \quad (2.29)$$

The oxidation of carbon atoms into CO_2 is relatively easy. In general, at low reactant levels or for compounds which do not form important intermediates, complete mineralization and reactant disappearance proceed with similar half lives, but at higher reactant levels where important intermediates occur, mineralization is slower than the degradation of the parent compound. However, before TiO_2 photocatalytic treatment can be proposed as a general and trouble free method, it is required that the chemistry of various classes of pollutants under these conditions is known in detail. Since the chemistry of such processes is complex, careful analytical monitoring using different techniques is essential in order to control all transformation steps, to identify harmful intermediates and to understand and interpret the reaction mechanism. The assessment of pollutant disappearance in the early steps is not sufficient to ensure the absence of residual products because the heterogeneous photocatalytic treatment may give rise to a variety of organic intermediates which can themselves be toxic, and in some cases, more persistent than the original substrate [49].

From an analytical viewpoint, the task that entails the most difficulty is, without doubt, qualitative and quantitative evaluation of the intermediates or degradation products (DPs). As hydroxyl radicals are not selective in their attacks, numerous DPs form on the path toward complete mineralization. There are five main types of DPs:

- Hydroxylated and dehalogenated products, the latter of these derived from the loss of the halogenated substitute in the original contaminant, if it had one.
- Products from the oxidation of the alkali chain, if it had one.
- Products derived from the opening of the aromatic ring in aromatic contaminants.
- Products of decarboxylation.
- Products of isomerization and cyclation.

The chemical analysis of these complex reaction mixtures is difficult, so that in the majority of the cases, not much attention is paid to their identification and analytical evaluation is limited to tracing the disappearance of the initial pollutant, combined with following decrease in TOC and the appearance of inorganic ions. Thus, the kinetic degradation of contaminants and the mineralization rate during the process are evaluated. However, a greater knowledge of the DPs originated would be necessary. It may be observed in Fig. 13 that most of the DPs with high molecular weight appear after exposure to sunlight and reach their maximum concentration at short treatment time. From here on, they begin to decrease and carboxylic acids appear. Until now, the analyses of fragments resulting from the degradation of the aromatic ring have revealed formation of aliphatics (organic acids and other hydroxylated compounds), which explains why total mineralization takes much longer than dearomatization, as mineralization of aliphatics by photocatalysis is the slowest step [47,50].

2.5. Analytical and toxicological tools

The basic parameters (necessary for relevant information on process kinetics and assure consistent results) to be evaluated are:

- Mineralization, as described below.

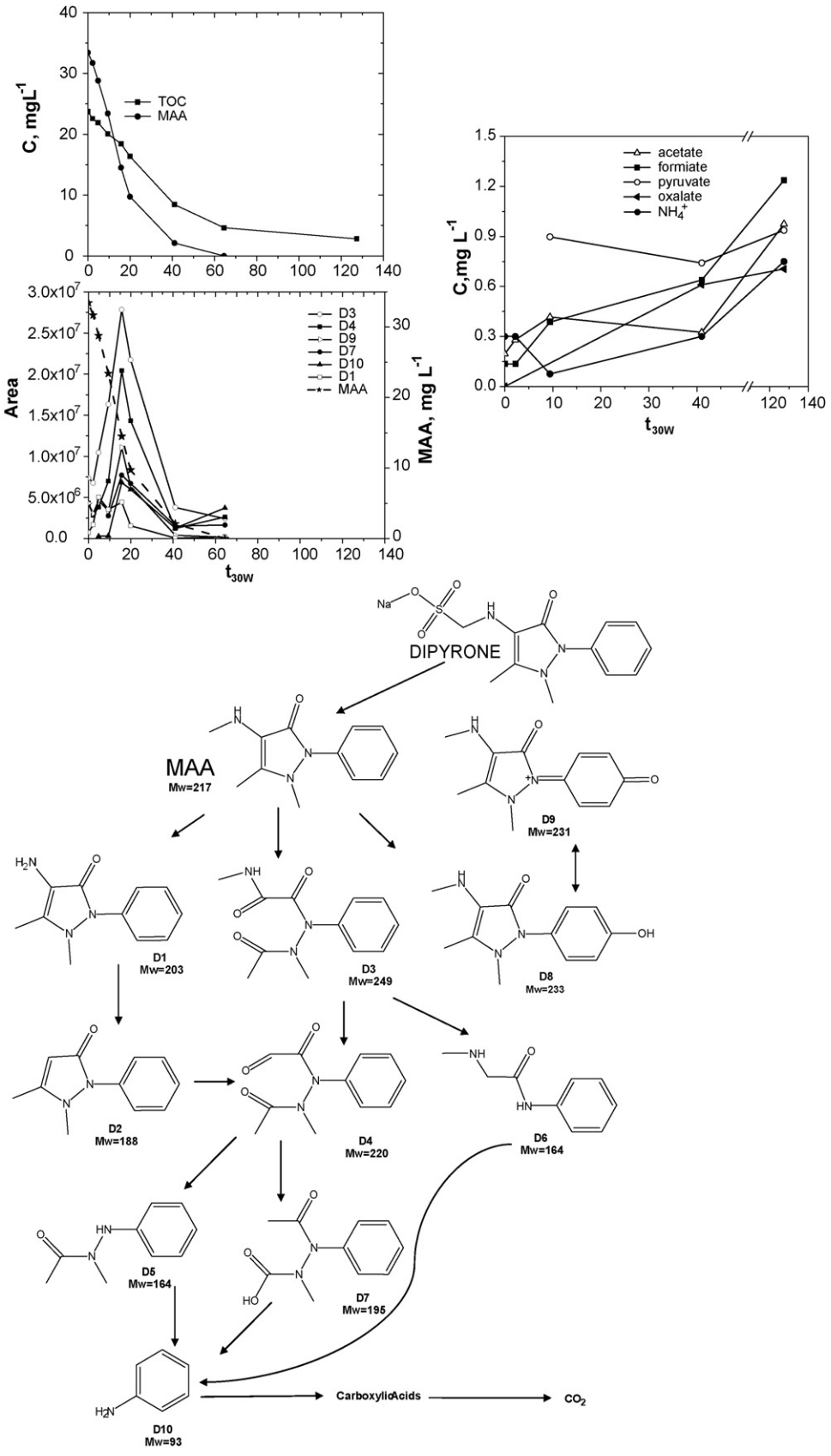

Fig. 13. (a) Dipyrone degradation (dipyrone is readily hydrolysed to 4-methylaminoantipyrine) kinetics during solar photocatalysis, kinetics of the most important DPs formed, evolution of the main carboxylic acids and inorganic species detected. (b) Degradation pathway.

- Concentration of the original pollutant. Use of Liquid Chromatography with UV detection (LC-UV) is recommended for this as the most reliable and versatile technique for analysis of organic pollutants dissolved in water. A commonly used method of measuring the original pollutant is UV–visible spectroscopy. However, as the components in the reaction mixture are not separated before their determination, the intermediates generated during degradation of an organic pollutant can easily interfere with its measurement, making results inconsistent.
- Concentration of inorganic ions. In this case Liquid Chromatography with electric conductivity detection (LC-IC) is recommended. This analytical method also makes it possible to determine low-molecular-weight carboxylic acids, which assists in establishing the degradation pathway of the compounds treated, since these acids are usually the last step before pollutant mineralization. The most common are formic, acetic, oxalic, glycolic, propanoic, and pyruvic acid, etc.

A complete mass balance of photocatalytic degradation processes is imperative and is generally reported in studies that envisage application of photocatalytic water treatment. Formation of CO_2 can be followed using headspace gas chromatography with a TCD detector after acidification of the solution. Another method for the kinetics determination of CO_2 formation consists on flushing by oxygen the CO_2 produced, into a flask containing a $Ba(OH)_2$ solution. The conductivity of the solution is followed by a conductivity meter. CO_2 precipitates as $BaCO_3$, thus decreasing the ionic conductivity in water. However, in the presence of real wastewaters the monitoring of inorganic ions and CO_2 gives only a general estimation on the correct functioning of the treatment, but does not provide information on the real decay of the contaminant. In such cases the determination of total organic carbon (TOC) and/or the measurement of the chemical oxygen demand (COD) of the irradiated solution are generally used for monitoring the mineralization. It is appropriate to analyze the chemical oxygen demand (COD) when CO_2 or TOC determination is unavailable, since it is a cheaper method. However, the information that it provides on mineralization of the compounds is not as reliable as TOC, because COD analyses are usually not accurate for pollutants concentrations in the order of mg/L (very common in photocatalysis) and because oxidizable inorganic species cannot be distinguished from the organic pollutants.

Therefore, the analysis of reaction mixtures containing one or several contaminants and their DPs requires analytical methods that enable the separation and identification of the large number of compounds, with very different chemical properties present in a wide interval of concentrations [51–60]. In practice, this is possible through the use of sophisticated analytical tools, such as gas chromatography coupled with high-resolution mass spectrometry (GC-HRMS); nuclear magnetic resonance spectroscopy (NMR); Fourier transformation infrared spectroscopy (FT-IR); liquid chromatography coupled to mass spectrometry (LC-MS/MS), etc. These methods or combinations of them can confirm the identity of the DPs present in a reaction mixture, however, they require specific expertise and the process is usually time-consuming. In the last 10 years, analytical instrumentation and techniques have undergone rapid development. Very sophisticated equipment and techniques, especially in the field of GC-MS and LC-MS, have been developed to enable efficient determination of organic compounds. Gas chromatography coupled to mass spectrometry (GC-MS) has doubtlessly been the most applied technique, since it offers important advantages in the analysis of complex samples and its use is relatively simple and there is established experience in the field.

Gas chromatography with atomic emissions detector (AED) has also demonstrated to be a very useful tool for the identification of DPs in photocatalytic processes [53]. With GC-AED, samples can be analysed by element to identify peaks of primary interest. The calculation of empirical formulas with AED also simplifies the spectral mass interpretation of unknown compounds. Thanks to Compound-Independent Calibration, the DPs can be quantified without the need of the corresponding analytical standard. The most important advantages of the methods based on GC-MS are:

- Highly sensitive and efficient separation, avoiding overlapping of compounds with similar structures.
- High potential for identification, thanks to abundant structural information provided by the mass spectra.
- Possibility of using commercial spectra libraries that facilitate the identification of unknown DPs.

In spite of the doubtless potential of the GC-MS techniques for identification of reaction intermediates, there are limitations inherent in the technique, such as its limited capacity for analysing very polar, poorly volatile or thermally unstable compounds and especially the difficulty in quantifying DPs in the absence of commercial standards.

Liquid chromatography coupled to mass spectrometry (LC-MS) is progressively gaining acceptance, since it presents several advantages over gas chromatography, some of which are very important for identification of reaction intermediates in AOPs: (i) direct analysis of aqueous samples avoids possible loss of polar DPs during the extraction process; (ii) compounds that are highly polar, not very volatile and/or thermally labile are easier to analyse; little or no cleaning of the system is necessary between samples. LC-MS techniques have achieved identification of DPs in a wide range of polarities. The LC-MS Atmospheric Pressure Ionisation interfaces, such as Atmospheric Pressure Chemical Ionisation (APCI) and electrospray (ES), provide structural information. This enables identification of very polar and thermolabile compounds as well as direct analysis of aqueous samples, thus avoiding possible modification of their concentration during extraction. Furthermore, time-of-flight analysis (TOF-MS) with electrospray ionization (ESI) has gained popularity due to its sensitivity, theoretically unlimited mass range, high mass resolution and capability for highly accurate mass determination [61].

Although, techniques for direct injection of aqueous samples have recently begun to be applied in liquid and gas chromatography, the fact is that to date, the determination of the degradation products present in samples of water treated by photocatalysis has involved the application of an extraction step prior to analysis. This extraction enabled pre-concentration of the samples between, so that trace compounds present at concentrations of less than μg/L are detectable. However, to develop an adequate method of extraction, able to recover a high number of compounds with chemical properties that may be very different from each other, is not simple.

The traditional method applied, liquid–liquid extraction (LLE), has serious limitations that include loss of polar compounds in the aqueous phase and strong interference by the matrix, since the technique is not very selective. From a practical point of view, LLE also has important disadvantages, such as the difficulty in breaking up emulsions that are formed during the extraction and difficulty in its automation. Therefore, solid phase extraction techniques (SPE) have been gaining acceptance in recent years [62,63]. These more selective techniques cause less interference by the matrix, which is an important advantage for subsequent analysis. On the other hand, there is a wide range of adsorbents on the market such as alkyl-bonded silica (C-18), porous polymers (styrene-divinylbenzene, PRP-1 and PLRP-S) and modified carbon (PGC). These materials have different properties and their behaviour in break-up capacity and sample volume, vary depending on the compounds to be analysed. This enables appropriate adsorbents to be selected for determining the analytes in a wider range of polarities.

Although C-18 is the material most used in extracting aqueous samples, its application to the study of intermediates in reaction mixtures has some limitations, such as (i) limited capacity for retaining high-polarity compounds and (ii) instability of the adsorbent at pH below 2 and above 10. Both aspects represent a serious problem for the extraction of reaction intermediates generated in degradation processes since these often have a higher polarity than the initial pollutants and may be ionised. The advantage of the new polymeric materials over C-18 materials is that they can be used in a wider pH interval without decomposing the adsorbent and have a greater capacity for retaining polar compounds.

An additional advantage of SPE is the possibility of designing sequential extraction schemes using different adsorbents and modifying the pH of the sample appropriately. Application of this technique allows simultaneous extraction of a large number of compounds with very different polarities. For example, a possible scheme would consist of initially extracting with C-18 at pH 7, to recover neutral hydrophobic compounds. Afterwards, the volume eluted by C-18 phase at pH 7 can be passed through a polymeric adsorbent that enables compounds with intermediate polarity to be retained. During the subsequent third and fourth steps, the samples can be acidified to pH 4.5 and 2.5, respectively, to extract the majority of the acid compounds with a polymeric or carbon adsorbent.

2.5.1. Toxicological tools

To shorten phototreatment time is of major concern for the cost and energy efficiency benefits of the overall treatment process (see also Section 4.5). Therefore, to investigate toxicity could be considered as a suitable overall indicator capable of giving information on the evolution of biocompatibility of the water solution contaminated with organic pollutants during the photo-treatment in order to dispose to the environment or promote biotreatment. But due to the complexity of the studied process and the specificity and sensitivity of the toxicity test, this approach has to be considered and discussed with caution. Besides, a more detailed study of DPs as well as other inorganic species produced in addition with toxicity analyses should be achieved in order to improve the knowledge of the implicated degradation pathways and molecular interactions. Considering the removal of the initial contaminants on one hand and the mineralization of the organic carbon on the other hand, two main categories of behaviours can be outlined. When the DPs demineralize shortly, toxicity usually decreases gradually in the course of the photodegradation. But when the reaction intermediates degradation takes a long time (after disappearance of the target contaminants), the level of toxicity is not predictable. However in the end, the toxicity tends to decrease.

Toxicity assessment of a chemical using a single species test reflects the sensitivity of that test only; it may overestimate or underestimate the potential toxicity for that particular substance. Accordingly, recent research has focused on the development of representative, cost-effective, and quantitative test bioassays, which can detect different effects using a variety of endpoints [64]. However, such a complete battery of bioassays for mixed chemical compounds is not yet feasible, in particular for industrial effluents. Furthermore, potential synergistic or antagonist effects may occur and can be problematic to study.

Fig. 14 shows the evolution of representative toxicity curves (% inhibition) for three bioassays performed during solar photocatalytic experiments. Chemicals added to the water for photocatalysis were removed prior to bioassays. These are not the results of a single toxic response, because in the experiments they are affected not only by the parent compound, but also by the presence of other intermediate compounds produced during its photodegradation. *Daphnia magna* was biochemically the most complex

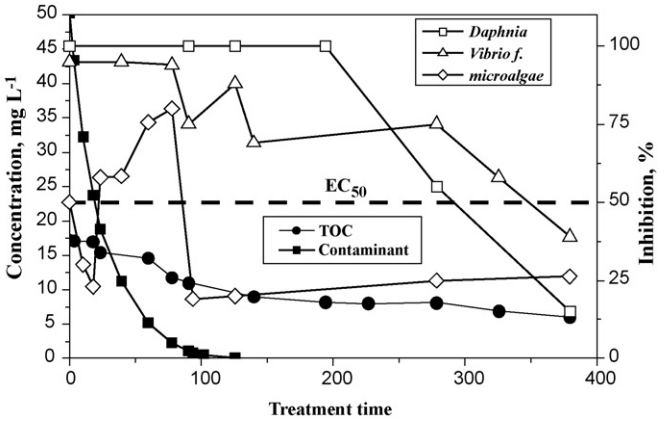

Fig. 14. Degradation mineralization and evolution of toxicity (right axis) during a photocatalytic treatment in a pilot plant.

test system and also the most sensitive. *Selenastrum capricornotum* (microalgae) behaviour is different, as toxicity increases during the photocatalytic tests and decreases again to below EC_{50} when the parent compound has almost disappeared. So toxicity is clearly related to the intermediates generated during photooxidation. At a TOC of 5 mg/L, all bioassays performed showed inhibition below 50%. *Daphnia magna* showed inhibition over 50% until TOC is less than 7.5 mg/L. But *Selenastrum capricornotum* and *Vibrio fischeri* showed different behaviour. Therefore, it may be concluded that different intermediates formed by both treatments show different toxicities for the two microorganisms. This means that TOC alone is an inadequate parameter for determining the efficiency of different photocatalytic methods, because for the same TOC, the toxicity is very different.

Toxicity could also be an alternative indicator for biodegradation assessment of partially phototreated wastewaters [65]. Overall, acute toxicity testing has been shown to represent dynamics and efficiency of phototreatment. Very often toxicity changes continuously during the treatment, and therefore, toxicity evaluation is not a suitable way to determine the moment when biodegradability is most enhanced. However, reduced toxicity results are indicative of an extended biodegradability achieved during the process. These assays must therefore be complemented with biodegradability studies. Thus even if it cannot provide a reliable biodegradability assessment by itself, toxicity can help identifying samples to be tested by biodegradability assessment methods (see also Section 4.5.3), which are quite time-consuming.

2.6. Solar photocatalytic treatment plants

The first outdoor engineering-scale reactor developed was a converted solar thermal parabolic-trough collector in which the absorber/glazing-tube combination had been replaced by a simple Pyrex glass tube through which contaminated water could flow [66]. Since that time, research all over the world has advanced a number of reactor concepts and designs, including concentrating and non-concentrating reactors [67]. The design procedure for a solar photocatalytic system requires the selection of a reactor, catalyst operating mode (slurry or fixed matrix), reactor-field configuration (series or parallel), treatment-system mode (once-through or batch), flow rate, pressure drop, pretreatment, catalyst and oxidant loading method, pH control, etc. Usually, a photocatalytic plant is constructed with several solar collectors. All the modules are connected in series or parallel, but with valves that permit to bypass any number of them.

Centrifugal pumps with an electric motor (calculated to provide sufficient flow when the maximum length of the system is used)

have to be installed to move the treatment water through the reactor. Either a flow-rate control loop made up of a flow meter connected to a controller, which in turn governs an automatic electric valve, or an electric pump with a speed controller has to be installed to regulate the flow to the rate desired. The most important sensors required for the system are temperature, pressure and dissolved oxygen (at least in the reactor outlet). Other sensors, such as pH, selective electrodes, etc., could be useful depending on the type of wastewater to be treated. A UV radiation sensor must be placed in a position where the solar UV light reaching the photoreactor can be measured, permitting the evaluation of the incident radiation as a function of hour of the day, clouds, atmospheric or other environmental variations. Solar photocatalytic plants are frequently operated in a recirculating batch mode. The fluid is continuously pumped between a reactor zone and a tank in which no reaction occurs, until the desired degradation is achieved. The systems are operated in a discontinuous manner by recirculating the wastewater with an intermediate reservoir tank and centrifugal pump.

But during the last years more installations have been constructed, mainly based on non-concentrating collectors since parabolic-trough concentrators are not the best option, as stated in Section 2.3.2. Dillert et al. have treated biologically pretreated industrial wastewaters from the factories Wolfsburg (Germany) and Taubaté (Brazil) of the Volkswagen AG in laboratory and bench-scale experiments. The results of the experiments were so promising, that a pilot plant was installed in the Wolfsburg factory during the summer 1998. The flowsheet of a more recent version of this pilot plant which was installed in 2000 has been recently published by Bahnemann [33]. This pilot plant which is operated in a recycle batch mode consists of 12 double-skin sheet photoreactors (DSSRs, manufactured by Solacryl) with a total irradiated area of 27.6 m^2. The water coming from the biological treatment plant is pumped into the tank and mixed with a catalyst slurry. The solar photocatalytic treatment starts after the tank has been filled. The suspension recycles between the tank and the DSSRs for 8–11 h during the daytime. After the desired treatment time of the solar photocatalytic process the suspension is pumped out of the reactors into the tank. The photocatalyst is allowed to settle during the night. After this sedimentation period, the supernatant liquid is pumped out of the tank and the treatment cycle can be started again by filling the tank with a new batch of wastewater. More than 50% of the organic pollutants initially present in the mixed water inside the pilot plant could thus be degraded within 8–11 h of illumination. In general, the total mass of the degraded contaminants was found to depend on the initial pollutant concentration, the time of illumination, and, in particular, on the solar UV energy flux density.

In 1997 Freudenhammer et al. reported their results from a pilot study using TFFBR (Thin Film Fixed Bed Reactor) reactors which was performed in various Mediterranean countries and showed that biologically pretreated textile wastewater can be cleaned by solar photocatalysis with a maximum degradation rate of 3 g COD h^{-1} m^{-2}. It was concluded that photocatalysis should be a suitable technology as the final stage of purification of biologically or physically pretreated wastewater in particular in sun-rich areas. Based on these results, a pilot plant, financed by the European Commission, has been built at the site of a textile factory in Tunisia (Menzel Temime). The TFFBR was chosen because previous studies showed sufficient degradation rates with the selected textile wastewater in combination with its simple, low cost construction and the low energy consumption. However, to integrate results obtained with suspended catalysts showing in some cases a higher efficiency than the fixed system, the possibility of using suspended catalysts has also been considered. The pilot plant and the flow chart have been published recently [68]. Two TFFBR reactors with a width of 2.5 m and a length of 10 m each, corresponding to a total illuminated area of 50 m^2, were built in concrete and are oriented to the south with an inclination angle of 20°.

Under the "SOLARDETOX" project (Solar Detoxification Technology for the Treatment of Industrial Non-Biodegradable Persistent Chlorinated Water Contaminants), a Consortium (coordinated by Plataforma Solar de Almería, Spain) has been formed in Europe for the development and marketing of solar detoxification treatments for recalcitrant water contaminants. The main goal (financed by the EC-DGXII through the Brite Euram III Program, 1997–2000) was to develop a commercial non-concentrating solar detoxification system using the compound parabolic collector technology (CPC), with a concentration ratio = 1. Field demonstration was intended to identify any pre or post-processing requirements, potential operating problems, and capital and operating costs. Based on accumulated experience in pilot plant design, construction and testing [29], a full-size demonstration plant was erected. This plant was designed to treat 1 m^3 of water contaminated with 100 m^2 of collector aperture area (see Fig. 15). The concentrated TiO_2 slurry and the air necessary for the reaction are injected in the circuit. Once the water is detoxified, the entire volume leaves to the sedimentation tank and the system is filled

Fig. 15. Photographs of solar detoxification demonstration plant constructed in "SOLARDETOX" project at HIDROCEN (Madrid, Spain). Left: TiO_2 separation system. Right: compound parabolic collector.

with more wastewater for another batch. Meanwhile, the detoxified water and the TiO_2 in the sedimentation tank undergo pH adjustment to achieve fast sedimentation of the catalyst. The concentrated catalyst slurry is transferred from the bottom of the sedimentation tank to another smaller tank from which the catalyst enters the photoreactor.

Recently (2004) a new CPC-based plant has been installed. In the area of El Ejido, a town in the province of Almería in southern Spain, intensive agriculture in 400 km^2 of greenhouses consumes approximately 2.0 million plastic bottles of pesticide per year. So far, these empty plastic bottles have simply been discarded. The solution is to selectively collect these containers for recycling. But before the plastic can be recycled, it must be washed and the water used for it becomes polluted by the pesticides. This water must be treated before it is discharged. It is in the detoxification of this water that Solar Photocatalysis intervenes. The water will still contain solid waste, which is eliminated by a rough screen and then to another tank where reactants needed for the photocatalytic reaction are added. The plant has been constructed to treat 1.6 m^3 of water contaminated with 150 m^2 of collector aperture area. Operation is fully automatic and maintenance requirements are minimum. The size of the solar field was calculated according to Eq. (2.30), where V_{tot} is the total yearly volume of water to be treated, T_s is the number of hours of operation yearly, $I_{G,UV}$ is the yearly average local global solar UV irradiation (sunrise to sunset) and Q is the solar energy necessary to degrade the pesticides per unit of solar reactor volume obtained from preliminary pilot plant tests (see Eq. (2.7)):

$$A = \frac{QV_{tot}}{T_s I_{G,UV}} \tag{2.30}$$

The last step in solar photocatalytic treatment plants has been a hybrid solar photocatalytic-biological plant with a 4 m^3 daily treatment capacity. It consists of a solar photo-Fenton (see Section 4) reactor with 100 m^2 of CPCs, and an aerobic biological treatment plant based on an immobilised-biomass (plastic pall rings) activated-sludge reactor (IBR, 1 m^3). CPC photoreactors illuminate a volume of 1260 L (glass tubes), with a recirculation tank that can hold up to 3 m^3. The IBR, filled with 700 L of Pall rings, is connected to a conditioner tank (2 m^3) in a closed loop. The water discharged from the solar photo-Fenton reactor must be neutralized, and may need conditioning (removal of Fe^{+3} and/or H_2O_2) before it is fed to the biological process, so there is a neutralisation tank (5 m^3) as the first step in the biological process. This plant treats a highly saline industrial wastewater containing around 600 mg L^{-1} of a non-biodegradable compound (α-methylphenylglycine) and 400–700 mg L^{-1} total organic carbon. The purpose of this treatment strategy was to achieve sufficient biodegradability of the photo-oxidized effluent to allow its discharge into the IBR. This two-step field treatment was operated in semi-continuous mode (solar photo-Fenton treatment in batch mode and the biological process in continuous mode), and overall efficiency was in the range of 85–95%, of which 50–65% were removed in the solar photo-Fenton treatment and 20–45% in the IBR [69].

3. Enhancing solar semiconductor photocatalysis

3.1. Introduction

Using the semiconductor photocatalysis to remediate the problem of chemical wastes is a promising approach and has attracted extensive attention. TiO_2 is a widely investigated photocatalyst and has been found to be capable of decomposing various kinds of organic and inorganic wastes in both liquid and gas phases because of its excellent functionality, long-term stability and non-toxicity. Most of these investigations have been carried out under ultraviolet (UV) light, because TiO_2 photocatalyst shows relatively high activity and chemical stability under UV light, which exceed the band-gap energy of 3.0 or 3.2 eV in the rutile or anatase crystalline phase, respectively. The process presents recognized advantages, such as the low price and the possibility to combine the process with biological decontamination methods. However, only 5% of the solar spectrum at the earth surface can be utilized.

On the other hand, one practical problem in using TiO_2 as a photocatalyst is electron/hole recombination, which, in the absence of proper electron acceptors, is extremely inefficient and thus represents a major energy-wasting step as well as limiting the achievement of a high quantum yield. Oxygen has been chosen in most of the applications for this purpose, although its role is not only related to electron scavenging (see Section 2.2.7). But with only dissolved oxygen as an oxidant, low mineralization photoefficiencies (production of CO_2) are usually obtained. Therefore, several approaches in order to improve the photocatalysis efficiency of TiO_2 have been carried out:

- Use of chemical oxidants.
- Use of doped and modified TiO_2.
- Coupling of TiO_2 photocatalysis with photosensitizers.
- Coupling of semiconductor photocatalysis with other AOPs.

3.2. Use of chemical oxidants

One strategy for inhibiting e^-/h^+ recombination is to add other (irreversible) electron acceptors to the reaction. The addition of other oxidising species could have several different effects [70]:

- Increase the number of trapped e^- in the e^-/h^+ pairs and, consequently, avoid recombination.
- Generate more $^{\bullet}OH$ and other oxidising species.
- Increase the oxidation rate of intermediate compounds.
- Avoid problems caused by a low O_2 concentration/O_2 starvation.

It must be mentioned here that in highly toxic waste water where degradation of organic pollutants is the major concern, the addition of an inorganic anion to enhance the organic degradation rate may often be justified. For better results, these additives should fulfill the following criteria: dissociate into harmless by-products and lead to the formation of $^{\bullet}OH$ or other oxidising agents. There is another advantage related to the use of this type of oxidant when solar energy is the photon source. Although scientific research on photocatalytic detoxification has been conducted for at least the last three decades, industrial/commercial applications, engineering systems and engineering design methodologies have only been developed recently. In this type of installation, the photoreactor is by far the most expensive component and a barrier to commercialisation. The increase of the photocatalytic reaction rate with these additives would decrease photoreactor dimensions and overall costs proportionally.

3.2.1. Hydrogen peroxide

Hydrogen peroxide is one of the first oxidants tested in this type of applications. It can increase the efficiency of the process and it has been tested with a large number of compounds since earliest 90s. Furthermore, it is a very commonly used chemical and therefore cheap. Due to its electron acceptor nature, it reacts with conduction band electrons (Eq. (3.1)) to generate hydroxyl radicals,

which are required for the photomineralization of organic pollutants:

$$H_2O_2 + e^- \rightarrow {}^{\bullet}OH + OH^- \quad (3.1)$$

Reactions (3.2) and (3.3) can also produce $^{\bullet}OH$ (reaction (3.3) does not take place with solar radiation, only at $\lambda < 300$ nm):

$$H_2O_2 + O_2{}^{\bullet-} \rightarrow {}^{\bullet}OH + OH^- + O_2 \quad (3.2)$$

$$H_2O_2 + h\nu \rightarrow 2{}^{\bullet}OH \quad (3.3)$$

It is necessary to discuss some aspects related to the effect of this electron acceptor. In some cases, the addition has been found to be beneficial, increasing the degradation rate. The effect depends on the H_2O_2 concentration, generally showing an optimum range of concentration. At higher concentrations the improvement starts to lessen. Whereas this beneficial effect can easily be explained in terms of prevention of electron/hole recombination and additional $^{\bullet}OH$ production through reactions (3.1)–(3.3), inhibition could be explained in terms of TiO_2 surface modification by H_2O_2 adsorption, scavenging of photoproduced holes (Eq. (3.4)), and reaction with hydroxyl radicals (Eq. (3.5)):

$$H_2O_2 + 2h_{VB}^+ \rightarrow O_2 + 2H^+ \quad (3.4)$$

$$H_2O_2 + {}^{\bullet}OH \rightarrow H_2O + HO_2{}^{\bullet} \quad (3.5)$$

The inhibition of adsorption not only depends on the characteristics of the pollutant but also on the hydrogen peroxide/organic concentration ratio. This may be explained in terms of Langmuir/Hinshelwood kinetics, $r_C = k_r KC/(1 + KC)$ and competitive adsorption (see Section 2.2.1). If pollutant concentration (C) is too low and H_2O_2 concentration too high, organic adsorption decreases because of adsorption of hydrogen peroxide and, therefore, r_C decreases. When C is higher, the radicals react more easily and r_C increases. When C is still higher, the reaction rate is not as affected by adsorption ($1 + KC \approx KC$; $r_C = k_r$). In the latter situation the reaction rate is only dependent on $^{\bullet}OH$ concentration related to favourable (Eqs. (3.1)–(3.3)) and unfavourable reactions (Eqs. (3.4) and (3.5)). There is an optimum ratio of H_2O_2/C under these circumstances, whereby organic material is sufficient to consume generated hydroxyl radicals and to avoid detrimental reactions, if the peroxide concentration is not too high. An optimal molar ratio (H_2O_2/contaminant) between 10 and 100 has been found by different authors [71–74]. At high molar ratios an inhibition effect would be expected, because the unfavourable reactions become more and more pronounced. All these may be summarized as: first, if pollutant concentration is low, the hydrogen peroxide easily inhibits the degradation rate and, second, if the molar ratio between H_2O_2 and pollutant is too high, the same is true.

3.2.2. Peroxodisulphate

Peroxodisulphate (or persulphate) is a powerful oxidizing agent with a standard potential of $E^\circ = 2.01$ V and can be decomposed to $SO_4{}^{\bullet-}$ radical by UV radiation ($\lambda \leq 270$ nm). In homogeneous reactions, the peroxodisulphate ion accepts an electron and dissociates (Eq. (3.6)). This radical goes through the reactions explained below (Eqs. (3.8) and (3.9)). Peroxodisulphate can therefore be a beneficial oxidising agent in photocatalytic detoxification because $SO_4{}^{\bullet-}$ is formed from the oxidant compound by reaction with the photogenerated semiconductor electrons ($e_{CB}{}^-$, Eq. (3.7)). In addition, it can trap the photogenerated electrons and/or generate hydroxyl radicals.

The sulphate anion radical ($SO_4{}^{\bullet-}$) is a very strong oxidant ($E^\circ = 2.6$ V) and engages in at least three reaction modes with organic compounds: by abstracting a hydrogen atom from saturated carbon, by adding to unsaturated or aromatic carbon and by removing one electron from carboxylate anions and from certain neutral molecules [75,76]. Sulphate radicals are also capable of oxidizing chloride producing $Cl^{\bullet}$, $Cl_2{}^{\bullet-}$, Cl_2 and HOCl. $Cl^{\bullet}$ could react with organic radicals and the free chlorine species such as HOCl with the organic material giving rise to chlorinated derivatives from the transformation of non-chlorinated organics [77]:

$$S_2O_8{}^{2-} + e_{aq}{}^- \rightarrow SO_4{}^{\bullet-} + SO_4{}^{2-} \quad (3.6)$$

$$S_2O_8{}^{2-} + e_{CB}{}^- \rightarrow SO_4{}^{\bullet-} + SO_4{}^{2-} \quad (3.7)$$

$$SO_4{}^{\bullet-} + e_{CB}{}^- \rightarrow SO_4{}^{2-} \quad (3.8)$$

$$SO_4{}^{\bullet-} + H_2O \rightarrow {}^{\bullet}OH + SO_4{}^{2-} + H^+ \quad (3.9)$$

3.2.3. Other oxidants

Other compounds could also potentially increase the reaction rate because they are also electron acceptors. The most frequently tested so far in heterogeneous photocatalysis are described in Eqs. (3.10)–(3.13):

$$IO_4^- + 8e^- \xrightarrow{8H^+} 4H_2O + I^- \quad (3.10)$$

$$ClO_3^- + 6e^- \xrightarrow{6H^+} 3H_2O + Cl^- \quad (3.11)$$

$$BrO_3^- + 6e^- \xrightarrow{6H^+} 3H_2O + Br^- \quad (3.12)$$

$$HSO_5{}^- + e^- \rightarrow {}^{\bullet}OH + SO_4{}^{2-} \quad \text{or}$$
$$HSO_5{}^- + e^- \rightarrow OH^- + SO_4{}^{\bullet-} \quad (3.13)$$

Chlorate has been proven insufficient to improve effectiveness. However, both $IO_4{}^-$ and bromate increase the mineralization rates in all cases tested. Nevertheless, these additives are very expensive compared to hydrogen peroxide and peroxydisulphate, and their application would dramatically increase treatment cost. Even more importantly, they do not dissociate into harmless products (Br^- and I^-), because hundreds of mg/L of these anions are undesirable in water. Potassium peroxymonosulphate (PMS, commercially called oxone®, commercialized by Dupont) was also examined as an irreversible electron acceptor. The formula of this salt is $2KHSO_5{\cdot}KHSO_4{\cdot}K_2SO_4$, written in aqueous solution as $HSO_5{}^-$. PMS is a powerful oxidizing agent $E^\circ = 1.84$ V, which undergoes radiolytic and photolytic reactions [78] but not photochemical decomposition unless it is irradiated in the UV region with the wavelength $\leq$260 nm. However, in the presence of photocatalysts efficient decomposition of PMS has been observed with light of wavelength $<$390 nm. Upon accepting an electron from the conduction band, $HSO_5{}^-$ would dissociate into two different pathways (Eq. (3.13)). Madhavan et al. [79] carried out a comparison of the efficiency of the oxidants peroxymonosulphate and peroxodisulphate (both at 1.25 mM) in degradation of the mono azo textile dye acid Red 88 (5×10^{-5} M), using Degussa P-25 TiO_2. In the photocatalytic degradation of the dye over TiO_2, the addition of peroxymonosulphate enhances the degradation rate by 2.7 times whereas the addition of peroxodisulphate (PDS) increases the rate by a factor of 1.3. While 87% decolorisation of the dye in 30 min was achieved only when the concentration of PDS was 100 times (5 mM) that of the dye, a complete decolorisation could be achieved with 25 times of PMS, which clearly demonstrates the efficiency of peroxymonosulphate over that of peroxodisulphate. Interesting studies have been published by Anipsitakis and Dionysiou related with by the interaction of transition metals and peroxymonosulphate in the presence and absence of UV/vis [80,81].

An enhanced efficiency of peroxymonosulphate over peroxodisulphate can be rationalised since peroxymonosulphate becomes decomposed through both e_{CB}^- (Eq. (3.13)) and h_{VB}^+ (Eq. (3.14)) of the semiconductor photocatalysts whereas peroxodisulphate can be decomposed only by e_{CB}^-. The disadvantage is its high molecular weight. Many grams of the precursor oxone® salt are necessary for 1 active mol (HSO_5^-):

$$HOOSO_3^- + h_{VB}^+ \rightarrow SO_5^{\bullet -} + H^+ \quad (3.14)$$

$$2(SO_5^{\bullet -}) \xrightarrow{H_2O} 2HSO_4^- + O_2 \quad (3.15)$$

Malato et al. [82] studied suspensions of TiO_2 (Degussa P-25), irradiated with natural solar light in a large experimental plant (collector surface 384 m^2, photoreactor 500 L), catalyzing the oxidation of pentachlorophenol (PCP). The addition of oxidants, the concentration of which was kept constant during treatment, such as hydrogen peroxide, peroxymonosulphate and peroxydisulphate increased the rate of photodegradation of PCP in the following order: $S_2O_8^{2-}$ > Oxone > H_2O_2. The results presented demonstrate that hydrogen peroxide and oxone do not considerably enhance the photocatalytic reaction rate and the consumption of oxidant was enormous. These previous results led to the use of additional oxidants in the photocatalytic degradation of a complex mixture of 10 commercial pesticides [70]. A CPC solar pilot plant used for the tests has 8.9 m^2 of collector surface and a total volume of 247 L. Experiments were performed with H_2O_2 and $S_2O_8^{2-}$, but only peroxydisulphate was chosen for optimisation, because better results have been obtained with it. Hydrogen peroxide increases reaction rate by approximately a factor of 2. However, oxidant consumption was very high (200 mM to lower TOC from 110 to 20 mg L^{-1}). Moreover, the mineralization rate was clearly inhibited at around TOC 20 mg L^{-1}. This may be explained by changes in the H_2O_2/contaminant molar ratio during the experiment, since they were lower at the beginning than at the end. However, the use of peroxydisulphate leads to a very significant reduction of the energy necessary for total mineralization (at least six times for initial TOC around 100 mg L^{-1}). This reduction would also reduce the solar collector surface necessary to degrade the organics in the process water by the same factor. The consumption of peroxydisulphate was linearly dependent on the TOC degraded and not on the initial TOC at the beginning of degradation.

3.3. Use of doped and modified TiO_2

TiO_2 is a catalyst which works at mild conditions with mild oxidants. However, as concentration and number of contaminants increase, the process becomes more complicated and challenging problems, such as catalyst deactivation, slow kinetics, low photoefficiencies and unpredictable mechanisms need to be solved. It is clear that unmodified TiO_2 usually needs help to undertake practical applications of industrial and environmental interest and this could lead to the loss of some of the charm of its mild operation. Moreover, even reactor set-ups using artificial light, and the cost of running the lamps involved in them, will be much cheaper if visible radiation can be employed.

The redox process is based on the migration of electrons and holes to the semiconductor surface and two further oxidation and reduction steps (see Fig. 2). Two basic lines of R&D attempt to balance both half-reaction rates, one by adding electron acceptors (additional oxidants, already commented in Section 3.2) and the other by modifying catalyst structure and composition. Both try to promote competition for electrons and avoid recombination of e^-/h^+ pairs. A third approach has focused not only on increasing quantum yield but finding new catalysts with band gaps that match the solar spectrum better. The development of photocatalysts exhibiting high reactivity under visible light ($\lambda > 400$ nm) should allow the main part of the solar spectrum, even under poor illumination of interior lighting, to be used. Unfortunately, the choice of convenient alternatives for substituting titanium dioxide in photocatalytic detoxification systems is limited. The appropriate semiconducting material should be: (i) non-toxic, (ii) stable in aqueous solutions containing highly reactive and/or toxic chemicals, (iii) not undergoing photocorrosion under band gap illumination and (iv) economical, that is, an increase in photocatalytic reaction rates must be always be accompanied by a non-proportional increase in overall process costs.

3.3.1. Modification of the surface of TiO_2 by noble metals

Noble metals, such as Ag, Pt, Ni, Cu, Rh, Pd, have been studied and showed to be very effective for enhancement of TiO_2 photocatalysis. The Fermi levels of these noble metals are lower than that of TiO_2; photo-excited electrons can be transferred from conduction band to metal particles deposited on the surface of TiO_2 (see Fig. 16). These metals reduce the possibility of electron–hole recombination, causing efficient charge separation and higher photocatalytic reaction rates. Therefore, noble metals with these properties can help electron transfer, leading to higher photocatalytic activity [83]. Different metal particle deposition methods, such as impregnation, photodeposition and deposition–precipitation were also tested. Optimal loading of metal must be kept into consideration, since too much metal particle deposition might reduce photon absorption by TiO_2 and might also become electron–hole recombination centers, negatively affecting photocatalysis efficiency. Since Pt and Au are very expensive, more research is needed to find low-cost metals with acceptable improvement of photocatalytic activity. For example, Ni and Ag

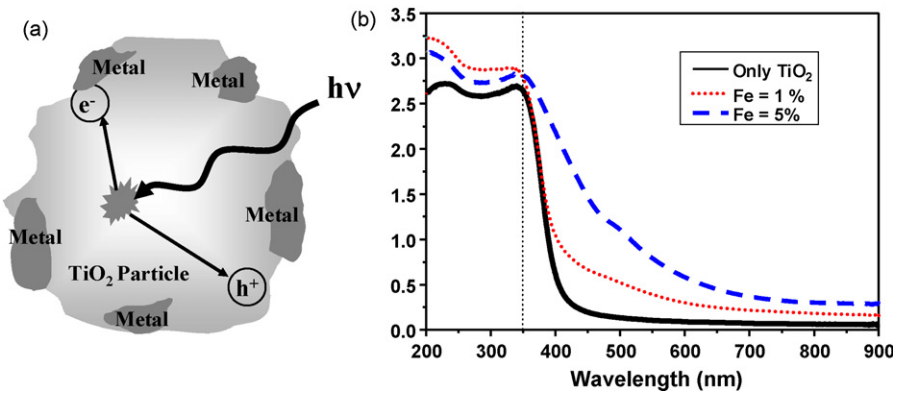

Fig. 16. (a) Electrons capture by a metal in contact with a semiconductor surface. (b) UV–vis spectra of iron-doped titania catalysts.

low-cost metals, were also found to be effective for improvement of photocatalytic activity. These low-cost although effective metals are expected to be promising materials to enhance photocatalytic TiO_2 activities for practical applications. In any case, use of metals should take into account possible metal toxicity issues and leaching from the catalyst.

3.3.2. Ion doping

During the last several years, transitional metal ion doping and rare earth metal ion doping have also been investigated for enhancing photocatalytic activity of TiO_2. Doping with metal ions could extend the photo-response of TiO_2 into visible spectrum (Fig. 16b). Metal ion are incorporated into the TiO_2 lattice, therefore impurity energy levels in the band gap of TiO_2 are formed ((3.16) and (3.17)):

$$M^{n+} + h\nu \rightarrow M^{(n+1)+} + e^-_{CB} \quad (3.16)$$

$$M^{n+} + h\nu \rightarrow M^{(n-1)+} + h^+_{VB} \quad (3.17)$$

where M is metal and M^{n+} is metal ion dopant. Moreover, electron (hole) transfer between metal ions and TiO_2 can modify electron-hole recombination:

$$M^{n+} + e^-_{CB} \rightarrow M^{(n-1)+} \quad \text{as electron trap} \quad (3.18)$$

$$M^{n+} + h^+_{VB} \rightarrow M^{(n+1)+} \quad \text{as hole trap} \quad (3.19)$$

$M^{n+}/M^{(n-1)+}$ energy level should be less negative than TiO_2 conduction band edge, while the energy level of $M^{n+}/M^{(n+1)+}$ should be less positive than TiO_2 valence band edge. As photocatalytic reaction can only occur, when the trapped electron and hole are transferred to the surface, carrier transport is as important as carrier trapping. Consequently, metal ions should be doped near the surface of TiO_2 particles for a better charge transfer. Otherwise, in case of deep doping, metal ions likely behave as recombination centers, as electron/hole transferring to the interface is more difficult. Moreover, there exists an optimum of doped metal ion concentration, above which the photocatalytic activity decreases due to the increase in electron/hole recombination.

It was found that Fe, Rh, Mo, V, Ru, Re, and Os ions can increase photocatalytic activity, while Al and Co ions cause detrimental effects. Different effects result from the different activity of various metal ions with regards to trapping and transferring electrons/holes. Fe and Cu ions can trap not only electrons but also holes, and the impurity energy levels introduced are near to conduction band as well as the valence band edge of TiO_2. For that reason, doping of either Fe or Cu ions is recommended for enhancement of photocatalytic activity [84].

In the same way, the effects of doping transition metal ions (Cr, Mn, Fe, Co, Ni and Cu) on photocatalytic efficiency of TiO_2 also have been studied. As, Cu, Mn, and Fe ions can trap both electrons and holes, doping of these metal ions may be better than doping with Cr, Co and Ni ions, as the latter metal ions can only trap one type of charge carrier. Likewise, enhanced photocatalytic activities were observed at certain doping content of different rare earth metal ions (La, Ce, Er, Pr, Gd, Nd and Sm) doped into TiO_2. It is remarkable that Gd ions were found to be most effective in enhancing the photocatalytic activity due to their higher ability to transfer charge carriers to the interface (on TiO_2 surface).

Nowadays, the use of anion doping to improve photocatalytic activity of TiO_2 under visible light is increasing [85–88]. Doping of anions (N, F, C, S, etc.) in TiO_2 crystalline could increase its photoactivity into the visible spectrum. Unlike metal ions (cations), anions less likely form recombination centers and, therefore, are more effective to enhance the photocatalytic activity. There are three main opinions about modification mechanism of TiO_2 doped with nonmetals:

(i) Band gap narrowing: Asahi et al. [89] found N 2p state hybrids with O 2p states in anatase TiO_2 doped with nitrogen because their energies are very close, and thus the band gap of N-TiO_2 is narrowed and able to absorb visible light.
(ii) Impurity energy level: Irie et al. [90] stated that TiO_2 oxygen sites substituted by nitrogen atom form isolated impurity energy levels above the valence band. Irradiation with UV light excites electrons in both the valence band and the impurity energy levels, but illumination with visible light only excites electrons in the impurity energy level.
(iii) Oxygen vacancies: Oxygen-deficient sites formed in the grain boundaries are important to evoke visible light activity and nitrogen doped in part of oxygen-deficient sites are important as a blocker for reoxidation [91].

The modification mechanism of anatase doped with nonmetals was also investigated by Zhao and Liu [92]. They investigated N-TiO_2 and concluded that TiO_2 doped with substitutional N has shallow acceptor states above the valence state. In contrast, TiO_2 doped with interstitial nitrogen has isolated impurity states in the middle of the band gap. These impurity energy levels are mainly hybridized by N 2p states and O 2p states.

The N-doped TiO_2 was reported to be effective for methylene blue decomposition, for disinfection [93] and for phenol degradation [94] under visible light ($\lambda > 400$ nm). S doping had resulted in a similar band gap narrowing, although the S ionic radius was reported to be too large to be incorporated into the TiO_2 lattice. C and P were found to be less effective as the introduced states were so deep that photo-generated charge carriers were difficult to be transferred to the surface of the catalyst. When TiO_2 was doped with S, the mixing of S 3p states with the valence band of TiO_2 increased the width of valence band, resulting in band gap narrowing. Since the band gap narrowing was caused by valence band upward shifting, the conduction band remained unchanged. S-doped TiO_2 is more efficient than pure TiO_2 under visible light radiation. Although the valence band was shifted upwards, the oxidation ability was found to be still high. Similar to S-doping, N-doping also causes a valence band upward shift resulting in a narrow band gap and less oxidizing holes. It was reported that N-doped TiO_2 was unable to oxidize $HCOO^-$.

3.3.3. Composite (coupling) semiconductors

Semiconductor composition is another method to utilize visible light to improve photocatalytic efficiency. When a large band gap semiconductor is coupled with a small band gap semiconductor with a more negative conduction band level, conduction band electrons can be injected from the small band gap semiconductor to the large band gap semiconductor. Thus, a wide electron–hole separation is achieved (see Fig. 17).

Successful coupling of the two semiconductors for photocatalytic applications under visible light irradiation can be achieved when the following conditions are met:

(i) Semiconductors should be photocorrosion free.
(ii) The small band gap semiconductor should be able to be excited by visible light.
(iii) The conduction band of the small band gap semiconductor should be more negative than that of the large band gap semiconductor.
(iv) Electron injection should be fast as well as efficient.

Coupled CdS (band gap 2.4 eV) with TiO_2 for 2-chlorophenol degradation under UV irradiation was reported [95]. The

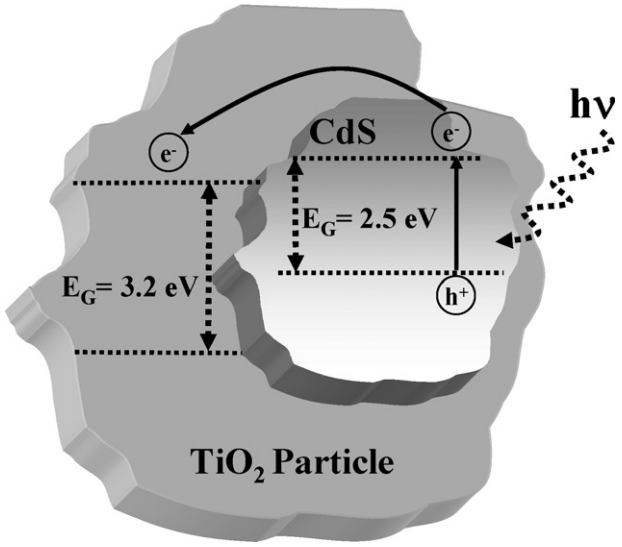

Fig. 17. The excitation process in a semiconductor–semiconductor photocatalyst.

combination of the two semiconductors showed better photocatalytic activity due to better charge separation. The conduction band electrons of CdS were injected to TiO_2 conduction band, while the TiO_2 valence band holes were injected to CdS valence band. It was found that coupling of CdS–TiO_2 was more effective than CdS and TiO_2 used separately. Moreover, optical absorption spectra analysis showed that CdS–TiO_2 could absorb photons with wavelengths up to 520 nm.

Besides coupling with small band gap semiconductors, TiO_2 coupled with a large band gap semiconductor has also been investigated and proven to be more efficient under UV irradiation. It was observed that photocatalytic oxidation of methylethylketone (MEK) was increased by coupling TiO_2 with WO_3 (2.7 eV band gap) and SiC (3.0 eV band gap) [96]. As the conduction band of SiC was more negative, electron transfer to the conduction band of TiO_2 could be more efficient. On the other hand, the conduction band of WO_3 was less negative than that of TiO_2, and thus electrons were transferred from the conduction band of TiO_2 to WO_3, resulting in a wide electron–hole separation. These composite semiconductors were found to be more effective than TiO_2 for MEK oxidation due to efficient charge separation.

3.3.4. Metal ion implantation

Metal ion implantation has been recently reported as an effective method to modify semiconductor electronic structures to improve visible light response [97,98]. In this method TiO_2 is bombarded, accelerated by high voltage, with high-energy transitional metal ions. This process modifies TiO_2 electronic structure and shifts its photo-response to the visible region up to 600 nm. These metal ions can have different interactions with the sample surface depending on their kinetic energy. In the metal ion-implantation, metal ions are accelerated enough to have a high kinetic energy (50–200 keV) and can be implanted into the bulk of TiO_2 samples [99].

Intensive studies of visible light-responsive photocatalysis have been carried out in order to harness the abundant and safe potential of solar energy. There have been various attempts to sensitize TiO_2 for much larger visible light regions. One of these investigations has been the chemical doping of TiO_2 with transition metals ions or oxides [100].

Although TiO_2 chemically doped with metal ions can induce visible light response, most of these catalysts do not show long-term stability nor have sufficiently high reactivity for a wide range of applications. When metal ions or oxides are incorporated into the TiO_2 by a chemical doping method such as impregnation, a small absorption band appears at 400–550 nm as a shoulder peak due to the formation of the impurity energy levels in the band gap of TiO_2. Such impurity energy levels may act as recombination centers for the excited electrons and holes, thus, decreasing the photocatalytic activity.

When TiO_2 is bombarded with such high energy transition metal ions accelerated by high voltage, the ions can be implanted into the lattice without destroying the TiO_2 surface structure. The absorption band of TiO_2 physically implanted with such metal ions such as Cr, Fe, Ni and V was found to shift smoothly to visible light regions up to 600 nm, depending on the kind of metal implanted, indicating that the band gaps of the physically ion-implanted TiO_2 are much smaller than that of the original TiO_2. Nevertheless, the spectra of chemically ion-doped TiO_2 are quite different from the spectra of physically ion-implanted TiO_2, exhibiting a shoulder peak in visible light regions, although it is not a smooth shift. Fig. 18 shows the band structures of the original TiO_2, chemically ion-doped TiO_2 and physically ion-implanted TiO_2. This effective narrowing of the band gap is attributed to the substitution of the Ti ions in the TiO_2 lattice with the metal ions. Takeuchi et al. [101] found that the application of the metal ion-implantation method allows the modification of the electronic states of TiO_2 thin film catalyst. The chemically ion-doped TiO_2 photocatalysts showing a shoulder in the visible light region exhibited a drastic decrease in photocatalytic reactivity under ultraviolet irradiation as compared with that of the undoped original TiO_2 since the doped ions induce impurity energy levels within the band gap and the energy level

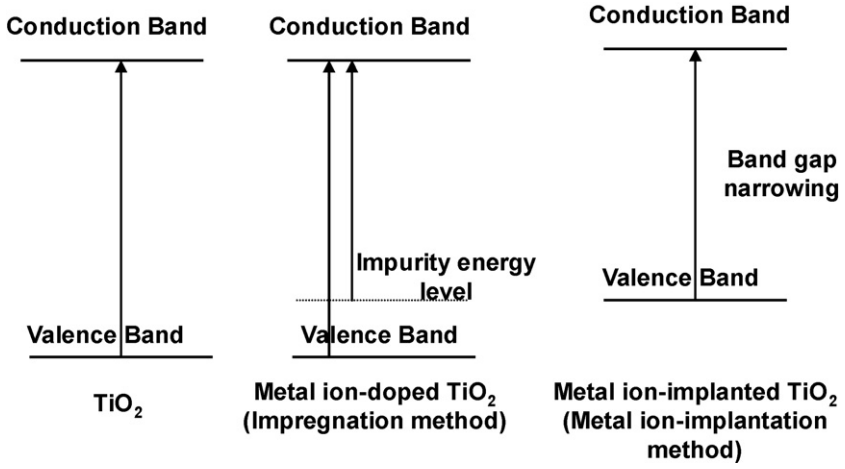

Fig. 18. Scheme of TiO_2 band structures, chemically ion-doped TiO_2 and physically ion-implanted TiO_2.

plays an important role in the recombination of the photoformed electrons and holes, leading to a drastic decrease in the photocatalytic reactivity. Nevertheless, under UV irradiation, the physically ion-implanted TiO_2 catalysts exhibited the same photocatalytic activity for the decomposition of NO and the complete oxidation of 2-propanol to CO_2 and H_2O as the unimplanted original TiO_2 photocatalysts, indicated that the implanted metal ions did not act as electron–hole recombination centers since they were present in the TiO_2 catalysts in a highly dispersed state.

Spectroscopic investigations, as ESR, SIMS and XAFS, showed that the substitution of octahedrally coordinated Ti ions in the bulk TiO_2 lattice with the implanted metal ions was a major factor in the TiO_2 modification to absorb under visible light irradiation. Furthermore, all molecular orbital calculations on the basis of a density functional theory method revealed that the mixing of the Ti(d) orbital of the Ti-oxide and the metal(d) orbital of the implanted metal ions under a low electric charge was essential in decreasing the energy gap between the Ti(d) and O(p) orbitals of the Ti-oxide. These results indicate that the substitution of Ti ions with the isolated metal ions implanted into the lattice TiO_2 position was the origin of the effective narrowing of the band gap.

Presently metal ion implanted TiO_2 is believed to be the most effective photocatalyst for solar energy utilization and is in general called as the "second generation photocatalyst" [102].

3.4. Coupling of TiO_2 photocatalysis with photosensitizers

For energy conversion of visible light, dye sensitization is widely used. Some dyes having redox property and visible light sensitivity can be used in photocatalytic systems as well as in solar cells [103,104]. The excited dyes can inject electrons to conduction band of semiconductors to initiate the catalytic reactions under illumination by visible light. The process is similar to composite semiconductors, the difference is that electrons are injected from the excited dye to semiconductor, rather than from one semiconductor to another semiconductor. The photo-excitation, electron injection and dye regeneration can be expressed as follows:

$$\text{dye} + h\nu \rightarrow \text{dye}^* \tag{3.20}$$

$$\text{dye}^* \xrightarrow{\text{TiO}_2} \text{dye}^+ + e^- \tag{3.21}$$

$$\text{dye}^+ + e^- \rightarrow \text{dye} \tag{3.22}$$

Fig. 19 illustrates the excitation, charge transfer and regeneration steps. If the energy level of the excited state of the dye is more negative than the semiconductor conduction band, then the dye can transfer the electron to the conduction band of the semiconductor. The electron in turn can be transferred to reduce an organic acceptor adsorbed on the surface. Without the presence of a redox couple, the dye-semiconductor system can also be used in oxidative degradation of the dye itself. This is important considering the large number of dye substances found in industrial textile waste water. Sensitized photocatalysis usually leads to a rapid destruction of chromophore structure to form smaller organic species, leading to the final mineralization of the dye [105–108].

Table 2
Frequently used dyes.

Dye	Type	λ_{max} (nm)
Thionine (TH^+)	Thiazines	596
Toluidine blue (Tb^+)	Thiazines	630
Methylene blue (MB)	Thiazines	665
New methylene blue	Thiazines	650
Azure A	Thiazines	635
Azure B	Thiazines	647
Azure C	Thiazines	620
Phenosafranin (PSF)	Phenazines	520
Safranin-O (Saf-O/SO)	Phenazines	520
Safranin-T (Saf-T/ST)	Phenazines	520
Neutral red (NR)	Phenazines	534
Fluorescein	Xanthenes	490
Erythrosin	Xanthenes	530
Erythrosin B	Xanthenes	525
Rhodamin B (Rh. B)	Xanthenes	551
Rose Bengal	Xanthenes	550
Pyronine Y (PY)	Xanthenes	545
Eosin	Xanthenes	514
Rhodamin 6G	Xanthenes	524
Acridine orange (AO)	Acridines	492
Proflavin (PF)	Acridines	444
Acridine yellow (AY)	Acridines	442
Fusion	Triphenyl methane derivatives	545
Crystal violet	Triphenyl methane derivatives	578
Malachite green	Triphenyl methane derivatives	625
Methyl violet	Triphenyl methane derivatives	580

To obtain a higher efficiency in converting absorbed light into direct electrical energy (for solar cells) or oxidation reactions, fast electron injection and slow backward reaction are required. The recombination times were found to be mostly in the order of nanoseconds to microseconds, sometimes in milliseconds on electron/hole recombination of dyes [109], while the duration of electron injection is in the order of femtoseconds [110]. The quick electron injection and slow recombination reaction make dye-sensitized semiconductors feasible for energy conversion. Jana [111] reported the most frequently used dyes with their absorption wavelength maxima; these dyes are listed in Table 2.

3.5. Coupling of semiconductor photocatalysis with other AOPs

In general, a combination of several methods gives high treatment efficiency compared with individual treatment. For example, a certain organic compound can hardly be degraded by ozonation or photolysis alone and the treated wastewater may be more dangerous as a result of ozonation but a combination of several treatments methods, such as O_3/VUV (ozone/vacuum ultraviolet), O_3/H_2O_2/UV and UV/H_2O_2, improves the removal of pollutants from the wastewater [112].

A combination of photocatalysis together with ozone, also a strong oxidant, is reasonable for the treatment of difficult to

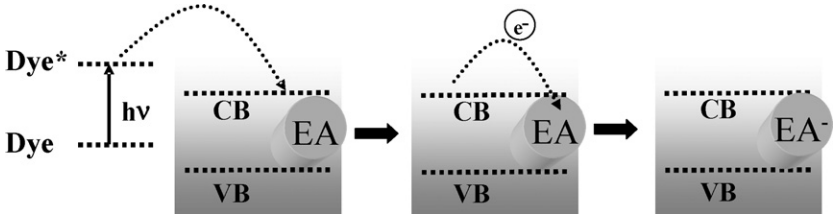

Fig. 19. Steps of excitation with a sensitizer in the presence of an adsorbed organic electron acceptor (EA).

degrade organic compounds since the organic compounds are then expected to decompose more quickly in the presence of ozone, to carbon dioxide, water, and inorganic ions. Sanchez et al. [113] combined these two methods for the removal of aniline from water and found that the decomposition rate of aniline is greater than when individually treated by either of the two methods. Wang et al. studied the decomposition of formic acid in an aqueous solution using photocatalysis, ozonation, and their combination. As a result, the decomposition rate of formic acid by the combination of photocatalysis and ozonization was found to be higher than the sum of the decomposition rates when formic acid was individually decomposed by a combination of the two methods, which indicates the presence of a synergistic effect of photocatalysis and ozonation [114].

Ozone is a powerful oxidant, which is generally produced by an electric corona discharge method in the presence of air or oxygen. Two reactions of ozone with dissolved organic substance can be distinguished in water [115]:

(i) A highly selective attack of molecular ozone takes place on the organic molecules at low pH.
(ii) Additional free hydroxyl radicals can be produced in the aqueous media from ozone by pH modification.

The use of ozone for the destruction of organics in water is also a well-known water treatment technique. Unlike photocatalysis, ozonation, due to its capability for selective destruction of recalcitrant organics and its easy and practical application, is applied as a pretreatment step before ordinary biological techniques, thus being more efficient for highly contaminated wastewater. The simultaneous application of ozonation and photocatalysis has the capability for efficient treatment of organically contaminated waters over a wide range of concentrations [116].

Sanchez et al. [113] in their investigation, found that although the strategy of ozonation pretreatment followed by photocatalysis would be a satisfactory route for aniline degradation, the simultaneous ozonation and photocatalysis methodology resulted in much higher TOC removal, but also to higher energy and material demands. Such a combination could be preferred from an application point of view. In fact, besides the direct ozonation of the intermediate compounds, in the presence of TiO_2 under illumination, ozone can generate $^{\bullet}OH$ radicals through the formation of an ozonide radical ($O_3^{\bullet-}$):

$$TiO_2 + h\nu \rightarrow e^- + h^+ \quad (3.23)$$

$$O_3 + e^- \rightarrow O_3^- \quad (3.24)$$

The generated $O_3^{\bullet-}$ species rapidly reacts with H^+ in the solution to give $HO_3^{\bullet}$ radical, which evolves to give O_2 and $^{\bullet}OH$ as shown in Eqs. (3.25) and (3.26):

$$O_3^{\bullet-} + H^+ \rightarrow HO_3^{\bullet} \quad (3.25)$$

$$HO_3^{\bullet} \rightarrow O_2 + {}^{\bullet}OH \quad (3.26)$$

In photocatalysis, the hydroxyl radical is generally considered to be mainly responsible for the attack on organics. It must be considered that the $^{\bullet}OH$ radical can react with O_3 in competition with organic compounds:

$$^{\bullet}OH + O_3 \rightarrow O_2 + HO_2^{\bullet} \quad (3.27)$$

Moreover, the $O_2^{\bullet-}$ species take part in a closed loop reaction scheme, which leads to a continuous consumption of ozone. In the absence of O_3, dissolved O_2 itself can accept TiO_2 conduction band electron and generate $O_2^{\bullet-}$:

$$O_2 + e^- \rightarrow O_2^{\bullet-} \quad (3.28)$$

Which can be protonated to form $HO_2^{\bullet}$:

$$O_2^- + H^+ \rightarrow HO_2^{\bullet} \quad (3.29)$$

Unlike $HO_3^{\bullet}$ (see Eq. (3.25)), this species cannot give $^{\bullet}OH$ radicals in a single step and an alternative reaction pathway exists to account for $^{\bullet}OH$ radical's generation from $HO_2^{\bullet}$:

$$2HO_2^{\bullet} \rightarrow H_2O_2 + O_2 \quad (3.30)$$

$$H_2O_2 + O_2^{\bullet-} \rightarrow {}^{\bullet}OH + HO^- + O_2 \quad (3.31)$$

This mechanism needs a total of three electrons for the generation of a single $^{\bullet}OH$ species, which is a less favoured situation if compared with the one electron needed through the $O_3^{\bullet-}$ reaction pathway.

To obtain more information about the photocatalytic ozonation processes, Kopf et al. measured [117] the ozone decomposition during illumination of aqueous TiO_2 suspension in the absence of organic compounds. The pH 3 solutions were saturated with ozone. After stopping the gas supply, illumination was started. Illumination induced ozone decomposition, and the reaction rate is proportional to the light intensity. These results show that a real photocatalytic reaction takes place in the suspension, not the radiation alone but the combination of radiation and photocatalyst starts a decomposition reaction of ozone. Oxygen should have influence on the photocatalytic ozonation. Besides other reaction paths, such as direct ozone attack, or direct electron transfer from TiO_2 to the ozone molecule (Eqs. (3.23)–(3.26)), a further possible reaction path is proposed. Charge separation (3.23) and charge transfer of positive charge (3.32):

$$h^+ + H_2O \rightarrow {}^{\bullet}OH + H^+ \quad (3.32)$$

Electron transfer (3.28) and further reactions ((3.25), (3.26) and (3.29)) including (3.33) and oxidation of the organic compound R–H ((3.34) and (3.35)):

$$O_2^{\bullet-} + O_3 \rightarrow O_3^{\bullet-} + O_2 \quad (3.33)$$

$$^{\bullet}OH + R - H \rightarrow R^{\bullet} + H_2O \quad (3.34)$$

$$^{\bullet}OH + R \rightarrow R^{\bullet} - OH \quad (3.35)$$

The difference between photocatalytic ozone decomposition and ozone decomposition in aqueous solution is the initiation of the reaction. The starting radical is formed photochemically by an electron transfer from titanium dioxide to oxygen and not, like in the Weiss-mechanism [118], by the reaction of OH^- ion with ozone. In both cases primarily $O_2^{\bullet-}$ is formed. $O_2^{\bullet-}$ reacts with ozone forming the ozonide ion (Eq. (3.33)). After protonation $^{\bullet}OH$ radicals are formed (Eqs. (3.25) and (3.26)). The formation of $^{\bullet}OH$ radicals in acidic solutions via direct electron transfer from the catalyst to the ozone molecule or via $O_2^{\bullet-}$ explains the compounds organic degradation by photocatalytic ozonation which react very slowly with the ozone molecule or with $HO_2^{\bullet}$, one of the primary oxidising species in photocatalytic processes.

Moreover, a synergistic effect occurs when the photocatalytic and ozonation treatments are carried out simultaneously. Two possible mechanisms are considered for the synergistic effect. Firstly, it is considered that in the photocatalytic reactor, the dissolved ozone could accept electrons produced on the surface of titanium dioxide according to the mechanism [114]:

$$O_{3(ads)} + e^- \rightarrow O_{3(ads)}^- \quad (3.36)$$

The recombination of electrons and positive holes could be blocked by the reaction between ozone and electrons on the surface of titanium dioxide. Therefore, a larger number of radicals are produced, thereby accelerating the photocatalytic reaction. Secondly, it is considered that a larger number of hydrogen peroxide and hydroxyl radicals were produced from the dissolved ozone as a result of UV-irradiation. The hydroxyl radical is produced by ozonation under UV-irradiation according to the following mechanism ((3.37)–(3.41), jointly with (3.25) and (3.33)):

$$O_3 + H_2O \xrightarrow{h\nu < 300\,nm} H_2O_2 + O_2 \quad (3.37)$$

$$H_2O_2 \xrightarrow{h\nu < 300\,nm} 2^{\bullet}OH \quad (3.38)$$

$$H_2O_2 \leftrightarrow HO_2^- + H^+ \quad (3.39)$$

$$O_3 + HO_2^- \rightarrow O_3^{\bullet -} + HO_2^{\bullet} \quad (3.40)$$

$$HO_2^{\bullet} \rightarrow O_2^{\bullet -} + H^+ \quad (3.41)$$

Farré et al. [119] suggested that for the photocatalytic ozonation system, the reaction proceeded through radical attack at the organic molecule. Consequently, the $^{\bullet}OH$ radical is produced by: (i) reaction of absorbed H_2O molecule with photogenerated holes at the illuminated TiO_2 particle and (ii) reaction of absorbed O_3 and photogenerated electrons at the TiO_2 particles (Eqs. (3.23)–(3.26)). The presence of dissolved ozone in the irradiated TiO_2 aqueous suspension increases the $^{\bullet}OH$ radical production and decreases the electron–hole recombination, increasing the efficiency of the photocatalysis process.

A kinetic model based on Langmuir–Hinshelwood (L–H) equations adequately describes the reactivity results and provides the values of kinetic constant and equilibrium adsorption constant in the degradation of organic compound using photocatalytic ozonation methods [120]. Beltrán et al. [121] reported that phenol removal followed first order kinetic. Balcioglu et al. [122] reported in their investigation, which also employed the combined method, that decomposition followed pseudo-first order kinetics.

On the other hand, in addition to Fenton-related technologies [123], if the semiconductor is used as an anode, those electrons can be extracted into an external circuit, thus retarding recombination. Peralta-Hernández et al. [124] presented the results of a study in which a sintered nanocrystalline TiO_2 semiconductor electrode (NSE) coupled as an anode in a photo-electrochemical reactor with a carbon-cloth cathode working under potentiostatic conditions at room temperature. The coupled electrochemical and photo-electrochemical reactions that take place in slightly acidic oxygen-saturated aqueous solutions (pH 2–4) resulted in the efficient production of H_2O_2. With the addition of ferrous ion, this reactor was found to destroy a model pollutant compound (Direct Yellow-52 dye) at a significant rate, as indicated by the decrease of the dye's optical absorbance as well as by the rapid reduction of dissolved TOC.

Among the existing AOPs, sonochemical oxidation has received considerable attention because of its particular efficacy toward volatile and/or hydrophobic compounds [125,126]. Ultrasound irradiation of aqueous solutions leads to acoustic cavitation, i.e., the cyclic formation, growth and adiabatic implosion of micro-bubbles. Under these conditions, organic substances with an elevated fugacity character are pyrolised [127], while non-volatile compounds are degraded by hydroxyl radicals coming from water and oxygen dissociation [128]. Hydrophobic substrates are mainly degraded at the interface of bubbles and solution. Because of the short lifetime of $^{\bullet}OH$ radicals, a large fraction recombine at the interface of the bubble before reacting with hydrophilic substances. Thus, polar organic compounds are eliminated in the solution bulk, to a much lower extent than volatile and hydrophobic substrates [129].

Enhancement of the photocatalysis efficiency using low-frequency ultrasound (20–100 kHz) has been widely investigated [130,131]. However, in spite of the notable performance of high-frequency ultrasound (frequencies >100 kHz) for degrading organic compounds, only a few reports have addressed the combination of photocatalysis and high-frequency ultrasound. Moreover, the synergistic effect between these two processes is a controversial matter. Stock et al. [132] reported that, after 4 h of treatment using a combined high-frequency ultrasound/photocatalysis system, the mineralization rate of an azo dye was greater than that resulting from an additive effect of the individual AOPs. In contrast, Théron et al. [130], studying the degradation of phenyltrifluoromethylketone, reported the absence of synergy between the same two AOPs.

In this sense, Torres et al. [133] coupled sonolysis (300 kHz, 80 W) and solar photocatalysis using titanium dioxide for the degradation of a model organic pollutant, bisphenol A (BPA), an endocrine disrupting chemical widely used in the plastic industry. Initially, the performances of the two separate processes in both the elimination and mineralization of BPA were compared. Even if identical BPA by-products were formed, the two processes were complementary, while ultrasound was better able to eliminate the target pollutant, photocatalysis proved to be more efficient for reaching mineralization. Using the combined system, an interesting synergistic effect, which depended on the titanium dioxide loading, was observed for BPA mineralization. The best synergistic effect was found a low catalyst loading (0.05 g L^{-1}). The poor synergistic effect at high catalyst loading can be explained by an inhibiting effect of the titanium dioxide on the cavitational activity.

4. Solar photo-Fenton processes—applications and process integration

4.1. Introduction

For the treatment of industrial wastewater Fenton and Fenton-like processes are probably among the most applied Advanced Oxidation Processes [134,135]. The first proposals for wastewater treatment applications were reported in the 1960s [136]. Several classical works report on the chemistry of the Fenton process [137,138] and a radical mechanism is generally accepted today, whereas the exact mechanism and the nature of the actual oxidizing species are still under discussion [139,140]. Quite recent reviews give good overviews of the Fenton chemistry [136,141].

Yet, it was not until the early 1990s, when the scientists working in the field of environmental sciences published results on the role of iron in atmospheric chemistry [142], which called the attention of scientists and engineers working in the wastewater treatment field. Soon afterwards, first works of the application of the photo-Fenton process (or photoassisted/light enhanced Fenton process) for the treatment of wastewater were published by the groups of Pignatello, Lipcznska-Kochany, Kiwi, Pulgarín and Bauer [141].

Since then the publication activities regarding the photo-Fenton process rose continuously surpassing 500 peer-reviewed publications up-to-date (source: http://www.scopus.com, 07 April 2008, search criteria "photo-Fenton" and "solar photo-Fenton"). Though such a simple search does not necessarily include every single article, it still serves to prove the general trend of an ever increasing interest of the scientific community. Fig. 20 shows the evolution of these publication activities. Fig. 20 also illustrates that much of the literature treating the photo-Fenton process takes into account the possibility of driving the process with solar radiation

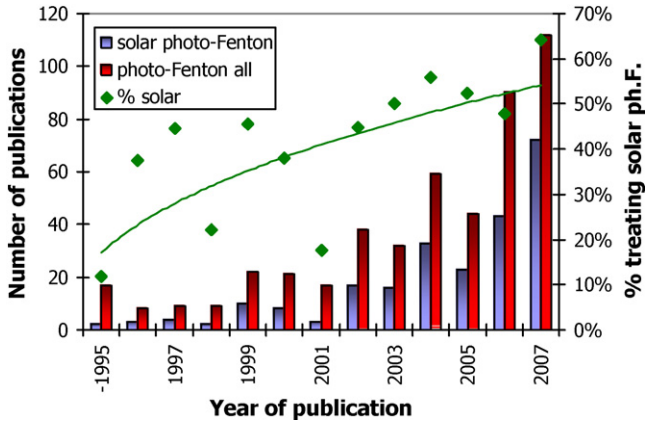

Fig. 20. Publications treating photo-Fenton and the share treating solar-driven photo-Fenton (source: http://www.scopus.com, 2008, search terms "photo-Fenton" and "solar" within these results).

with an evermore increasing share with respect to the total publications on the process. This fact is due to that a priori the photo-Fenton process seems to be the most apt of all AOPs to be driven by sunlight, because soluble iron-hydroxy and especially iron-organic acid complexes absorb even part of the visible light spectrum, not only ultraviolet radiation. Consequently, the photo-Fenton system is a very efficient reaction system for the generation of radicals available for oxidative processes.

Research on photo-Fenton undertaken covers the treatment of many pollutants, such as pesticides [143,144], chlorophenols [5], natural phenolic pollutants [145,146], and pharmaceuticals [147,148]. It was also successfully applied to waste water with high organic load in the order of 10 up to 25 g L^{-1} total organic carbon [149–151].

Within the investigated limits in these studies (maximal iron concentration 2.6 mM, maximal temperature 70 °C) an increase of the respective parameter always caused an increase in reaction rate. Only two studies examine the result of alternating time intervals with and without illumination [150,151]. They suggest the formation of precursors in the dark prone to rapid photolysis upon irradiation. Consequently, by alternating dark and illumination periods a decrease of necessary number of photons can be achieved compared to constant illumination. Provided the assumption that photons are one of the most important cost factors in the process (still theoretically solar light implies costs for the solar reactor), this phenomenon may be crucial to reduce costs, but still lacks thorough investigation.

Another issue that complicates the chemistry behind the process is the influence of ions on the process. Whereas the influence of phosphate is rather clear through the co-precipitation with ferric iron, other ions such as halogens and sulphate form complexes with the catalyst altering its activity and/or promote the formation of radicals less reactive than the hydroxyl radical. Formation of these complexes is largely dependent on the concentrations of these ions and the solution's pH value [152]. To know the resulting influence on the process is important, because usually any industrial or other wastewater stream contains one or several different ions, where concentrations may vary from close to zero to dozens of grams of dissolved salts.

Other studies deal with the application of iron as a heterogeneous catalyst, e.g., in the form of suspended oxides [153], fixed on a support structure [154] or even a combination of both [155]. While an easy separation and the possibility of working without pH adjustments are advantages of this approach, the drawback is generally diminished reaction rates compared to the homogeneous photo-Fenton process. This is mainly related to mass transfer limitations of the heterogeneous process and worsened light penetration into the photoreactor in the presence of solids [156]. Another approach to avoid the need for acidification of the wastewater to maintain iron stably dissolved is performing the photo-Fenton reaction in the presence of complexing agents [157]. In case of these complexes are also photoactive in the visible region, also a beneficial effect on the reaction rate may occur. This is way several authors proposed either the addition of oxalic acid or the direct application of ferric oxalate as iron source [158]. Also, different solar photoreactors have been proposed for applying the photo-Fenton method, trying to take into account the specific needs of the process [145,159,160].

Similar as in literature on other AOPs, originally toxic waste water has been proven to lose its toxicity upon treatment by photo-Fenton process before total mineralization has been achieved. Loss of toxicity usually is accompanied by an enhancement of biodegradability of the treated waste water [161,162]. Consequently, photo-Fenton process and AOPs in general have been proposed as a pretreatment to biological treatment for toxic wastewater streams [163].

Whereas the given citations do not aim to form a complete list, the following chapters will try to rationalize the findings of the topics mentioned shortly in this introduction, give an overview of compounds studied and efficiencies found, pilot-plant scale studies conducted and existing solar hardware. We will subsequently address the need and ways to integrate variations of the photo-Fenton process in a complete treatment train with a special focus on the combination with biological treatment. Finally, at the end of this section, we will provide recommendations for further development needs to bring the photo-Fenton process from the current research phase closer to applicability at pre-industrial, and industrial scale taking into account economical and environmental aspects.

4.2. Chemical fundamentals

Though as mentioned in the introduction several excellent and comprehensive reviews on the Fenton chemistry exist [136,141,164], for the sake of completeness and clarity of the following discussion we will give a short summary of the principles of reactions occurring in the photo-Fenton system.

4.2.1. Aquatic iron chemistry

Behind oxygen, silicon and aluminium, iron is the fourth most abundant element in the earth's crust. It occurs in oxidation numbers from −II to +VI with coordination numbers of 3–8 [165]. In aqueous solution the most abundant iron species have an oxidation number of +II (ferrous iron) and +III (ferric iron). Other iron species are highly unstable and are therefore not dealt with here in detail. Dissolved ferrous and ferric iron species are present in octahedral complexes with six ligands in water. Iron is complexed by water and hydroxyl ligands provided that no other complexing substances are present. How many of these ligands are hydroxyl ions, depends on the solution's pH, which influences directly the acid/base equilibrium of the aquo complex. Ferric iron is the more critical iron species in the photo-Fenton process, because its hydroxides precipitate at lower pH than those of ferrous iron. Consequently, only the acid/base equilibrium for the ferric iron aquo complex is described here, Eqs. (4.1)–(4.3). For simplification, coordinated water molecules in the coordinate sphere will not be included in the chemical formulae from hereon. Formation of dimers, Eq. (4.4), and oligomeres is possible as well, with the dimer being the most important at pH below 3 [166].

$$[Fe(H_2O_6)]^{3+} \rightleftarrows [Fe(H_2O)_5(OH)]^{2+} + H^+ \qquad K = 6.3 \times 10^{-3}\,M \tag{4.1}$$

$$[Fe(H_2O)_5(OH)]^{2+} \rightleftarrows [Fe(H_2O)_4(OH)_2]^{+} + H^{+} \qquad K = 3.2 \times 10^{-4}\,M \tag{4.2}$$

$$[Fe(H_2O)_4(OH)_2]^{+} \rightleftarrows [Fe(H_2O)_3(OH)_3] + H^{+} \qquad K = 1 \times 10^{-6}\,M \tag{4.3}$$

$$2Fe_{aq}^{3+} \rightleftarrows Fe_2(OH)_2^{4+} + 2H^{+} \qquad K = 1.3 \times 10^{-3}\,M \tag{4.4}$$

Fig. 21 shows the equilibrium concentrations of the most important ferric iron aquo complexes in the absence of other complexing substances at different pH for a ferric iron concentration of 20 mg L^{-1}. The dimer concentration is rather low at this ferric iron concentration. As the formation of the dimer is a process of second order, the relative amount of this species augments at higher iron concentrations. It is evident that between pH 2.5 and 3 $[Fe(H_2O)_5(OH)]^{2+}$ is the dominant species.

Because of the low solubility product of ferric iron hydroxide ($K_S(Fe(OH)_3) \approx 10^{-37}$), precipitation starts at pH 2.5–3.5 depending on the iron concentration and the temperature. The precipitation process starts with the formation of dimers and oligomeres, which at continuation gradually polymerise further and lose water until forming finally insoluble iron hydroxides (e.g., goethite or hematite). This ageing process is slow and can take up to a 100 days [166]. The precipitation and aging processes are also temperature dependent and more and faster precipitation takes place at higher temperatures [167]. The resulting precipitate is of red brown colour (absorption over the whole UV/vis spectral range) and not stoichiometric. It contains a lot of water and has a strong cationic character, thus co-precipitating a lot of other ions but also organic substances. Therefore, ferric iron is often used as coagulant in wastewater treatment. The precipitate is difficult to re-dissolve through acidification (insoluble above pH ≈ 1–1.5), but it can be re-dissolved by complexing substances (e.g., oxalic acid) [168] or photoleaching processes [169]. Photoleaching refers to photoreduction of ferric to ferrous iron and subsequent leaching of the more soluble ferrous iron from the precipitate.

4.2.2. Fenton chemistry—reactions of Fe^{2+}, Fe^{3+} and H_2O_2 in aqueous solution

Hydrogen peroxide is decomposed to water and oxygen in the presence of iron ions in aqueous solution in the Fenton reaction, Eq. (4.5), which was first reported by Fenton in 1894 [170]. Classically, there were two suggestions for the mechanism, a radical and an ionic one, but after the work of Walling [138], the radical mechanism has been broadly accepted for reactions in acidic milieu. Yet, it should be mentioned that discussion is still on-going and the occurrence of ferrate and ferryl iron (+IV and +V), at least in intermediate complexes, has been proposed [139,140]. This has to be taken into account as an important issue, because oxidative reactions involving ferrate and ferryl complexes may, in many cases, be different from the reactions with the hydroxyl radical, in reactivity as well as with respect to reaction products.

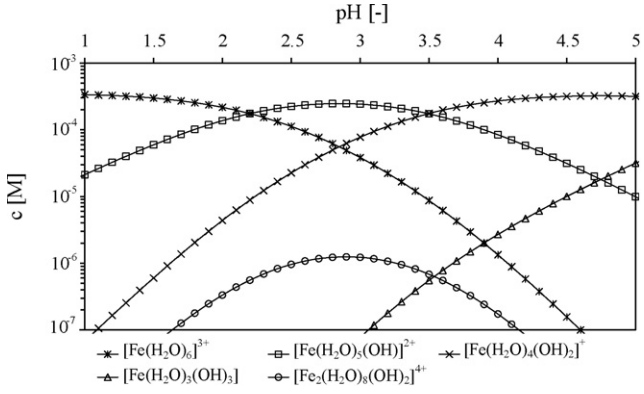

Fig. 21. Ferric iron species present in aqueous solution at different pH at a concentration of 20 mg L^{-1}, calculated with equilibrium constants from [166], T = 20 °C.

Mixtures of ferrous iron and hydrogen peroxide are called Fenton reagent. If ferrous is replaced by ferric iron it is called Fenton-like reagent. Eqs. (4.5)–(4.11) show the reactions of ferrous iron, ferric iron and hydrogen peroxide in the absence of other interfering ions and organic substances. The regeneration of ferrous iron from ferric iron by Eqs. (4.8)–(4.10), is the rate limiting step in the catalytic iron cycle, if iron is added in small amounts. The listed rate and equilibrium constants for Eqs. (4.5)–(4.14) were reported by Sychev and Isak [171]:

$$Fe^{2+} + H_2O_2 \rightarrow Fe^{3+} + OH^{-} + OH^{\bullet} \qquad k = 53\text{–}76\,M^{-1}\,s^{-1} \tag{4.5}$$

$$Fe^{2+} + OH^{\bullet} \rightarrow Fe^{3+} + OH^{-} \qquad k = 2.6\text{–}5.8 \times 10^{8}\,M^{-1}\,s^{-1} \tag{4.6}$$

$$Fe^{2+} + HO_2^{\bullet} \rightarrow Fe^{3+} + HO_2^{-} \qquad k = 0.75\text{–}1.5 \times 10^{6}\,M^{-1}\,s^{-1} \tag{4.7}$$

$$Fe^{3+} + H_2O_2 \rightarrow Fe^{2+} + HO_2^{\bullet} + H^{+} \qquad k = 1\text{–}2 \times 10^{-2}\,M^{-1}\,s^{-1} \tag{4.8}$$

$$Fe^{3+} + HO_2^{\bullet} \rightarrow Fe^{2+} + O_2 + H^{+} \qquad k = 0.33\text{–}2.1 \times 10^{6}\,M^{-1}\,s^{-1} \tag{4.9}$$

$$Fe^{3+} + O_2^{\bullet -} \rightarrow Fe^{2+} + O_2 \qquad k = 0.05\text{–}1.9 \times 10^{9}\,M^{-1}\,s^{-1} \tag{4.10}$$

$$OH^{\bullet} + H_2O_2 \rightarrow H_2O + HO_2^{\bullet} \qquad k = 1.7\text{–}4.5 \times 10^{7}\,M^{-1}\,s^{-1} \tag{4.11}$$

Furthermore, radical–radical reactions have to be taken into account:

$$2OH^{\bullet} \rightarrow H_2O_2 \qquad k = 5\text{–}8 \times 10^{9}\,M^{-1}\,s^{-1} \tag{4.12}$$

$$2HO_2^{\bullet} \rightarrow H_2O_2 + O_2 \qquad k = 0.8\text{–}2.2 \times 10^{6}\,M^{-1}\,s^{-1} \tag{4.13}$$

$$HO_2^{\bullet} + OH^{\bullet} \rightarrow H_2O + O_2 \qquad k = 1.4 \times 10^{10}\,M^{-1}\,s^{-1} \tag{4.14}$$

Finally, the following equilibrium reactions have to be regarded [172]:

$$H_2O_2 \rightleftarrows HO_2^{-} + H^{+} \qquad K = 2.63 \times 10^{-12}\,M \tag{4.15}$$

$$[Fe]^{3+} + H_2O_2 \rightleftarrows [Fe(HO_2)]^{2+} + H^{+} \qquad K = 3.1 \times 10^{-3}\,M \tag{4.16}$$

$$[Fe(OH)]^{2+} + H_2O_2 \rightleftarrows [Fe(OH)(HO_2)]^{+} + H^{+} \qquad K = 2 \times 10^{-4}\,M \tag{4.17}$$

$$HO_2^{\bullet} \rightleftarrows O_2^{\bullet -} + H^{+} \qquad K = 3.55 \times 10^{-5}\,M \tag{4.18}$$

$$OH^{\bullet} \rightleftarrows O^{\bullet -} + H^{+} \qquad K = 1.02 \times 10^{-12}\,M \tag{4.19}$$

$$HO_2^{\bullet} + H^{+} \rightleftarrows H_2O_2^{\bullet +} \qquad K = 3.16\text{–}3.98 \times 10^{-12}\,M \tag{4.20}$$

4.2.3. Fenton reaction in the presence of inorganic and organic substances

If organic substances (quenchers, scavengers or in the case of wastewater treatment pollutants) are present in the system Fe^{2+}/Fe^{3+}/H_2O_2, they react in many ways with the generated hydroxyl radicals. Yet, in all cases the oxidative attack is electrophilic and the rate constants are close to the diffusion-controlled limit. The

following reactions with organic substrates have been reported [134]:

- Hydrogen abstraction from aliphatic carbon atoms, Eq. (4.21).
- Electrophilic addition to double bonds or aromatic rings, Eq. (4.22).
- Electron transfer reactions, Eq. (4.23).

$$OH^{\bullet} + RH \rightarrow R^{\bullet} + H_2O \quad (4.21)$$

$$R - CH = CH_2 + OH^{\bullet} \rightarrow R - C^{\bullet}H - CH_2OH \quad (4.22)$$

$$OH^{\bullet} + RX \rightarrow RX^{\bullet +} + OH^{-} \quad (4.23)$$

The generated organic radicals continue reacting prolonging the chain reaction. Depending on the oxidation–reduction potential of the organic radical generated, reactions (4.24)–(4.27) can take place. The organic peroxide generated in reaction (4.27) can further react with ferrous iron similar to the Fenton reaction, (4.28). Of special interest is the reaction with dissolved oxygen (Dorfman-mechanism), Eqs. (4.29) and (4.30) [173], because the peroxyl radical can regenerate hydrogen peroxide by reaction ((4.7) and (4.25)) and thereby contribute to reduce the consumption of oxidant in wastewater treatment by Fenton and photo-Fenton method:

$$R^{\bullet} + Fe^{3+} \rightarrow R^{+} + Fe^{2+} \quad (4.24)$$

$$R^{\bullet} + Fe^{2+} \rightarrow R^{-} + Fe^{3+} \quad (4.25)$$

$$R^{\bullet} + R^{\bullet} \rightarrow R - R \quad (4.26)$$

$$R^{\bullet} + HO_2^{\bullet} \rightarrow RO_2H \quad (4.27)$$

$$Fe^{2+} + RO_2H \rightarrow Fe^{3+} + OH^{-} + OR^{\bullet} \quad (4.28)$$

$$R^{\bullet} + O_2 \rightarrow RO_2^{\bullet} \quad (4.29)$$

$$RO_2^{\bullet} + H_2O \rightarrow ROH + HO_2^{\bullet} \quad (4.30)$$

In the case of aromatic pollutants the ring system usually is hydroxylated before it is broken up during the oxidation process. Substances containing quinone and hydroquinone structures are typical intermediate degradation products, e.g., produced by reactions equivalent to Eqs. (4.31) and (4.32). These are especially worth mentioning because they provide an alternative, quicker pathway for ferrous iron regeneration through Eqs. (4.33) and (4.34) accelerating thereby the process. Resulting benzoquinone structures can also be reduced as in Eq. (4.35). Thereby, each molecule can reduce several ferric iron ions in a catalytic cycle. Anyway, sooner or later this catalytic cycle is interrupted, because in competition with reactions (4.31)–(4.35) also ring opening reactions occur, which further carry on the mineralization of the molecule [174]:

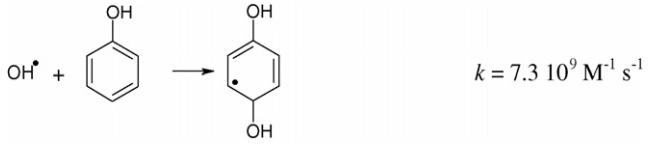

(4.31)

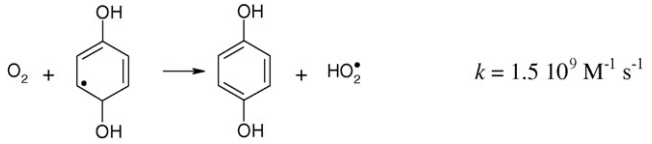

(4.32)

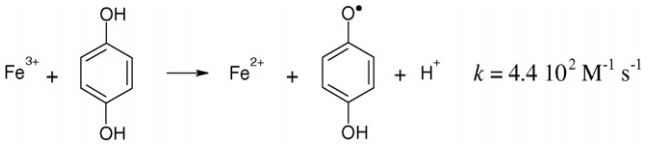

(4.33)

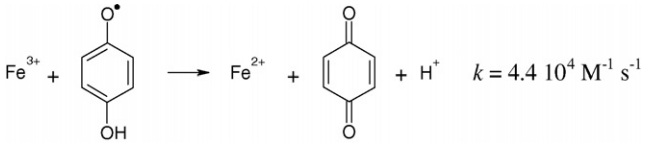

(4.34)

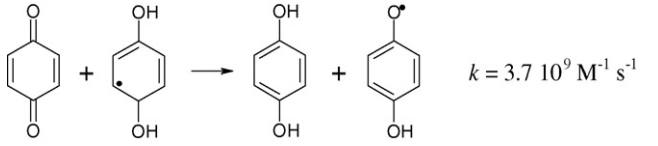

(4.35)

There is one great setback of the Fenton method. Especially when the treatment goal is the total mineralization of organic pollutants, carboxylic intermediates cannot be further degraded. Carboxylic and dicarboxylic acids are known to form stable iron complexes, which inhibit the reaction with peroxide [175]. Hence, the catalytic iron cycle reaches a standstill before total mineralization is accomplished, Eq. (4.36):

$$Fe^{3+} + nL \rightarrow [FeL_n]^{x+} \xrightarrow{H_2O_2,\,dark} \text{no further reaction} \quad (4.36)$$

L: mono- and dicarboxylic acids.

Due to the high oxidation potential of the hydroxyl radical, it can also react with inorganic ions present in the solution. Several authors have described the strong negative effect of the presence of carbonate and phosphate in the Fenton reaction, while the effect of other ions such as chloride or sulphate is not as strong [152,173,176,177]. Phosphate has a double detrimental effect; first, it precipitates iron and second, it scavenges hydroxyl radicals.

De Laat et al. [152] presented a rather comprehensive review of the additional reactions and equilibria of importance in the presence of significant amounts of chloride and sulphate. Both ions are capable of complexing ferric as well as ferrous iron. They can thereby hinder reactions or also open completely new reaction pathways for the decomposition of hydrogen peroxide in the presence of dissolved iron. Also, hydroxyl radicals generated can react with these ions, creating chlorine radicals and sulphate radicals. Some representative reactions are shown in Eqs. (4.37)–(4.40):

$$OH^{\bullet} + Cl^{-} \rightarrow [ClOH]^{\bullet -} \qquad k = 4.3 \times 10^{9}\ M^{-1}\ s^{-1} \quad (4.37)$$

$$[ClOH]^{\bullet -} + H^{+} \rightarrow [HClOH]^{\bullet} \qquad k = 3.0 \times 10^{10}\ M^{-1}\ s^{-1} \quad (4.38)$$

$$[HClOH]^{\bullet} + Cl^{-} \rightarrow Cl_2^{\bullet -} + H_2O \qquad k = 8.0 \times 10^{9}\ M^{-1}\ s^{-1} \quad (4.39)$$

$$OH^{\bullet} + HSO_4^{-} \rightarrow H_2O + SO_4^{\bullet -} \qquad k = 3.5 \times 10^{5}\ M^{-1}\ s^{-1} \quad (4.40)$$

De Laat and co-workers further calculated, that below pH 4 practically all hydroxyl radicals end up in chlorine radicals (calculations done for 100 mM NaCl solution). In the presence of sulphate the conversion of hydroxyl radicals is considerable at acidic pH as well. Yet, it should be mentioned that these

calculations were performed for solutions without any other scavenging substances (e.g., organic pollutants). There are two negative effects; first, the chlorine and sulphate radicals are potentially weaker oxidants and the overall process efficiency becomes diminished and second, chlorine radicals can electrophilically add themselves to double bonds similar to hydroxyl radicals and generate undesired chlorinated intermediate reaction products, such as detected by Kiwi et al. [176].

4.2.4. Photochemical reactions

The primary step of the photoreduction of dissolved ferric iron is a ligand-to-metal charge-transfer (LMCT) reaction. Subsequently, intermediate complexes dissociate as shown in reaction (4.41) [142]. The ligand can be any Lewis base able to form a complex with ferric iron (OH^-, H_2O, HO_2^-, Cl^-, R–COO^-, R–OH, R–NH_2, etc.). Depending on the reacting ligand, the product may be a hydroxyl radical such as in Eqs. (4.42) and (4.43) or another radical derivated from the ligand. The direct oxidation of an organic ligand is possible as well as shown for carboxylic acids in Eq. (4.44):

$$[Fe^{3+}L] + h\nu \rightarrow [Fe^{3+}L]^* \rightarrow Fe^{2+} + L^\bullet \quad (4.41)$$

$$[Fe(H_2O)]^{3+} + h\nu \rightarrow Fe^{2+} + OH^\bullet + H^+ \quad (4.42)$$

$$[Fe(OH)]^{2+} + h\nu \rightarrow Fe^{2+} + OH^\bullet \quad (4.43)$$

$$[Fe(OOC{-}R)]^{2+} + h\nu \rightarrow Fe^{2+} + CO_2 + R^\bullet \quad (4.44)$$

Depending on the ligand the ferric iron complex has different light absorption properties and reaction (4.41) takes place with different quantum yields and also at different wavelengths. Consequently, the pH plays a crucial role in the efficiency of the photo-Fenton reaction, because it strongly influences which complexes are formed (e.g., see Eqs. (4.1)–(4.4), Fig. 21). Thus, pH 2.8 was frequently postulated as an optimum pH for photo-Fenton treatment (e.g., [177,178]), because at this pH precipitation does not take place yet and the dominant iron species in solution is $[Fe(OH)]^{2+}$, the most photoactive ferric iron–water complex. In fact, as shown in its general form in Eq. (4.41), ferric iron can form complexes with many substances and undergo photoreduction. Of special importance are carboxylic acids because they are frequent intermediate products in an oxidative treatment. Such ferric iron–carboxylate complexes can have much higher quantum yields than ferric iron–water complexes. It is therefore a typical observation that a reaction shows an initial lag phase, until intermediates are formed, which can regenerate more efficiently ferrous iron from ferric iron accelerating the process. This can either happen through a photochemical pathway, Eq. (4.44), a thermal pathway, e.g., Eqs. (4.31)–(4.35), or a combination of both.

The addition of oxalate has been proposed to overcome the initial lag phase [158,178]. Thereby, the wastewater throughput in a photo-Fenton plant can be raised, but these gains have to be compared to the increased reagent cost due to the addition of oxalate, because oxalate is not acting as a catalyst, as it is as well degraded during this photochemical reaction. Other chelating agents have been proposed as well with the additional aim of working at neutral pH [157,179]. The photolysis of ferric iron–oxalate complexes has been known for a long time and is used in actinometry for its high and well-defined quantum yield for Eqs. (4.45) and (4.46):

$$Fe(C_2O_4)_3^{3-} + h\nu \rightarrow Fe^{2+} + 2C_2O_4^{2-} + C_2O_4^{\bullet-} \quad (4.45)$$

$$C_2O_4^{\bullet-} + Fe^{3+} \rightarrow 2CO_2 + Fe^{2+} \quad (4.46)$$

Finally, another photochemical reaction should be mentioned, which is the photoreduction of quinones to semiquinones, Eq. (4.47) [180]. By this reaction intermediate quinonic reaction products can be reduced and can further contribute to accelerate the reduction of ferric iron by Eq. (4.34). As a side product even a hydroxyl radical is generated:

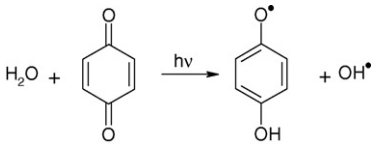

(4.47)

Fe(III) complexes present in mildly acidic solution, such as $Fe(OH)^{2+}$ absorb light appreciably in the UV and into the visible region. The quantum yield for Fe^{2+} formation in Eq. (4.42) is wavelength dependent. It is 0.14–0.19 at 313 nm and 0.017 at 360 nm [181]. Fe(III) may complex with certain target compounds or their by-products. These complexes typically have higher molar absorption coefficients in the near-UV and visible regions that the aquo complexes. Polychromatic quantum efficiencies in the UV/visible range from 0.05 to 0.95 are common [141]. Fe(III)–oxalate complexes (Eq. (4.45)) is efficient up to 500 nm (quantum efficiency 1.0–1.2).

4.3. Process parameters and their influence

4.3.1. pH

The need for acidification in the photo-Fenton process is often outlined as one of its major drawbacks. Not only does this mean additional cost through the consumption of reagents for acidification and subsequent neutralization but also an increase of the treated water's salt load. Still one cannot get around acidification, if the application is based on dissolved iron salts and the application requires maintaining the iron dissolved for longer than a few minutes. Exceptions and proposed strategies are to be mentioned below.

Those scientists treading the conventional path accepting the need for acidification have searched from the very beginning for an optimal pH and several authors soon proposed a pH around 2.8 as the optimum operating condition [177,178]. A pH of 2.8 avoids iron precipitation (at least under low to moderate iron concentration below approx. 1 mM), but maximizes the concentration of mono- and dihydroxylated iron(III) aquo complexes, which absorb UV light more efficiently than the non-hydroxylated iron(III) complexes (see also Fig. 21). This was accepted by many authors as a matter of fact and henceforth many publications appeared applying this pH.

Nevertheless, considering that the chemistry of dissolved iron is much more complex, mainly due to the fact that iron can form complexes with many Lewis bases, evidently a number of scientists proposed that in the presence of complexing agents the need for acidification could be circumvented [157,179,182]. Also, simply through the presence of organic acids in the wastewater, which are also generated through the oxidation process itself, not always a pH as low as 2.8 is necessary, e.g., a pH of 4–5 was sufficiently low to maintain iron (2–6 mM) dissolved in the case of olive mill wastewater with high organic load (approx. 20 g/L initial dissolved organic carbon) [150].

Usually, the reduction of ferric iron is the rate limiting step in Fenton and photo-Fenton applications. Photoreduction of ferric iron complexes (Eqs. (4.41)–(4.44) takes place at longer wavelengths, when aquo and hydroxyl ligands are replaced with stronger complexing agents. Hence, if present, upon irradiation with sunlight (a polychromatic radiation source with only a few percent of its irradiance power pertaining to the UV range) these complexes contribute more to the photoreduction than the aquo and hydroxyl complexes. Consequently, one must state that the

early explanation for an optimum pH of 2.8 based on the absorbance spectra of different aquo and hydroxyl ferric iron complexes seems only plausible in the absence of complexing agents. This is seldom the case, as carboxylic acids are formed in the oxidation process. Hence, the only real constraint seems to be the need of avoiding iron precipitation.

4.3.2. Iron concentration and iron source

In "normal" photo-Fenton applications (i.e., pH < 3, dissolved iron as catalyst), where equal or less than 1 mM of dissolved iron was studied as maximum concentration [145,183–185], an increase in iron concentration always led to an increased reaction rate as well. Yet, this increase is not directly proportional but levels off as higher concentrations are applied. Other studies applying higher iron concentrations up to 450 mg/L [186–188] still continued to find increasing reaction rate up to their maximum iron concentration applied.

One of the principle characteristics of a photoreactor is its optical pathlength, e.g., in the case of a tubular reactor the tube diameter. A ray of light is attenuated along the optical pathlength as a function of the solution's extinction coefficient, which is closely related to the iron concentration. In general the photoreactor (i.e., the solar collector in the case of a solar-driven photocatalytic plant) constitutes a substantial part of the investment cost of the installation. Hence, one aim in the design of a photoreactor is that nearly the whole volume of the photoreactor is illuminated. A too high iron concentration generates dark zones in the photoreactor, because the incident ray is attenuated too strongly along the optical pathlength [159]. Nevertheless, as photo-Fenton chemistry involves also significant thermal reactions (e.g., Eqs. (4.8)–(4.10) and Eqs. (4.31)–(4.35) for the thermal reduction of ferric iron), usually an increase of iron concentration beyond the needed concentration to absorb all photons inside the photoreactor will still lead to a further increase of reaction rate. Still, then, the same result may be achieved with a different photoreactor, with less optical pathlength and which may be cheaper to construct.

The inner filter effects present in the solution are another important issue regarding the effect of iron concentration on the reaction rate. Inner filter effects are the competitive absorption of photons by other light absorbing species, usually the contaminants present in the wastewater. Whereas this competitive light absorbance may lead also to some direct photolysis reactions, photolysis reactions normally have a low quantum yield. Hence, if photolysis is not effectively taking place, photons absorbed by the contaminants instead of the catalyst may be considered lost in terms of efficient photon use. Oliveros et al. [187] studied the influence of the irradiation source on the process and found that a medium pressure mercury lamp (majority of photons irradiated between 300 and 400 nm) performed superior compared to a low pressure mercury lamp (254 nm) and an excimer lamp (222 nm). They attributed this to the inner filter effects present at low wavelengths for their model wastewater (containing xylidine). Also, Gernjak et al. [145] found an improved performance applying sunlight compared to a medium pressure mercury lamp for model compounds absorbing in the UV region (in this particular case vanillin). In a similar sense it can be explained why Torrades et al. [188] found an increased reaction rate until very high iron concentrations (450 mg/L), as they treated a strongly coloured cellulose bleaching effluent, as a high catalyst concentration is being needed to compete efficiently for the photons in the highly coloured wastewater.

Consequently, one may state that iron concentration optimization must take into account the solar collector geometry (or vice versa [149]) and the inner filter effects. Also, to reduce inner filter effects, sunlight seems an ideal irradiance source. This ability to make use of photons of a wavelength beyond the UV region may also be one of the main reasons why photo-Fenton compares favourably to TiO_2 photocatalysis, when applied to highly coloured wastewaters [149]. Only logically following then is that another strategy to overcome inner filter effects is procuring that iron complexes are present that absorb at higher wavelengths than the contaminants present in wastewater, which is part of the reason, why applying iron sources containing already iron chelating ligands have been proposed such as ferric oxalate [158,189], ferric citrate [182] or also other chelating agents [179]. Whereas there are several obvious advantages (higher reaction rate through absorption of more solar photons, possibility to raise the pH) literature has not discussed the influence on the economy of the process in the sense of enhanced reagent costs. Not only is there an additional cost for adding the chelating agent, also, as the chelating agent is being oxidized as well more hydrogen peroxide ought to be needed to abate the target contamination.

Another interesting finding of the group of Sun and Pignatello [179] was, that partly oxidised chelates may even cause a further enhancement of the reaction rate compared to the same chelates in their none-oxidised form, or expressed in a different way, an initial lag-phase was observed. A later work of the same group [174] explained such an observed phenomenon by the involvement of hydroquinones and quinones. Consequently, an enhancement of reaction rate may not only be achieved by selecting an iron source containing chelates, but also by blending the wastewater with partly oxidised wastewater. Such a blending may be done on purpose in a batch mode of operation, but also may be a desirable side-effect of operation schemes that involve continuous operation mode.

Another possibility is the application of iron as a heterogeneous catalyst, as commented in Section 4.1, e.g., in the form of suspended oxides [153], fixed on a support structure [154,190] or even a combination of both [155]. While an easy separation and the possibility of working without pH adjustments are advantages of this approach, the drawback are generally diminished reaction rates compared to the homogeneous photo-Fenton process. This is mainly related with mass transfer limitations of the heterogeneous process and worsened light penetration into the photoreactor in the presence of solids [156].

Taking into account the comparably high price of the solar collector, a loss of reaction rate (i.e., an increase of needed collector surface) directly is reflected in the treatment costs and Gumy et al. [190] found a difference of approx. 50% and 75% between homogeneous and heterogeneous photo-Fenton reaction, depending on the solar collector applied. Though this is a single case study making such an economical comparison, it nicely highlights that science should not only focus on developing new catalysts but also on how these catalysts could be applied minimizing costs.

4.3.3. Influence of temperature

When investigated, increasing temperature always had a beneficial effect on reaction kinetics [160,183,186]. Within the investigated limits in these studies (maximal iron concentration 2.6 mM, maximal temperature 70 °C) an increase of the respective parameter always caused also an increase in reaction rate, e.g., by about 5 times by raising temperature from 20 to 50 °C [183]. In another study already mentioned [188] a maximum "process efficiency" was found to be around 55 °C. Yet, this study takes into account the hydrogen peroxide consumption efficiency, because at higher temperatures more hydrogen peroxide is consumed to reach the same level of TOC mineralization. This can be explained by looking at the thermal reactions involved in the reduction of ferric iron, particularly Eqs. (4.8)–(4.10) as opposed to the photoreduction of ferric iron. Whereas in the thermal pathway hydrogen peroxide is consumed for the reduction of ferric iron

without producing hydroxyl radicals, in the photoreduction pathway hydrogen peroxide is not consumed. This seems an obvious and easy explanation, but normally the issue becomes complicated when other reactions are involved as the already mentioned reactions with hydroquinones and quinones, Eqs. (4.31)–(4.35) and (4.47).

To our knowledge no study has ever tried to solve the tricky problem that presents the estimation of hydrogen peroxide consumption based on first principle models (i.e., the chemical equations) in the presence of organic contaminants taking into account the influence of temperature. For practical purposes in the optimization of the application the trade-off situation (increased reaction rate vs. higher oxidant consumption) has to be regarded as such, but theoretical studies may be helpful, particularly on the issue, how hydrogen peroxide consumption may be lowered.

4.3.4. Irradiance wavelength, light penetration and irradiance intensity

The first of the three aspects in the heading has been dealt with previously (Sections 4.3.1 and 4.3.2) and here, as a summary from the previous sections, we would only like to point out that sunlight has been found as an adequate polychromatic irradiation source, compared to shorter wavelength UV lamp sources. This is because the longer wavelengths are able to overcome inner filter effects better by photolysing ferric iron complexes [145,187]. Also, to make efficient use of this effect and to increase the share of photons used, another option is to apply iron sources [158,179], which augment the concentration of complexes, which may be photolysed by wavelengths of the visible part of the solar spectrum.

Light penetration is related to solar collector engineering, as ideally the whole photoreactor is illuminated [159]. This goal is not always as simple to achieve, because due to the formation of intermediate degradation products the absorbance of a wastewater may change considerably during the treatment. Whereas this is of an intrinsic logic (e.g., the objective of dye wastewater treatment may be its decolourization), it may have considerable influence on the reaction rate along the process, impeding photons from entering the reactor. Also, wastewater, which initially is not strongly coloured may develop colour during the treatment. An example is given in Fig. 22, where 1 g/L of alpha-methyl phenyl glycine was treated in a solar collector with 5 cm diameter tubes (as described by [186]) applying 1 mM of ferrous iron sulphate. This figure clearly illustrates the dilemma of the engineer for choosing an appropriate optical pathlength for the solar collector as different points during the degradation may be chosen as the design point.

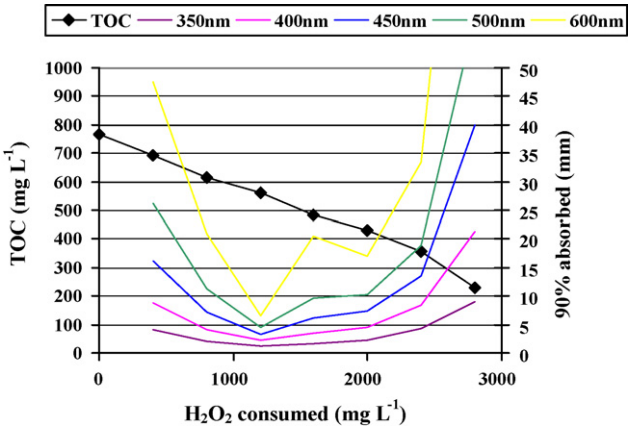

Fig. 22. Experiment in pilot-plant. α-Methyl phenyl glycine = 1 g L^{-1}; C_{Fe} = 1 mM, V = 75 L. Optical pathlength, after which 90% of radiation is absorbed. Initial sample not shown, because the contaminant does not absorb at wavelengths above 300 nm.

Finally, the third aspect, radiation intensity, was not investigated in dedicated studies as such to our knowledge. Either, some investigations focused on the variation of optical pathlength, e.g., or on the difference between direct sunlight/shadowy conditions [184] or midday/afternoon sunlight [191]. These studies found always a higher reaction yield / incident photons, when less irradiance power per volume was applied as is shown in the last column of Table 3 for the data from the paper from Krutzler et al. [184]. Provided that solar collector area is one the most important influences on the costs of the process, this paper contains valuable information. Whereas the explanation is obviously again related with the parallel occurrence of thermal reactions, few investigation was performed to explain with more detail a tool for plant optimization.

Another approach would be the investigation of alternating time intervals in the dark and under illumination such as performed by two studies [183,192]. Both studies found promising results regarding the reduction of necessary light amount, supposedly through the formation of precursors in the dark, which then readily photolyse upon irradiation. Gernjak et al. [183] could reduce the amount of necessary photons to achieve a defined reaction progress (50 and 80% of TOC mineralization) by a factor of approximately 2.5. This was achieved by reducing the solar collector area by a factor 5 maintaining the volume constant. Also, these studies provide interesting data, but they focus on a single parameter (kinetics of TOC mineralization). Future studies should take also into account such effects as enhanced pumping energy

Table 3
TOC mineralization rates for the oxidation of 3 mM 4-chlorophenol in the presence of 0.75 mM iron at an initial pH of 2.8. The reactor is a basin with varied depth, area 0.4 m^2 and was exposed to shadow and direct sunlight conditions. The first 4 columns are obtained from Krutzler et al. [184], the other TOC mineralization rates have been calculated based on the data given in this paper.

Run	Depth (cm)	I (W/m^2)	Different TOC mineralization rate constants			
			(mg TOC/L min)	(mg TOC/min)	(mg TOC/kJ L)	(mg TOC/kJ)
1	0.5	518	10.1	20.2	0.81	1.62
2	1	717	13.4	53.6	0.78	3.11
3	2	555	9.1	72.8	0.68	5.47
4	3	623	8.5	102	0.57	6.82
5	4	176	2	32	0.47	7.58
6	5	544	3.6	72	0.28	5.51
7	0.5	224	8.3	16.6	1.54	3.09
8	1	110	3.7	14.8	1.40	5.61
9	2	106	2.8	22.4	1.10	8.81
10	3	137	3	36	0.91	10.95
11	4	98	1.9	30.4	0.81	12.93
12	5	88	1.6	32	0.76	15.15

(though the amount of solar collector is reduced, the time needed for completion of mineralization goal is doubled).

4.3.5. Substrate concentrations and chemical characteristics

Many studies have included the influence of the contaminant concentration in the scope of their investigation. Basically, the logical outcome was that higher pollutant concentrations needed a longer treatment time under otherwise identical process conditions. Yet, the already mentioned filter effects are prone to increase at higher concentrations (see also Fig. 22). Consequently, Krutzler et al. [184] found that an increase from 1 to 5 mM 4-chlorophenol lower the TOC mineralization rate from 14.9 mg/L min TOC to 8.9 mg/L min TOC (calculated for a 50% TOC mineralization degree). So, if the influent concentration is to be expected to change in an application, the correct scaling and design of the photoreactor may be complicated, because the correlation of necessary treatment time and substrate concentration must not be directly estimated, but always be determined by experiment.

To our knowledge the influence of chemical characteristics of the substrate was never studied explicitly and no such studies exist, which try to rate the reactivity of a broad range of chemicals rationalizing their behaviour based on a chemical description of the target molecule (e.g., in the sense of a QSAR study). Nevertheless there exist a series of papers, which compare the degradation of several compounds under otherwise identical conditions [143–145,193–195]. Some of these papers also perform TiO_2 photocatalysis on the same model wastewaters [193,195], which helps to point out several aspects specific to photo-Fenton. Several conclusions may be drawn from comparing the data of these papers. First, Fallmann et al. [143] found that among the ten pesticides tested Methamidofos was most difficult to degrade due to its ability to release phosphate into the solution and precipitate the iron catalyst. Among the others tested Vydate had an unusual long initial lag phase, which was also confirmed by Oller et al. [195]. The latter paper did not find a similar lag phase during TiO_2 photocatalysis, though unfortunately it is not clarified if these lag phase was caused by active ingredient, oxamyl, or other compounds present in the commercial formulation applied. As iron measurements confirmed the presence of the dissolved iron and the effect was not observed in the TiO_2 application, it remains clear that dissolved iron is being complexed and inactivated. In the same study 1,3-dichlorpropane was studied and in this case the photo-Fenton reaction occurred extraordinarily quickly showing the preference of the photo-Fenton reaction towards the electron rich bonds. The effect could not be observed to a similar extent in the comparison of the oxidation of chlorinated solvents (chloroform, dichloromethane and 1,2-dichloroethane) by Malato et al. [194].

In two studies, atrazine was observed to be more recalcitrant to photo-Fenton treatment than other compounds treated in comparison with data obtained by TiO_2 photocatalysis [144,193], which is likely due to the low electron density in the aromatic ring. Several compounds were shown to be impossible to be quickly completely mineralized, such urea herbicides [193] and atrazine [193], the latter one being impossible to degrade further than cyanuric acid. In the case of diuron it may depend on the process conditions, because another study reports complete mineralization [158].

On the other hand phenolic compounds are always very quickly degraded and just in agreement with the studies of Chen and Pignatello [174] those substances reacted fastest, which are more oxidized (gallic acid > protocatechuic acid > vanillin > p-coumaric acid > l-tyrosine) and hence sooner will form hydroquinones and benzoquinones contributing to an accelerated redox cycle of the iron catalyst. This study confirmed also the preference of the oxidant species for the phenolic structures by measuring in a mixture of these five phenols the phenol index dropped to zero already at approx. 50% of TOC mineralization. It may be concluded that aromatic and phenolic contamination can be abated by the photo-Fenton reaction with high reaction rates as shows the comparison with another AOP. In the case of aliphatic substances or aliphatic intermediates the performance may be less favourable. Also, the photo-Fenton reaction may be strongly influenced by inorganic ions released during the degradation process, particularly phosphate. Also, if large amounts of ammonia are released this may cause a problem through an increase of pH and subsequent catalyst precipitation.

4.3.6. Salinity

Excellent theoretical studies exist by the group of De Laat on the effect of chloride and sulphate in Fenton systems (e.g., [152]). Basically, the study states that at low pH (below 3) an ever increasing amount of hydroxyl radicals are converted into chlorine radical species and, to a lesser degree, sulphate radicals. These radicals are less reactive and hence they postulate an effect on the degradation efficiency. The effect can have several aspects, among them an effect on process kinetics, loss of oxidant power (thermodynamic effect) and less efficient use of oxidant. Whereas first and third effect bore down proportionally on the costs of the process, a loss of oxidant power may imply that certain pollutants or intermediate degradation products may not been degraded in the presence of salts.

Other applied studies found, that though there is a significant influence on the reaction kinetics, the photo-Fenton still works even in salt concentrations as high as present in seawater [196,197], though with a reduced reaction rate. A recent paper [198] postulated that the negative effect of chloride on the kinetics of the photo-Fenton reaction may be circumvented by working at a pH slightly above 3. Only one paper [176] reported the formation of chlorinated intermediate degradation products, but since then no other study reported the same fact and it remains an open issue, because the generation of such degradation products would be highly undesirable. In the specific case of a chloride-rich environment, chlorine radicals are also formed following a sulphate radical (see reaction (4.40)) mediated attack on the chloride ion. A termination reaction of a chlorine radical with an organic radical could lead to the formation of chlorinated derivatives. Chlorinated derivatives were indeed formed, but due to the dual effect of chlorine and sulphate radicals [77].

4.3.7. Oxidant concentration

The influence of oxidant concentration on the kinetics was investigated by several studies and the main findings can be reduced to the fact that neither too low hydrogen peroxide concentration (leading to a rate reduction of the Fenton reaction) nor a too high concentration may be applied (H_2O_2 competes successfully for hydroxyl radicals and becomes decomposed with oxidizing the pollutant). Usually, there is a rather broad concentration interval in between both extremes, where none of both phenomena occurs. Hence, it has been found that the H_2O_2 concentration, i.e., its consumption may be used to predict the progress of a photo-Fenton application [183,196,199], i.e., hydrogen peroxide addition can also be used to control the mineralization degree desired in an application. This fact is an advantage insofar as the control of hydrogen peroxide addition is relatively easy as in a wide range of variation of process parameter a change does not affect. But it is also a disadvantage, because it means that reducing hydrogen peroxide consumption is not easily done. The efficiency of the oxidant use with respect to the theoretically needed stoichiometric amount of hydrogen peroxide is highly dependent on the substrate and its concentration, with the data of ranging below the stoichiometric amount of hydrogen peroxide

[48] up to several times the stoichiometric need for the measured COD reduction [195].

Though theoretical explanations for a better-than-stoichiometric oxidant consumption efficiency may be given through the Dorfman mechanism [173], which was also experimentally evidenced for photo-Fenton reaction [200], no significant reduction of hydrogen peroxide consumption has been achieved up-to-date by working under continuous oxygen saturation under typical process conditions, i.e., higher substrate concentration and degradation rate. Another way of harvesting additional hydroxyl radical would be the photoreduction of quinones. Given the important influence of the hydrogen peroxide consumption on the process costs, additional research should be performed on how to reduce the oxidant consumption.

4.4. Solar hardware and engineering aspects relevant to photo-Fenton

Reports exist that provide excellent reviews of the needs towards the solar hardware for photocatalytic processes based on TiO_2 application including aspects of optics, geometry and reactor materials [48,67,159]. This literature also reviews the different solar collectors developed up-to-date and pilot-plant and industrial applications. They are also up-dated in this paper elsewhere, and this section will try to focus on the aspects relevant to photo-Fenton. Historically speaking, the first solar photoreactor designs for photochemical applications were based on line-focus parabolic-trough concentrators (PTCs). PTC concentrators represented a mature engineering concept due to their former similar development for solar thermal applications and were readily available, when solar photocatalysis was first implemented around 1990.

In this type of concentrators an absorber tube is placed in the focus of a parabolic reflector. The reflector redirects radiation parallel to the axis of the parable towards the absorber tube in the focus. Consequently, this type of concentrator has to track the sun and can use only parallel direct beam radiation. They can be easily set-up and scaled-up due to the simple engineering concepts involved (tubular plug-flow photoreactor with turbulent flow conditions). Turbulent flow ensures good mass-transfer and maintains TiO_2 particles in suspension in case of TiO_2 slurry photocatalysis. Another advantage is that the photoreactors are closed systems. Therefore, no vaporization of volatile compounds takes place. A disadvantage of PTCs is, that due to their geometry they can use only direct beam radiation, which makes them practically useless, when the sky is clouded. They also are rather expensive systems due to the necessary sun tracking system. This applies to the investment as well as to the maintenance costs, because moving parts are prone to require enhanced maintenance effort. Furthermore and most important, high irradiance in TiO_2 photocatalytic systems leads to a loss of quantum yield.

Subsequently, it took then around 10 years to develop and validate a series of different reactor concepts trying to overcome the intrinsic weaknesses of concentrating collectors, leading to the development of non- and low-concentrating reactors:

- Free-falling film: the process fluid falls slowly over a tilted plate with a catalyst attached to the surface, which faces the sun and is open to the atmosphere [201].
- Pressurized flat plate: consists of two plates between which the fluid circulates using a separating wall [202].
- Solar ponds: small, shallow, on-site pond reactors [203].
- Compound parabolic collectors: a tubular reactor above a reflector consisting of two truncated parables with a concentration factor (ratio of tube perimeter to aperture) of around one [29].

Our group strongly supported the development and application of compound parabolic collectors and more details on the background and their advantages are given elsewhere in this paper. Compared to TiO_2 photocatalysis (research since the seventies with a large boom starting towards the end of the eighties) photo-Fenton is like a little younger cousin (research starting in the early nineties with a boom starting around 10 years later). As a consequence, while growing up, the younger cousin had to wear the older cousin's used shoes, i.e., most researchers applied the same solar reactors for photo-Fenton that were applied previously for TiO_2 photocatalysis without taking into account that photo-Fenton treatment implies different constraints and opportunities for designing effective photoreactors. Hence, the situation can be compared to the early nineties, when PTCs, being readily available, were taken as a starting point for photoreactor design, although it soon had become clear that the reactors were not an optimal solution. Having it mentioned previously, that photo-Fenton application has limitations and yields opportunities regarding the solar collector, Table 4 now compares TiO_2 and photo-Fenton with respect to photoreactor design requirements.

As mentioned before the process differences provide several important opportunities for reactor optimization, where one of the obvious is being the beneficial effect of higher temperature. If the temperature is to be increased this implies an increased cost per square meter of collector as thermal insulation may be necessary. Then, such an approach would make use of the intrinsically present heat radiation in sunlight. Hence, the only cost for "heating" would be the enhanced cost of investment as solar radiation is "free". Processes that discharge hot wastewater (e.g., paper mill, dying industry) would be ideal candidates. Also, any other adjacent process providing waste heat could be incorporated easily. The photo-Fenton processes own heat could be recycled via heat exchangers as generally it is undesirable or even forbidden to discharge the wastewater hot.

A second way of making more heat efficient solar collectors may be learned from the solar thermal industry and would mean in a certain way to go back to the roots. As heat dissipation is largely proportional to the surface area of the photoreactor, a higher concentration ratio of the solar collector decreases the heat losses at a given temperature. Whereas this was ruled out as a good reactor concept for TiO_2 photocatalysis due to the decreased quantum efficiency at higher irradiance power, such an effect may not exist for photo-Fenton. Fig. 23 shows an example performed at our facilities, which compares the treatment of a synthetic wastewater treated in two different solar photoreactors (concentrating and low-concentrating) with two different AOPs (photo-Fenton and $TiO_2/S_2O_8^{2-}$). A mixture of 9 commercial pesticide formulations was prepared for degradation. The solution contained a TOC of 100 mg/L originating in equal parts from each pesticide formulation. Degradation experiments were performed in the Helioman reactor with photo-Fenton (20 mg/L iron) and $TiO_2/S_2O_8^{2-}$ (200 mg/L catalyst).

Concerning the two titanium dioxide experiments the Helioman reactor (see [67] for reactor details) turns out to yield clearly worse results than the CPC reactor (see [29] for reactor details). This is due to the low order dependency of the reaction rate on the irradiation intensity. So the non-concentrating reactor geometry leads to higher quantum yield. It can be also observed that in the case of the photo-Fenton process no such obvious effect can be observed. The somewhat better performance of the CPC type reactor could be explained by a slightly better optical efficiency of the collector. Hence, this attribute, also mentioned in the table, facilitates a whole new set of solar collector concepts for the photo-Fenton method.

These experiments were performed under clear sky conditions. In case of cloudy skies the CPC type collectors would of course yield a lot better results compared to the Helioman due to their ability to absorb also diffuse radiation. Nevertheless, it must be noted that

Table 4
Comparison of TiO_2 and photo-Fenton process aspects relevant to the photoreactor's design requirements.

	TiO_2	Photo-Fenton
Stress on reactor materials	Corrosive liquids: oxidative process, pH and salt concentration depend on application.	Corrosive liquids: oxidative process, H_2O_2, iron ions, usually acidic pH (2–3.5), salt concentration and temperature depend on application.
Cleaning procedures	TiO_2 may adsorb on the reactor walls preventing illumination, effective chemical cleaning agents are HCl, and mostly, H_2F_2.	Iron oxides may deposit on the reactor walls preventing illumination, effective chemical cleaning agents are chelating agents, such as oxalic acid and acidic pH.
Residence time in collector	Long residence time in the collector may cause dissolved O_2 depletion.	Long residence time in the collector may cause H_2O_2 depletion.
Temperature	Not relevant to process performance between 20 and 80 °C.	Strongly influential on process performance, beneficial if higher.
Flow conditions	Turbulent flow necessary to maintain TiO_2 suspension in solution and to avoid mass transfer limitations.	Homogeneous iron catalyst, hence no precipitation; no data available, if laminar flow leads to mass transfer limitations.
Reactor diameter/ depth—optical pathlength	Light distribution in the collector is largely governed by absorbance and scattering by the catalyst particle. A direct correlation between ideal catalyst concentration and diameter exists.	Light distribution is governed by absorbance of the solution, which is a function of catalyst concentration and wastewater. Absorbance varies strongly along the treatment due to the appearance and destruction of compounds.
Effective wavelength range	<390 nm for TiO_2, being approx. 4% of sunlight's irradiance power (sunny days).	Depends strongly on the presence of complexes, may be up to 550–600 nm being 28–35% of sunlight's irradiance power (sunny days).
Light intensity	Rate law changing from first through half order to zero-order dependency as the light intensity increases.	Little research performed, first order rate law suggested over a broad range of light intensity, applicable as long as ferric iron predominates over ferrous iron.
Dark zones	No reactions taking place in dark zones.	Fenton process takes place in dark zones, elevated temperature influences the reaction rate positively. Alternating dark and illumination intervals have shown to reduce the necessary illumination time.
Process control	Process control mainly includes the determination of treatment end.	Process control includes the determination of the treatment end. pH must be controlled to avoid iron precipitation.

the experiments were performed applying an air cooler (fan system) in the Helioman system to ensure similar temperatures in both reactors to enable comparison between both reactors. If the reactor had been allowed to heat up, the comparison clearly would have been favourable for the Helioman reactor in the case of photo-Fenton. To reach a final comparison it would have to be taken into account as well that the Helioman reactor implies higher investment costs than a comparable collector area of static CPC collectors.

The example of Fig. 23 may be used to discuss another of the aspects mentioned in Table 4. Whereas the volume is irradiated approximately 60% of the total treatment time in the CPC reactor (i.e., ratio of illuminated to total volume is 0.6), it is different in the Helioman, where the illuminated volume constitutes less than 15% of the total volume. As mentioned in TiO_2 photocatalysis dark zones are dead zones with respect to reaction rate, whereas in photo-Fenton they are not. As mentioned above highly promising results were obtained by reducing illumination time and enhancing dark times [146,183], whereas few research efforts have been dedicated up-to-now and none of the two cited studies provides theoretic insights explaining satisfyingly the phenomenon.

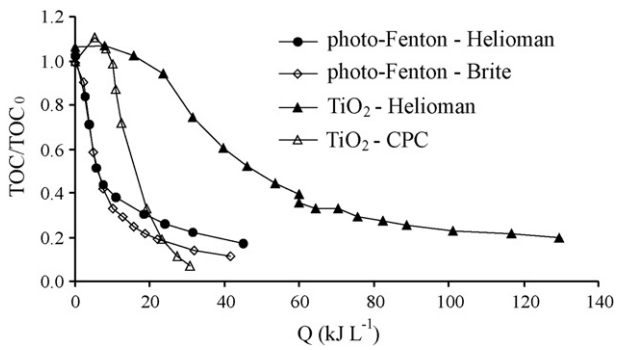

Fig. 23. Degradation of mixture of commercial pesticides, TOC_0 = 100 mg L^{-1}, Photo-Fenton: Fe = 20 mg L^{-1}, H_2O_2 consumption = 1.5 g L^{-1}; TiO_2: TiO_2 = 0.2 g L^{-1}, $Na_2S_2O_8$ consumption = 2.5 g L^{-1}.

One paper that suggested a solar collector including heat insulation and heat recovery was the work of Sagawe et al. [160]. The groups of Malato and co-workers [145,149] and Alfano and co-workers [204] developed flat-plate reactors, but few other works delved into aspects of reactor engineering taking into account the issues specific to the photo-Fenton process. Another topic is the effective radiation wavelength. Table 5 shows solar radiation data illustrating wavelength dependent irradiance power and related data. What becomes clear that the density of photonic flux proportionally increases even more than the irradiance power the longer the wavelength (which is of course due to the indirect proportional relation between photon energy and wavelength).

Table 5 shows clearly that UV transmissivity of the photoreactor and UV reflectivity of the collector is a critical issue for TiO_2 application. For example, roughly a third of the available photons in sunlight for TiO_2 photocatalysis have a wavelength shorter than 350 nm. Assuming that photo-Fenton operates at a wavelength up to 450 nm that share would only be 10%. Hence, there seems scope for the study of different materials for photo-Fenton. For example one of the reasons why low iron content borosilicate glass was preferred over fluoropolymers was its improved UV transmissivity [29]. A second reason was its lower investment price. Nevertheless the use of polymers adds to the durability of the plant and helps to keep maintenance costs low (less breakage). Also, given the information of Table 5 other reactor materials may be an option. Such developments should be supported by fundamental investigations on the effect of the irradiance wavelength on the process, especially regarding the quantum yield as it may vary strongly as a

Table 5
ASTM solar radiation data for global irradiance (AM 1.5), incident on a plane tilted 37° facing the sun [205].

Wavelength (μm)	Spectral irradiance (W/m² μm)	Integrated irradiance power up to wavelength (W/m²)	Fraction of total spectrum's irradiance power (%)	Spectral photon flux (μE/m² s nm)	Integrated photon flux up to wavelength (μE/m² s)
0.33	381	4.74	0.49%	1.05	12.8
0.35	466	14.3	1.49%	1.36	37.0
0.37	642	25.8	2.67%	1.98	71.9
0.39	695	39.6	4.11%	2.26	116
0.42	1141	72.0	7.46%	4.00	227
0.45	1471	110	11.36%	5.53	366
0.5	1493	186	19.26%	6.23	671
0.55	1505	268	27.80%	6.91	1002
0.6	1388	338	35.09%	6.96	1345

function of wavelength. A better understanding of the wavelength dependency will also give additional impetus to investigations regarding activating complexes, which increase the available pool of effective photons and diminish inner filter effects (usually less present at longer wavelengths). The results of such investigations may help enhancing the scientific rationale for the design of the optical wavelength of the photoreactor.

Generally speaking the treatment incurs three different types of costs: investment costs (design, equipment, installation), operating costs (reagents, energy, operation) and maintenance (replacements, repairs, cleaning). Of these costs the human resource factor (operation and maintenance) is one of the most important factors at the current development stage of the technology. Few papers exist, which address these topics and if they do, they address only single aspects. For example Bacardit et al. suggested models to control the treatment progress based on the hydrogen peroxide consumption [199], which was previously also suggested by Gernjak et al. [183] in our group, where also an algorithm for automatic dosing and maintenance of hydrogen peroxide was developed and tested [206]. Still, altogether little investigation exists on the topic and on how large-scale facilities (dealing at least several cubic meters per day) could be operated effectively. Particularly, we do not know of any work, which postulates how a photo-Fenton plant could be operated in a continuous way. This is especially important towards the process integration in a treatment train consisting of several treatment unit operations.

Finally, to our knowledge the effect of soiled collector and photoreactor surface was never investigated. Reactor soiling is inherent to a process to be performed outside and must be taken into account. From an engineering point of view the issue includes not only the effect of the surface deterioration but also the development of a reactor design, which enables easy cleaning procedures to recover the full reactor performance at a low cost (regarding consumables and human resource). The application of materials with low stickability or self-cleaning effects may be investigated. As a final conclusion to this section it seems clear that much scope remains for engineers and scientists to develop improved solar photoreactors taking into account the specific requirements of the photo-Fenton process and this process is meant to go hand-in-hand with fundamental investigations on topics scarcely touched by scientists up-to-date.

4.5. Designing a complete treatment—integration of photo-Fenton

In the sense of the review presented by Augugliaro et al. [41] several ways exist to enhance the performance of a treatment by an AOP. The first possibility is to position the AOP in a sequence of physical, chemical and biological treatments (not necessarily in this order). Many times such a treatment approach will at least involve an AOP step and a biological treatment step. Either way, putting AOP or biological treatment first in the treatment train, the global objective of minimal costs will closely resemble minimizing the treatment degree in the AOP and maximizing the treatment in the biological treatment, because of the large differences in costs of the two different treatments. The key issue is the correct design of the process, so that the process will be best in terms of overall economic and ecological performance. We will deal later in this section in detail with some examples and how such a design of treatment strategy is best performed.

A second option would be the real integration with another process, which may again be of physical, chemical or biological nature and we will first review several proposed possibilities for process integration.

4.5.1. Enhancing photo-Fenton by means of direct integration with other processes

Several authors have proposed the direct interaction of the oxidative mechanisms of photo-Fenton with other oxidative processes, e.g., the simultaneous combined action of photo-Fenton and ozone [207], TiO_2 [208–210] and ultrasound [133]. The addition of ozone yielded exceptionally high reaction rates, but adds strongly to the complexity of the process, especially when a large scale solar application is envisaged (e.g., maintaining the ozone concentration throughout the collectors). In the same sense currently ultrasound irradiation and solar collectors seem to form a mismatching pair, whereas the combined application of TiO_2 and photo-Fenton is rather straightforward, though the results obtained suggest that the combined application cannot compete in terms of reaction rate with the homogeneous process performed at acidic pH.

Nevertheless there exists scope in applications, in which it is critical to avoid pH modifications, i.e., acid and base additions adding up to salt, and where synergistic interactions between both processes [209–211] may well lead to feasible applications. Introducing electrochemistry to the photo-Fenton system leads to a process, which is generally termed photo-electro Fenton. This process is closely related to the electro-Fenton process and similar to the classical Fenton process the enhancement consists in the photoreduction of ferric iron complexes. This may be a promising process but lacks development at its current stage to allow thorough scale-up for applications [212].

A series of integration approaches exist for the simultaneous application of TiO_2 photocatalysis and physical separation processes (e.g., activated carbon, nanofiltration [41] or membrane distillation [43]). To our knowledge only one study suggests the application of nanofiltration for the removal of the catalyst [213]. No studies were ever suggested for the combination of photo-Fenton and membrane distillation or activated carbon, though some clear synergies may be easily envisaged such as the beneficial effect of increased temperature in either process, membrane distillation and the hot water regeneration of activated carbon. Neither was it ever tried to set up an integrated biological/photo-Fenton system to our knowledge, i.e., where the AOP is placed on the recirculation stream of the biological reactor. Hence, the AOP

may partially oxidize contaminants, which can be completely metabolized by the bacteria. This of course seems to be impossible for an application at pH 3, but a process performed at neutral pH involving low hydrogen peroxide concentrations may be suitable and worth investigation.

4.5.2. Application examples for photo-Fenton as part of a whole treatment

As photo-Fenton is applied only in research the applications in a whole series of treatments are scarce, but some examples may be given, where authors tried to find environmental problems, where two or more processes (being one of them photo-Fenton) could be joined together in a synergistic way, though not all applications applied solar photo-Fenton.

Yardin and Chiron investigated the subsequent extraction and degradation of TNT from soil [214]. They extracted the soil with methylated-β-cyclodextrin (5 mM) obtaining solutions containing 132 mg/L TNT. These solutions were then treated by photo-Fenton applying a low pressure mercury lamp. Their results indicated that MCD has a beneficial effect on the degradation rates of TNT. This relative improvement of TNT degradation rate (1.3 times) in presence of high amounts of hydroxyl radical scavengers was ascribed to the formation of a ternary complex (TNT–cyclodextrin–iron) which can direct hydroxyl radical reaction toward TNT.

Another application ensures transparency of the solution by a pretreatment aimed at removing solids. The authors [150] apply variations of pretreatments such as simple flocculation by polyaluminum compounds or a combination of chemical pretreatment by Fenton and flocculation/coagulation. The target wastewater was olive mill wastewater and by removing the solids the authors were able to treat this wastewater having an especially high organic load (around 20 g/L TOC) by photo-Fenton, although applying high reagents amounts (e.g., over 50 g/L H_2O_2). These authors also suggested the posterior use of the treated wastewater for fertilization by irrigation as the treated wastewater contains high amounts of nutrients, particularly potassium. Also, other chemicals were suggested to be adapted to this subsequent use, i.e., acidification by nitric acid and subsequent neutralization with potash. The authors supported their hypothesis by germination index studies with barley. This study gives a nice example how the process may be adjusted to achieve a revalorization through reuse instead of considering the wastewater solely as a source of problems.

Furthermore, there exist plenty of examples, which focus on the sequential combination of photo-Fenton treatment and biological treatment (aerobic in most cases) and some examples were mentioned already. A general approach for the development of a combined treatment will be discussed in the next section.

4.5.3. Combining photo-Fenton and biological treatment

As mentioned several times throughout this paper, the treatment of an industrial wastewater through AOPs should be pondered in the presence of organic pollutants that are toxic and/or non-biodegradable and therefore not treatable by conventional biological processes, because although biological treatment is often the most cost-effective alternative it is generally not effective for industrial effluents contaminated with bio-recalcitrant organic substances. The use of AOPs as a pretreatment step to enhance the biodegradability of waste water containing recalcitrant or inhibitory pollutants can be justified if the resulting intermediates are readily degradable by microorganisms in further biological treatment. Consequently, photo-Fenton process and AOPs in general have been proposed as a pretreatment to biological treatment for toxic wastewater streams [163].

Today combined photo-assisted AOP and biological processes are gaining in importance as treatment systems, as one of the main urban waste water treatment obligations imposed by European Union Council Directive 91/271/EEC is that waste water collecting and treatment systems (generally involving biological treatment), must be in place in all agglomerations of between 2000 and 10,000 population equivalents by 31st December 2005. Smaller agglomerations which already have a collecting system must also have an appropriate treatment system by the same date [215]. This means that nowadays, provided that the regulations have been implemented, AOP plants developed in the EU can discharge pretreated waste water into a nearby conventional biological treatment plant. The same is true for many other locations all over the world.

Similar as in literature on other AOPs, originally toxic waste water has been proven to lose its toxicity upon treatment by photo-Fenton process before total mineralization has been achieved [193]. Loss of toxicity usually is accompanied by an enhancement of biodegradability of the treated waste water [161,162]. Hence, the following approach may be taken to take a decision on the treatment strategy and the design of a treatment plant:

- Step 1: check if wastewater is potentially treatable by AOP and/or biotreatment.
- Step 2: selection of treatment strategy as a function of wastewater characteristics (only AOP, AOP–BIO, BIO–AOP, only BIO, and no treatment).
- Step 3: develop and optimize coupling strategy (if AOP–BIO was chosen in Step 2).
- Step 4: pilot-plant studies on process kinetics.
- Step 5: theoretical up-scaling.
- Step 6: economic study.
- Step 7: choose best-performing AOP.
- Step 8: final plant design.

4.5.3.1. Step 1: check if wastewater is potentially treatable by AOP and/or biotreatment. In Step 1 one should clarify the characteristics of the wastewaters, which could avoid their proper treatment by the studied AOPs: volatility and solubility of contaminants, concentration of contaminants in the wastewaters, and degradation kinetics of the organic content of the wastewater.

Volatility may be an issue because it would pose a reactor design constraint to avoid volatilization, which is furthermore incompatible with elevating the treatment temperature as suggested in the photo-Fenton treatment. Henry's constant could be envisaged to estimate the loss of organics to the atmosphere when applying AOPs. Dichloromethane ($H_{30\ ^\circ C}$ = 0.00265 atm m^3/mol), dichloroethane ($H_{30\ ^\circ C}$ = 0.00124 atm m^3/mol) and trichloromethane ($H_{30\ ^\circ C}$ = 0.00450 atm m^3/mol) were tested in our group [194]. By photo-Fenton dichloroethane was completely degraded even with 2 mg/L of Fe and after more than 3 h of treatment time without observing losses to the atmosphere. Dichloromethane was completely degraded only if short reaction times (<60 min) where achieved using high concentration of Fe (55 mg/L). Trichloromethane was release to the atmosphere in any case, releasing almost 25% of it to the atmosphere.

Another issue may be solubility, especially when a second phase is present. As the oxidative species are created in the aqueous phase any presence of solids or secondary liquid phases (e.g., oil films) leading to a separation may have a strong detrimental on the process kinetics and reproducibility, in which case process efficiency decreases and process design uncertainty increases. The contaminant concentration has to be considered as well and their influence on the process. As stated in different sections a high contaminant concentration may lead to high operation costs due to high reagents concentration and residence times in the photoreactor. On the other hand low contaminant concentrations means that the coupling with a biotreatment normally would not be necessary because of the very low organic content of the effluent.

4.5.3.2. Step 2: selection of treatment strategy as a function of wastewater characteristics. TOC (or COD) as a general parameter of wastewater treatment should always be known. Toxicity and biodegradability of wastewaters are very often related but not always. As a general rule one should test both parameters when dealing with real wastewaters. Knowledge of toxicity of the wastewater, as evaluated by a battery of different bioassays, should be necessary always. When the TOC, biodegradability and toxicity against different microorganisms are determined, one should follow the subsequent decision path (see also Fig. 24):

1. If the wastewater is biodegradable a biological pretreatment should be performed (unless legal discharge limits are already fulfilled, which is an unlikely case for industrial wastewater), because classical biological treatments are, at present, the cheapest and most environmentally compatible option. Then, after this biotreatment, the effluent quality has to be checked if further treatment is necessary or if the effluent can be safely disposed of in agreement with the legal discharge limits established.
2. If the wastewater is not biodegradable and TOC is high (>100 mg/L) AOP pretreatment before biotreatment should be envisaged. After the treatment the effluent quality has to be checked, to decide if it complies with legal requirements for effluent discharge.
3. If the wastewater is not biodegradable, TOC is low (<100 mg/L) but toxicity is high, one should design the appropriate AOP treatment for reducing the toxicity, but without a subsequent biotreatment, because such a low TOC would not produce pretreated effluent (this means, with lower TOC) suitable for a biotreatment. Very often this wastewater could be disposed to the environment after the AOP treatment or, which is more convenient, to a public sewage treatment system for polishing it.
4. If the wastewater is not biodegradable, TOC is low (<100 mg/L), toxicity is low, but other physical–chemical legal requirements are not met, also an AOP treatment without subsequent biotreatment should be envisaged. After the AOP treatment the effluent quality has to be assessed before discharge.
5. If the wastewater is not biodegradable, TOC is low (<100 mg/L), toxicity is low and all legal requirements for discharge are met, the wastewater can be safely discharged.

4.5.3.3. Step 3: develop and optimize coupling strategy (if AOP → BIO was chosen in Step 2). This step is truly multidisciplinary and requires knowledge of the biological and the chemical process. A series of analytical parameters needs to be measured ranging from chemical sum parameters (total organic carbon or chemical oxygen demand), chromatographic methods (HPLC-UV to quantify specific contaminants of interest), acute toxicity tests (typically various, e.g., *Vibrio Fischeri* and *Daphnia Magnae*) to biodegradability tests (BOD_5, Zahn–Wellens test, respirometry). Anions and cations can be important through various reasons. First, the nutrients are important for the biological process and monitoring the inorganic nitrogen species can give much information on the integrity of the biotreatment. Second, contaminants may contain heteroatoms, which can be released into solution as inorganic species as a consequence of mineralization. Hence, their measurement, either by ionic chromatography or tests designed for each specific ion (test kits are usually available), can yield valuable information on the process as typically a decrease of organic heteroatoms leads to decreased toxicity and higher biodegradability. Another series of parameters related to the process conditions should be monitored, which include the iron concentration, hydrogen peroxide concentration and the pH value. This whole series of analytical parameters will satisfy the needs for engineering purposes to design the coupling strategy. If further understanding of the underlying processes is sought, additional analytical methods may have to be applied, which allow the identification of unknown intermediate degradation products. Such studies involving a considerable effort of sophisticated analytical equipment and dedication occasionally were able to explain the fact, why acute toxicity may rise during a treatment by pinpointing single toxic intermediate degradation products with an increased toxicity compared to the original pollutant.

In coupled systems, the AOP pretreatment is meant to modify the structure of pollutants by transforming them into less toxic and easily biodegradable intermediates, which allows the subsequent

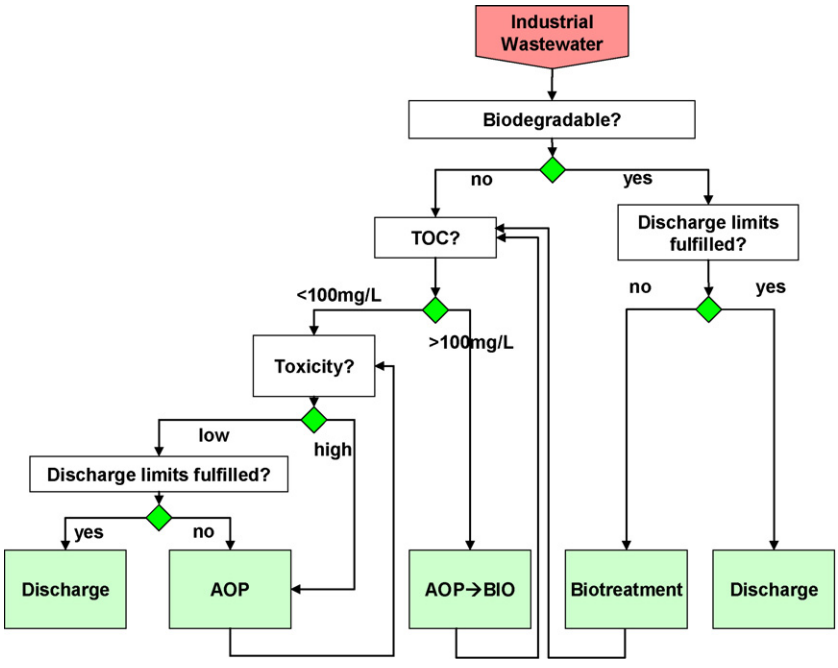

Fig. 24. Decision scheme for selecting the appropriate treatment train.

biological degradation to be achieved in a shorter time and in a less expensive way. The solution resulting from the phototreatment stage is considered to be biologically compatible after the elimination of: (i) the initial bio-recalcitrant compound, (ii) the inhibitory and/or non-biodegradable intermediates, (iii) the residual H_2O_2, or other inhibitory electron acceptors, whenever they are utilized for the phototreatment, and (iv) any necessary adjustments to the pH have been made.

These requirements, together with information concerning the evolution of toxicity and biodegradability of the phototreated solutions, allow the determination of an optimal phototreatment time, which corresponds to the best cost-efficiency compromise. However, if the fixed pretreatment time is too short, the intermediates remaining in solution could still be structurally similar to initial bio-recalcitrant compounds and therefore, non-biodegradable. Such behaviour was recently found to occur in heterocyclic compounds, where the heterocyclic moiety remained could only be broken up very slowly maintaining the toxicity high during the whole mineralization in the phototreatment [216].

In the OECD guidelines biodegradation tests are divided into three principal categories: tests for ready biodegradability, tests for inherent biodegradability and simulation tests [217]. Tests for ready biodegradability are the most stringent tests, offering only limited opportunities for biodegradation and acclimatization of the inoculum during a time span of the test of several days. These tests were compared by Reuschenbach et al. [218]. Recently another toxicity test based on the growth of the bacteria *Pseudomonas Putida* CECT 324 was suggested as a testing method for ready biodegradability [219]. However, these tests have limited capacity for the prediction of a biological treatment plant, as acclimatization may occur. This is especially true for modern biological treatments, which are often based on reactor technologies involving a much higher sludge age compared to the traditional activated sludge process (e.g., moving bed biofilm reactors, membrane bioreactors). In such a case tests for inherent biodegradability such as the Zahn–Wellens (Z–W) procedure is the most appropriate method for biodegradation assessment of partially photodegraded solutions of contaminants. But this analytical tool is quite time-consuming, typically between a few days in the case of quick evidence of biodegradability (i.e., samples with ready biodegradability) and in the case of a continuing negative test response the test must be prolonged for 4 weeks, which is the test duration according to the standard protocol.

Therefore, to limit the amounts of samples to be processed by the Zahn–Wellens test, we propose as an indicator of partially phototreated waters the complementary use of acute toxicity techniques, which yield a comparably quick response. A series of acute toxicity tests are available [220], but among the typical ones applied (e.g., invertebrates immobilization, fish toxicity tests, algae growth tests, luminescence bacteria tests, plant seed germination tests) the ones based on bioluminescent bacteria (*Vibrio fischeri*, *Photobacterium phosphoreum*) are probably the ones, which are most easily applied, quickest to yield a result and lest expensive. Another interesting cross between ready biodegradability tests and acute toxicity tests are short-term respirometric tests performed with activated sludge such as were proposed by the group of Amat et al. [221].

Being a quick test, acute toxicity can be evaluated regularly in the course of the experiments to be performed for the optimization of the coupling strategy. Frequent samples should be collected in order to observe the impact of the oxidative treatment on the toxicological level. Toxicity evolution is considered as an indicator of a progressive molecular transformation of the solution and the toxicity could level off or increase as treatment proceeds. An increasing toxicity reveals the production of reaction intermediates which are more toxic than the initial molecule. Thus, whenever the phototreated solution is considered sufficiently modified regarding its toxicological variations, the AOP can be interrupted and a consecutive Z–W assay should be carried out. This procedure should be applied to any point where toxicity suffers a substantial variation [65].

Another interesting parameter that could help to decide when to apply or not biotreatment (or which samples should be tested by Z–W) is the so-called Average Oxidation State (AOS), defined by Eq. (4.48), where TOC and COD are expressed in mM of C and mM of O_2, respectively [222]. AOS usually increases as a function of treatment time and attains almost a plateau after a certain time. These results suggest that more oxidised organic intermediates are formed at the beginning of the treatment and after certain time the chemical nature of most of them did not vary substantially anymore, even if the AOP was prolonged. Formation of more oxidized intermediates is an indirect indication of the ability of the treatment to improve the biodegradability. In the moment that AOS is stabilized, the chemical treatment is only mineralizing organic contaminants, but partial oxidation does not happen anymore. The AOS changes should be also taken into account for determining when to apply Z–W tests:

$$AOS = 4 \times \left(\frac{TOC - COD}{TOC}\right) \tag{4.48}$$

As a conclusion, Fig. 25 summarises the procedures to be followed to determine the best possible AOP–BIO coupling strategy, i.e., to determine, when to pass from chemical-oxidative (AOP) to a biological wastewater treatment. Once that promising AOP strategies regarding the coupling of chemical and biological treatment have been identified, these strategies have to be verified in pilot-plant experimentation, which includes a further optimization regarding process kinetics (step 4). Theoretical scale-up and cost analysis (steps 5 and 6) will allow choosing the possible operation conditions and treatment strategy (step 7). Finally, after this decision has been taken one can proceed to the design of the final treatment plant (step 8). Several of the works of our group illustrate the path from pilot-plant studies to a full-size demonstration plant application [197,223,224].

5. Solar photocatalytic disinfection

5.1. Introduction

5.1.1. Need of safe drinking water disinfection

The most important issue in water disinfection is, of course, safe drinking water. According to the WHO and UNICEF polluted drinking water and lack of sanitation is responsible for the death of approximately 4500–5000 children every day, and one billion people still lack access to safe drinking water [225].

The microbial contamination in different regions may have different anthropogenic and non-anthropogenic origins. If fecal wastewater from human settlements is not treated before being discharged into a river, it can cause contamination further downstream. Cattle husbandry close to rivers can cause microbial contamination of river water which is later used for irrigation, washing and sometimes even drinking. Fig. 26 shows an estimate of pathogens in lakes, rivers, streams and groundwater sources found in recent literature and summarized by the WHO Drinking-Water Guidelines [226]. Except for groundwater and the low figures in wilderness rivers and streams, all detected concentrations are infectious concentrations of pathogens highly significant for health. Therefore water disinfection is essential for the consumption of safe water.

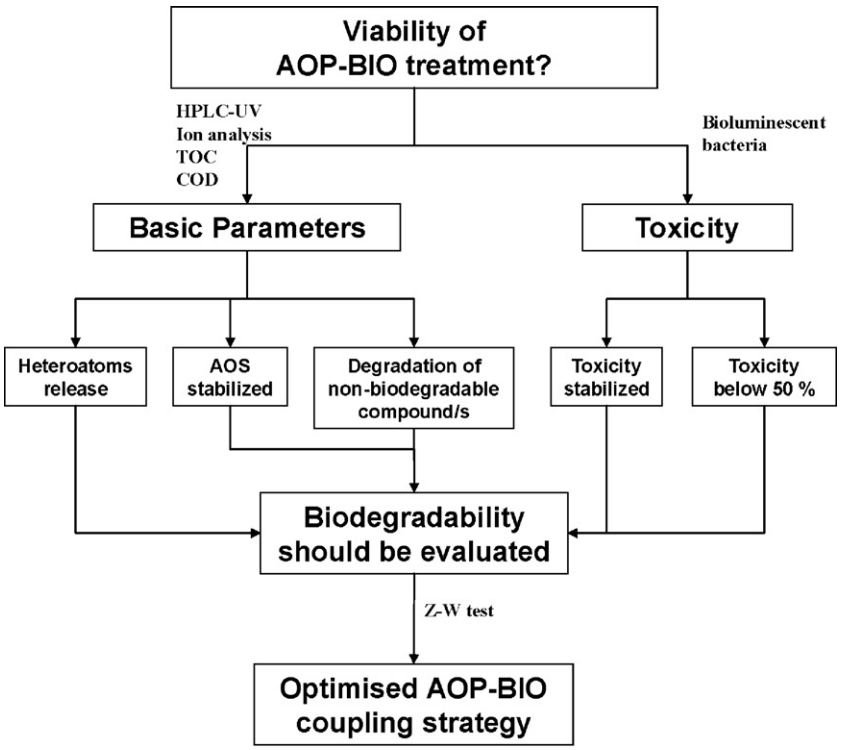

Fig. 25. Procedures that should be applied to decide an optimized AOP–BIO coupling strategy applied to wastewaters previously determined as suitable (see also Fig. 24).

5.1.2. Need of irrigation water disinfection

In addition to the well-known task of drinking water disinfection, the second most critical issue is the disinfection of water for agriculture. According to the Food and Agriculture Organization of the United Nations (FAO), agriculture consumes 70% of fresh water used worldwide. In developing countries, this increases to over 95% of the available fresh water. The average water used for crops is around 1000–3000 m^3 per ton of cereal harvested, or in other words, 1–3 tons of water are used to grow 1 kg of cereal. Bearing in mind that the daily drinking-water requirement per person is only 2–4 l, it is often forgotten that it still takes 2000–5000 L of water to produce a person's daily food requirement [227].

80% of land cultivated worldwide is today still exclusively rainfed, and supplies over 60% of the world's food. Irrigation could

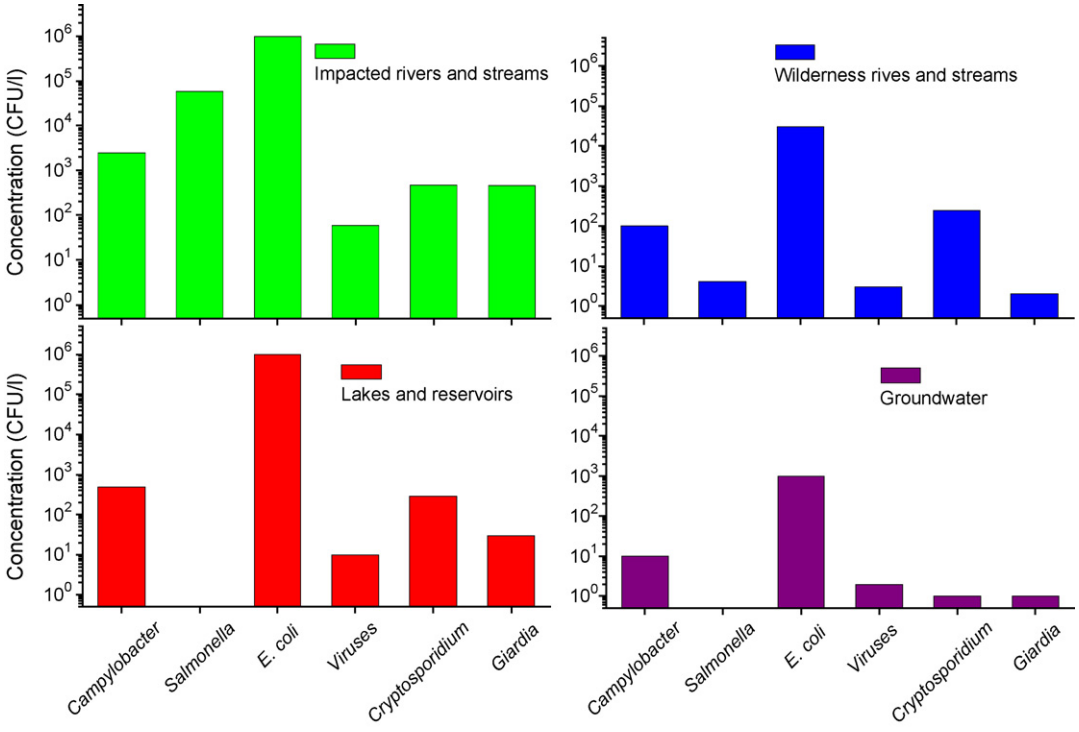

Fig. 26. Concentrations (in CFU per liter) of enteric pathogens and fecal indicators in different types of source waters from scientific literature [226].

Table 6
Disinfection by-products of chlorine and ozone [234].

Disinfectant	Significant organohalogen products		Significant inorganic products	Significant non-halogenated products
Chlorine	THMs	Chlorophenols		Aldehydes
Hypochlorous acid	Haloacetic acids	Halofuranones	Chlorate (mostly from hypochlorite use)	Cyanoalkanoic acids
	Haloacetonitriles	N-chloramines		Alkanoic acids
	Chloral hydrate	Bromohydrins		Benzene
	Chloropicrin			Carboxylic acids
Chlorine dioxide	Haloacetonitriles	Chloramino acids	Nitrate	
Chloramine	Cyanogen chloride	Chloral hydrate	Nitrite	Aldehydes
	Organic chloramines	Haloketones	Chlorate	Ketones
			Hydrazine	
Ozone	Bromoform		Chlorate	Aldehydes
	Monobromoacetic acid		Iodate	Ketoacids
	Dibromoacetic acid		Bromate	Ketones
	Dibromoacetone cyanogens bromide		Hydrogen peroxide	Carboxylic acids
			Hypobromous acid	
			Epoxides	
			Ozonates	

triple or quadruple this production. However, the FAO does predict a sharp increase in irrigation replacing rainfed agriculture [227]. Stored rainwater or surface water used for irrigation accumulates phytopathogens as phytopathogenic bacteria and fungi can be found almost everywhere. The plant and human pathogen *F. solani* has been reported as found almost everywhere, even in hospital water distribution systems [228].

Phytopathogens may be fought with organic disinfectants, also referred to as pesticides, which can be employed for disinfection of irrigation water, but this involves many negative aspects. Chlorine is used extensively, but has the drawback of the disinfection by-products and resistance (see Table 6). Furthermore, depending on how crops are cultivated, phytotoxicity has also been reported. Non-chemical disinfection methods are rare in agriculture, but some work on UV-C disinfection of pathogens, such as *Phytium* and *Phytophthora*, is reported [229]. Hydrogen Peroxide is also commonly used as a disinfectant in agriculture, but it quickly becomes phytotoxic, especially in hydroponic cultures, at doses as low as 50 mg/L [230]. Thus to improve its efficacy, H_2O_2 has been combined with germicidical UV-C radiation or ozone [231]. Both techniques are in use, but energy costs are very high. Recent research on solar and solar photocatalytic disinfection attempts to combine sustainability with low cost leading to an efficient disinfection method, not only for drinking water, but also for irrigation.

5.1.3. Standard methods for drinking water disinfection

Drinking water disinfection is mainly defined by the destruction of microorganisms causing epidemic diseases, like cholera and typhoid fever. The mechanism involved is most commonly explained as the destruction of the organism protein structure and inhibition of the enzymatic activities [232]. This definition leads to the general resistance order to widely used high-level disinfectants such as ozone and chlorine compounds. Most resistant infectious agents include prions, followed by coccidian (*Cryptosporidium*) and bacterial spores (*Bacillus*), mycobacteria (*M. tuberculosis*), viruses (poliovirus), fungi (*Aspergillus*), leading finally to Gram-negative (*Pseudomonas*) and Gram-positive bacteria (*Enterococcus*) (Fig. 27). This resistance is decisively determined by the cell wall permeability to the specific disinfectant, although size and complexity of the microorganism also influence its resistance.

Most bacteria, except the non-tuberculous mycobacteria, are relatively easy targets for chlorine disinfection. Nevertheless, they must be taken seriously because they are highly infectious and can multiply in water supply systems. Viruses (adenoviruses, enteroviruses, hepatitis A virus, hepatitis E virus, noroviruses and saproviruses, rotaviruses) can easily cause infections highly detrimental for health. Furthermore, they are moderately resistant to chlorine disinfection and persistent in water supply systems. Nevertheless, the most difficult targets for chlorine disinfection are the protozoa (*Acanthamoeba spp., Cryptosporidium parvum, Cyclospora cayetanensis, Entamoeba histolytica, Giardia intestinalis, Naegleria fowleri, Toxoplasma gondii*), which are infectious at very low concentrations and are moderately to highly persistent in water systems. Therefore protozoa in potential drinking water systems are very hazardous and have to be considered in the choice of treatment [226].

The existing drinking water pretreatment processes, coagulation, flocculation, and sedimentation remove a maximum of 90% of bacteria, 70% of viruses and 90% of protozoa. Filtration for drinking-water treatment (e.g., granular, slow sand, precoat and membrane filtration) with proper design and adequate operation, can act as a consistent and effective barrier for microbial pathogens leading to an approx. 99% bacteria removal. Depending on the water source, the remaining bacteria might still be able to cause disease, which makes filtration a good pretreatment, but not a completely safe disinfection technique. For highly resistant microorganisms filtration in combination with chlorine is recommended [226].

The commonly used drinking water disinfection techniques, chlorination (chlorine and derivates), UV-C, and ozonation are the safest against most of infectious agents. UV-C disinfection and ozonation have associated installation, electricity and maintenance costs. But both technologies are very effective in killing bacteria and reasonably effective in inactivating viruses (depending on type) and many protozoa, including *Giardia* and *Cryptosporidium*. 99% of bacteria can be removed with 0.02 mg of ozone

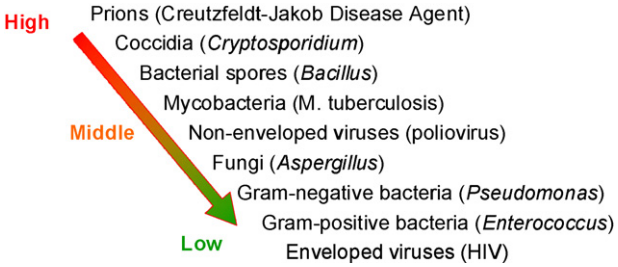

Fig. 27. Classification of infectious agents according to their resistance to disinfectant agents [233].

per min per liter at 5 °C and pH 6–7. For the disinfection of *Cryptosporidium*, the highest ozone concentration is needed: 40 mg per min per liter at 1 °C [234]. Despite its highly efficient inactivation of all microorganisms present, ozonation can also produce disinfection by-products (DBPs) (Table 6), depending on source-water quality.

Application of UV-C-lamps ($190\,nm < \lambda < 290\,nm$) is very effective against a wide range of microorganisms. The main advantage is that UV-C disinfection makes the storage and transport of reagents unnecessary although may also be limited depending on source-water turbidity. For clear water, average bacteria inactivation is 99% at 7 mJ/cm^2 and for *Cryptosporidium* at 5 mJ/cm^2. The total number of microorganisms reduced by UV-C is very similar for protozoa and bacteria, because of their similar susceptibility to UV-C damage [235].

Chlorine is a very effective disinfectant for most microorganisms. 99% of bacteria can be killed with 0.08 mg per min per liter at 1–2 °C and neutral pH. For disinfection of 99% of viruses, 12 mg per min per liter at 0–5 °C and neutral pH is sufficient, but for the inactivation of 99% of *Giardia*, 230 mg per min and liter are necessary at 0.5 °C and neutral pH, and *Cryptosporidium* cannot be safely inactivated with chlorine at all [226]. The protozoa *Cryptosporidium*, *Giardia* and *Acanthamoeba*, which are very highly resistant to chlorine, present a high risk of infection and are extremely persistent in water supply systems. Such significant resistance makes it clear that alternatives to chlorine as a general disinfectant must be found. These protozoa, as well as *C. jejuni, C. coli, Y. enterocolitica, P. aeruginosa*, have been successfully inactivated by solar or solar photocatalytic disinfection, as described further below.

Another alarming disadvantage of chlorine is the appearance of its by-products, organohalides, especially trihalomethanes (THMs), in chlorinated drinking water. Organohalides were first found in the 1970s, and later fully characterized (Table 6). These findings have led to severe criticism of its use in drinking water and even in irrigation water.

Research seeking alternative methods of drinking water disinfection is necessary to solve above mentioned limitations and issues. Any such solution will have to take into account many factors: (i) low cost, (ii) low power consumption, (iii) sustainability, and (iv) absence of negative effects on health, and taste.

5.1.4. Pesticides as disinfectants in agriculture

Since production of all kinds of chemicals began to increase in what is often referred to as the "Chemical Age" in the 1950s, phytopathogens have often been fought with organic chemicals called "pesticides", which includes any chemical used to inactivate or control pests. In agriculture, this refers to herbicides (weeds), insecticides (insects), fungicides (fungi), nematocides (nematodes), and rodenticides (rats and mice). Benefits of these agricultural techniques, well known under such terms as the "Green revolution", come from pesticides, especially in regions where food production relied on monocultures. Unfortunately, pesticides have also other non-desirable effects leading to disruption of predator–prey relationships and loss of biodiversity, which pose serious threats to the long-term survival of major ecosystems. Of course pesticides can also have significant consequences for human health.

Besides the shockingly high accumulation levels in plants and humans, these substances are often not biodegradable and therefore imply indefinite long-term effects on the health of humans and of whole ecosystems [236]. These substances are some of the list of persistent bioaccumulative and toxic (PBT) pollutants, which environmental organizations, such as the US Environmental Protection Agency (EPA), are fighting against. Many of these PBTs, like aldrin, dieldrin, chlordane, DDT, mirex, and toxaphene are now better monitorized and controlled, especially since the US-Environmental Protection Agency (EPA) launched its PBT program in November 1998. But the fight against PBTs goes on. Not only is a reduction in the use of PBTs an issue, but also keeping new PBTs from entering the marketplace [237].

Specific control of phytopathogenic fungi by fungicides, has had very limited success. This is due to their easily acquired resistance to systemic inhibitors. The problem is worldwide and therefore the use of fungicides is only recommended for specific conditions. The Fungicide Resistance Action Committee (FRAG) publishes a long list summarizing current and historical resistance problems in the UK and potential problems in other countries [238].

Besides the use of specific fungal chemicals and broadband pesticides, "soil disinfection" chemicals are applied, of which the most discussed is methyl bromide (MeBr). MeBr is an odorless, colorless gas used as a structural and soil fumigant in pest control for many years all over the world and across a wide range of agricultural sectors. The worst characteristic of MeBr is that it depletes the stratospheric ozone layer. Its strong negative impact motivated many EPA reports and commitments to reducing its use [238]. After a long struggle, its use was restricted and the amount of MeBr in agriculture was reduced incrementally as required by the Montreal Protocol on Substances that Deplete the Ozone Layer (Protocol) and the Clean Air Act (CAA) [239]. Nevertheless, the battle against MeBr has not yet been won, and its worldwide use has not yet stopped. The fight against MeBr has become one of the most important tasks for sustainable agriculture.

5.2. Factors affecting disinfection

The variables that influence a disinfection process by the use of a disinfectant agent can be the type of disinfectant, the nature of microorganism, the disinfectant agent concentration and contact time, pH, temperature, other chemical species in water, etc. Disinfectant agents affect the microorganisms' viability and survival attacking them through their different structures. Depending on the disinfectant agent capacity to break through the cell wall, the disinfectant can cause sequential damage in the different elements of the cell: external and internal membrane, different organelles of the cell, DNA molecules, etc. (Fig. 28).

Resistance to disinfection can vary depending on the type of microorganism; even within different strains of the same species. In general, it can be said that microorganisms that form spores are more resistant to disinfection than those that do not, even if they belong to the same type. The order of resistance of microorganisms to conventional disinfecting methods is the following: *Non-forming spores bacteria < Viruses < Forming spores bacteria < Helminths < Protozoa (oocysts)*.

In general microorganisms behave in many different ways during disinfection; it depends on the type of strain used and the culture. There are several disinfection studies of strains cultured in

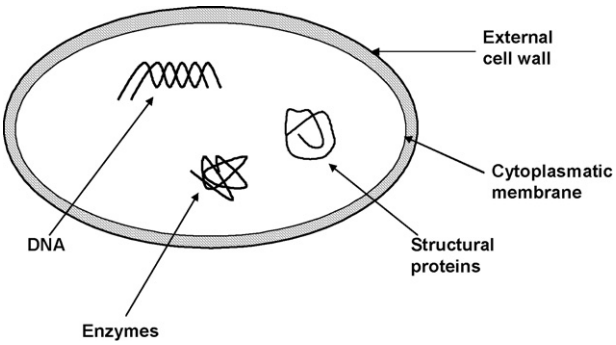

Fig. 28. Possible targets of biocide attack by a disinfectant agent.

laboratory and natural cultures showing very different results. Ward et al. found a resistance of *Flavobacterium spp.* 200 times stronger to chlorine cultured in natural conditions vs. laboratory cultured [240].

Disinfection of pathogens in contact with a disinfecting agent enhance with the time of contact. So the behaviour of the disinfection can be modelled in that case as a first order reaction [241]:

$$\frac{dN}{dt} = -kN_t \tag{5.1}$$

where N_t is the number of microorganisms in the time of reaction or contact with the disinfecting agent, t and k is the reaction constant. The expression can be as follows:

$$N = N_0 e^{-kt} \tag{5.2}$$

However, the field experiences with real waters show deviation of the kinetics that depends on the resistance of each microorganism and the heterogeneity of the existing population in the treated water (Fig. 29). The width and tail of these typical disinfection curves of the resistant populations show the survival level in subpopulation of very resistant pathogens or with high protection by other additional factors [242], although most authors agree that it is mainly due to grouping process of microorganisms.

For disinfection with chlorine or other biocide agents, the effectiveness of the disinfection process can be expressed as the product $C \times t$, being C the disinfectant concentration and t the time needed to inactivate a determined percentage of the pathogens population. The ratio between the disinfectant agent concentration and the contact time expresses Watson's law:

$$K = C^n t \tag{5.3}$$

For a type of microorganism exposed to a disinfectant concentration C (expressed in mg/L) under controlled pH, temperature, etc., conditions, the time needed to inactivate a determined percentage of the population (i.e., 90 or 95%) is called t in (5.3). Both parameters are related through the constants K and n. K represents the process efficiency and n is called "dilution coefficient" (Fig. 30, Bitton [244]).

Other expressions exist that relate the capacity of disinfection or the lethality (Λ) of a disinfectant to the concentration and time of contact necessary to obtain a disinfection of 99% of the

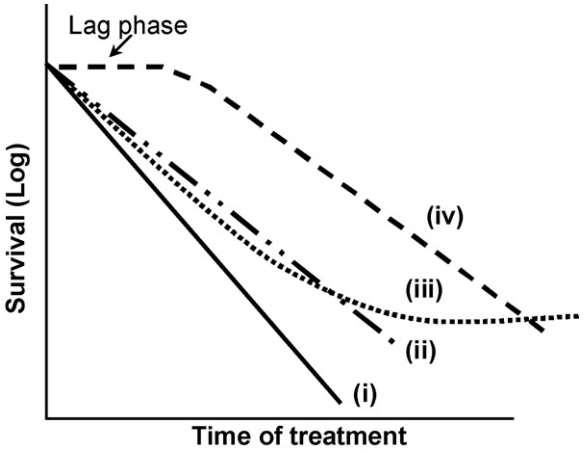

Fig. 29. Inactivation kinetics of microorganisms using a disinfecting agent. (i) Homogeneous microorganisms population sensitive to disinfection; (ii) homogeneous microorganisms population resistant to disinfection; (iii) homogeneous population partially protected by agglomeration (adapted from [243]; (iv) heterogeneous population partially resistant to the treatment [242].

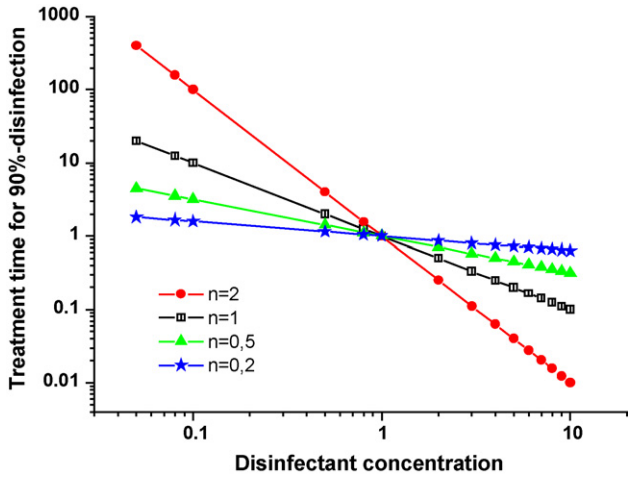

Fig. 30. Graphical representation of Watson's law.

population:

$$\Lambda = \frac{4.6}{Ct_{99}} \tag{5.4}$$

The influence of temperature on the chemical processes during disinfection is in general to increase the efficiency with an increase of temperature. In general, this effect can be expressed according to the equation of Van't Hoff–Arrhenius:

$$\ln\left(\frac{k_1}{k_2}\right) = -\frac{E_a}{R}\left(\frac{1}{T_2} - \frac{1}{T_1}\right) \tag{5.4}$$

In which k_1 and k_2 represent the constants of balance to temperatures T_1 and T_2, E_a is the energy of activation for reaction and R is the universal constant of gases.

The viability of the bacteria *Escherichia coli* depends to a great extent on its temperature of incubation. The resistance and sensitivity to the temperature depend in general of the type of microorganism. In the literature there are many specific studies and results for the different microorganisms. In general, the chemical composition of water as well as its content in suspended solid particles, their turbidity, etc., affects in a very important way the disinfection processes. Regarding chemical disinfection, it is clear that the presence of determined organic compounds will determine the efficiency of the process. In the same way, the efficiency of UV-C disinfection fundamentally depends on the optical properties of the water to treat, which is why the turbidity becomes this case in a determining parameter. It has been verified that the presence of faecal material, solid materials dissolved of black waters, etc., protect the microorganisms against radiation effect. In the case of the disinfection with chlorine, there are evidences of the negative influence of certain compounds like organic and inorganic nitrogen compounds, iron, manganese and hydrogen sulfide.

5.3. Damaging effects of light on microorganisms

The very energetic solar UV-C (200–280 nm) band is absorbed by the atmosphere, and is therefore not a component of the sunlight responsible for such phenomena as skin cancer. UV-C light (used, e.g., in disinfection lamps), when absorbed by the cell DNA, damages irradiated DNA, directly inducing pyrimidine and purine dimers and pyrimidine adducts. Some studies with viruses have demonstrated that the hazardous effect of UV-C photons is first produced in the viral DNA and then in the outer membrane (Fig. 31).

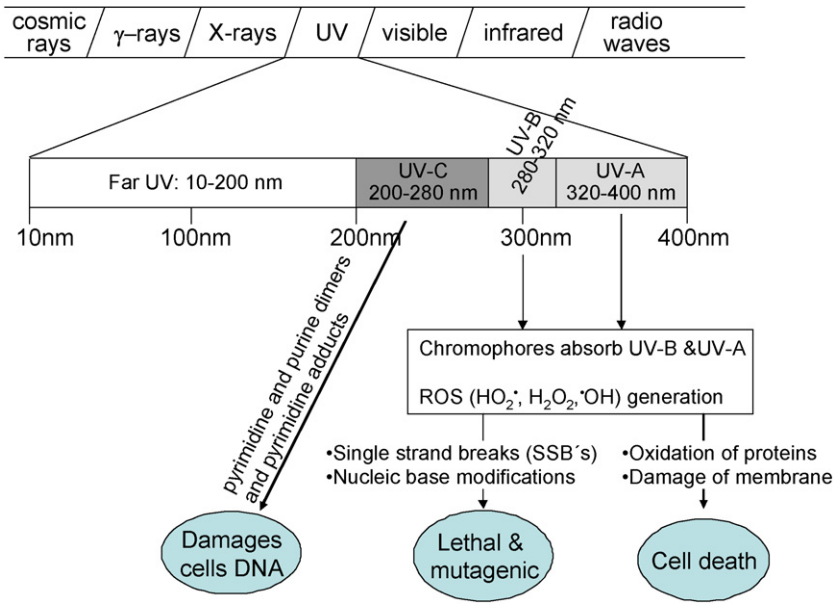

Fig. 31. UV radiation damages on microbial cells.

Although UV-C radiation treatment does not require any chemical additives, formation of oxidation by-products is possible, especially when using high-pressure UV systems. This is due to the generation of hydroxyl radicals in water when the water encounters UV radiation. However, conventional UV systems do not seem to produce any type of derivate known so far [235].

The resistance of different microorganisms to UV-C radiation has been studied. *Legionella pneumonphila* is one of the most sensitive to the treatment, while *Giardia muris* and *Cryptosporidium parvum* oocysts are the most resistant of those discussed in Table 7. Turbidity is often considered the most limiting factor of this process; however, sometimes due to light diffusion in the fluid turbidity may have a positive effect on the disinfection efficiency. So, absorbance in the UV-C range is considered as a general parameter to take into account in any case. The removal percentage depends on the initial concentration of microorganism, for this reason the data shown in Table 7 should be taken as a mere example.

The solar ultraviolet radiation that reaches the surface of the earth contains UV-B (280–320 nm) and UV-A (320–400 nm) light. In this wavelength range, only the UV-B region overlaps with the tail of DNA absorption. UV-B radiation is believed to be the component of sunlight mainly responsible for the majority of human skin cancers. Nevertheless, the UV-A region of sunlight is potentially carcinogenic and is certainly involved in photo-aging, so much research has been undertaken to understand the cell damaging action of both components (UV-A and UV-B). Today it is accepted that the damage caused by UV-A and UV-B light is mainly due to its absorption by cellular components called intracellular chromophores. The best known intracellular chromophore is probably L-tryptophan. Potential chromophores are also considered to contain unsaturated bonds such as flavins, steroids and quinines [245].

Table 7
Required UV-C dose to reach a 90% of inactivation with different microorganisms adapted from [244].

Microorganism	$[\text{UV-C dose}]_{90\%}$ (mW s cm^{-2})
Protozoa cysts	
Giardia muris	82
Cryptosporidium parvum	80
Giardia lamblia	63
Viruses	
Rotavirus SA 11	8
Poliovirus I	5
Hepatitis A Virus	3.7
Bacteria	
Pseudomonas aeruginosa	5.5
Escherichia coli	3
Salmonella Typha	2.5
Shigella dysenteriae	1.7
Legionella pneumonphila	0.38

The irradiation of intracellular chromophores with UV-A light is only toxic to cells in the presence of oxygen. Damage by light absorption through chromophores is therefore contributed to the generation of reactive oxygen species (ROS). The resulting oxidative stress damages the cells and cell components. Besides other cell damage, ROS can lead to lipid peroxidation, pyrimidine dimer formation and even DNA lesions. When ROS interacts with DNA, single strand breaks (SSB's) occur as well as nucleic base modifications which may be lethal and mutagenic. Furthermore oxidation of proteins and membrane damage is also induced.

ROS can be inhibited by scavenging enzymes, such as catalase, peroxidase and superoxide dismutase, which are found in all aerobic organisms. Scavenging agents not only act during UV-A-irradiation-induced oxidative stress, but also during normal cell life to correct oxidative lesions during the cell metabolism itself. These oxidative lesions can be caused during cell respiration by three active intermediates of the univalent reduction of molecular oxygen to water: peroxyradical ($HO_2^{\bullet}$), hydrogen peroxide (H_2O_2), and the hydroxyl radical ($^{\bullet}OH$). While intracellular UV-A absorption induces the superoxide radical directly, the intracellular $^{\bullet}OH$ radical formation can be attributed to the Fenton and Haber-Weiss reaction.

5.4. Bactericide action of solar radiation

The bacterial decontamination rate by solar radiation is proportional to the intensity of radiation and the temperature and inversely proportional to the depth of the water, due to the dispersion of the light. The amount of radiation attenuated by this effect depends on the range of wavelengths, for example, between

200 and 400 nm the reduction does not attain 5% per meter of depth and at longer wavelengths it can reach up to 40% per meter [246]. The first successful application of sunlight to drinking water disinfection was published in 1980. Acra et al. used sunlight for disinfection of oral rehydration solutions brought to developing countries as part of the World Health Organization (WHO) disease control program. In developing countries where it can be difficult to obtain drinking water free of pathogenic organisms, the need for an effective but practical water disinfection method is still of vital importance. Solar disinfection (SODIS) has been shown to be an effective household treatment method that is both practical and low in operational costs. Through a synergistic effect of mild heat and UVA light, microbial pathogens in drinking water contained in poly(ethylene) terephthalate (PET) bottles are inactivated within 6 h after exposure to sunlight [247].

It is widely accepted that solar UV inactivation of microbial cells occurs through a variety of mechanisms depending on the type of UV used for inactivation. Sunlight used during the SODIS process consists mainly of UVA and hence the main inactivation mechanism is a photooxidative process as well as the generation of reactive oxygen species (ROS). ROS include free radicals such as the superoxide anion radical as well as non-radicals such as hydrogen peroxide. When ROS interacts with DNA, single strand breaks (SSB's) occur as well as nucleic base modifications which may be lethal and mutagenic. Furthermore oxidation of proteins and membrane damage is also induced [248]. However, many aspects of UVA inactivation are still unclear. The most destructive wavelengths for the forms of microbial life are those of the near UV-A spectrum (320–400 nm), whereas the spectral band from 400 to 490 nm is the least harmful. Whereas differences in the speed of inactivation of bacteria to temperatures between 12 and 40 °C are negligible, when the temperature rises to 50 °C the bactericidal action is enhanced by a factor of 2, probably due to the synergistic effect between radiation and temperature [249]. The work of Joyce et al. on water disinfection with faecal bacteria at high concentrations (10^6 CFU/mL, Colony Forming Units per mL) shows very promising results on the bactericidal effect of solar heating, with a maximum of 55 °C [250].

5.4.1. Resistance of microorganisms to solar radiation

Many research works show that solar disinfection is efficient against a wide range of microorganisms using "batch" systems (a bottle or a glass with agitation of the fluid is used like photoreactors) under artificial or natural solar illumination. Nevertheless, few works of direct comparison between the results obtained with very different methodologies and under very different experimental conditions have been carried out. Most of the published investigations to date have been done using *Escherichia coli* (*E. coli*) as model microorganism, because it is a very well-known bacterium from all points of view (DNA, metabolism, structure and composition, morphology, behaviour under different nutrient media, pathogenicity, types, strains, etc.).

In order to know the relative resistance of different microorganisms to solar radiation it is necessary to take into account the efficiency of the reactor, with the aim of accurately analyzing disinfection results under real conditions that may occur in the environment where different microorganisms can be present simultaneously. For that reason, an analysis of the existing works on the resistance of different microorganisms is complicated and requires considering many factors. Gill and McLoughlin [251] published an interesting study on this issue where they analyze results obtained in "batch" systems, since they are most numerous in literature and, with some differences, can be taken as reference when designing disinfection recirculation systems. In this study, the microorganism selected as a reference is *E. coli* because it is a coliform entero-bacterium widely used and all the comparisons are standardized with respect to the behaviour of *E. coli* in the same conditions. The levels of solar radiation resistance of different specimens come from the results of diverse contributions; existing certain homogeny in these results.

The Gram-negative bacteria are of similar sensitivity to *E. coli* with the exception of *Vibrio cholera*, which is much more resistant. *Pseudomonas aeruginosa* (responsible for infections in the eyes and ears) and *Enterobacter cloacae* (causes infections in the urine and respiratory systems) requires half the UV energy compared to *E. coli*. The species of *Shigella*, related to diarrhoea and dysentery and *Salmonella enteritidis* (gastroenteritis) are also relatively easy to inactivate in comparison to *E. coli*, although *Salmonella typhimurium* and *Sh. Sonnei* are slightly more resistant. Gram-positive bacteria, represented by Enterococci sp. (*Enterococcus faecalis*) and *Bacillus subtilis*, are more difficult to disinfect. In fact, the solar disinfection technique is not effective for *Bacillus subtilis* spores. *Acanthamoeba polyphaga* (protozoa), common in soil and aquatic environments, is quite resistant, even compared with other protozoa.

Fungal pathogens as *Candida albicans* and *Fusarium solani* are more resistant than *E. coli* although their main route of infection is not via water, but via other media such as soil. Bacteriophage Poliovirus and MS-2 behave like virus with double resistance to solar radiation than *E. coli*. It is important to emphasize that almost all works on the matter are concentrated in the reduction of a single microorganism, but do not study the real water disinfection in the presence of turbidity, chemical compounds and other microbial atmospheres.

5.5. SODIS: practical demonstration of water disinfection with pathogens

Acra et al. reported that enteric bacteria were inactivated after exposure to 6 h of sunlight. Subsequently other organisms have been tested, including: *Salmonella thyphimuirum, Shigella dysenteria, Escherichia coli, Vibrio cholera* and *Pseudomonas aeuriginosa* [242,252,253], protozoan oocysts of *Cryptosporidium parvum* and cysts of *Giardia muris* [254], the yeast *Candida albicans*; the fungus, *Fusarium solani* [255], several phytopathogenic fungi of *Fusarium* genera [256] and *Polio* virus [257] (Table 8). A controlled field trial done immediately after a cholera epidemic also revealed that SODIS participants were 7 times less likely to contract cholera [258]. The resistance that microorganisms display to solar disinfection leads to variation in treatment times. Even the growth phase of the microorganisms influences their susceptibility to disinfection.

Table 8
Inactivation times of microorganisms during solar exposure (SODIS process).

Microorganism	Inactivation time under approx. 1000 W/m^2 global irradiance	Reference
Bacillus subtilis endospores	No inactivation after 8 h	[259]
Yersinia enterocolitica	3 h	[259]
Enteropathogenic E. coli	1.5 h	[259]
Staphylococcus epidermis	35 min	[259]
Campylobacter jejuni	20 min	[259]
Fusarium solani	5 h	[256]
Fusarium oxysporum	5 h	[256]
Cryptosporidium parvum	8 h	[260]
Giardia muris cysts	4 h	[254]
Acanthamoeba polyphaga (cysts)	6 h	[257]
Polio virus (NCPV #503)	6 h (40 °C)	[257]
A. polyphaga (Trophozoites)	6 h	[255]
Escherichia coli DH5 a	2.5 h	[255]
Pseudomonas aeruginosa	2 h	[255]
Candida albicans	6 h	[255]

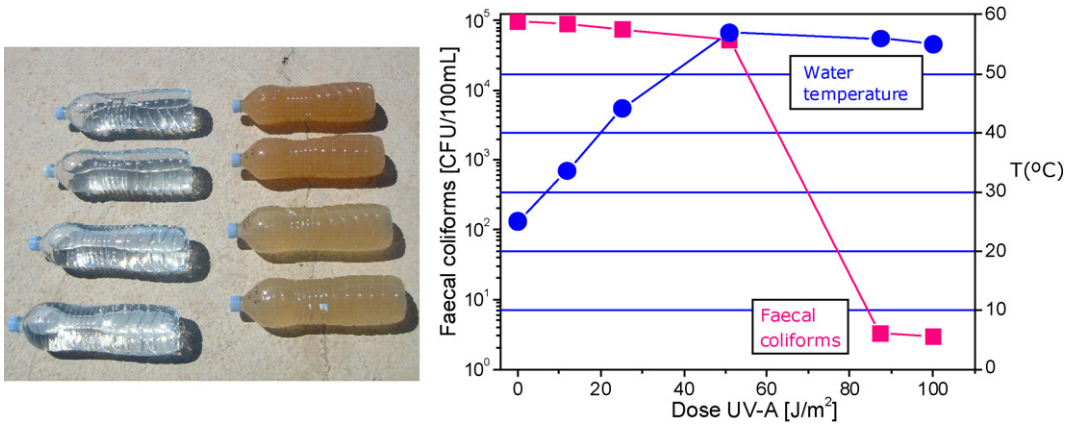

Fig. 32. PET-bottles filled with water samples at different turbidity values (0–300 NTU) exposed to the sunlight. Graph of temperature increase and reduction of faecal coliforms in a SODIS experiment.

One of most interesting applications of solar water disinfection is known as Solar Water Disinfection (SODIS). The term SODIS refers particularly to small (1.5–2 L) household solar disinfection in polyethylene terephthalate (PET) bottles and has already been tested successfully in real field applications under different projects worldwide [http://www.sodis.ch]. Thanks to the bactericidal effect of the radiation and solar heating, important reductions of microorganisms' concentration can be obtained (Fig. 32).

The results of SODIS are very promising. They guarantee the safety of drinking water not only in remote low-income areas without access to clean drinking water but also in urban slums less than 1 km from the centres of modern cities. Therefore, SODIS is used by millions of people throughout the world. The suitability of the SODIS technique for countries with a high incidence of waterborne disease is further illustrated by the fact that these countries lie in the latitude lines of 30 N and 30 S and hence receive sufficient sunlight to apply SODIS. In industrialized areas with fewer economic limitations, ozone, UV-C and chlorine disinfection are used. The effectiveness of the process depends on the source water quality, temperature, turbidity, and resistance of the specific microorganisms, irradiance and dissolved oxygen. Over 45 °C, there is synergy between thermal heating and solar UV inactivation which leads to improved disinfection. Even extremely turbid water (200 NTU) can be disinfected under Kenyan sunlight after storing for 7 h at temperatures of 55 °C or higher [250]. An increase in dissolved oxygen in the PET bottles after agitation leads to improved inactivation [261].

SODIS in PET bottles is limited by small treatment volumes (<3 L) and access to PET containers (there is no requirement for the bottles to be clean when they are obtained). Disinfection of larger volumes of water for various households with solar reactors is under study. Compound parabolic collector reactors (CPCs) are mostly used for this. Solar disinfection can be achieved even for real water sources in such reactors, but the effect has been noticeably improved by the presence of photocatalysts.

SODIS as a drinking water treatment has important advantages to alternative treatments (i) availability in low-income, sun-rich areas; (ii) acceptance due to natural odor and taste of the water (often not the case for chlorine); (iii) sustainability as no chemicals are consumed; and (iv) no need of posttreatment after disinfection. Following the standard SODIS operating guidelines, solar inactivation should be sufficient to render potable water safe for drinking [225].

These advantages led WHO to recommend SODIS for the reduction of health hazards related to drinking water on World Water Day on 22 March 2001. The acceptance of SODIS in many projects all over the world has been strongly supported by the Swiss Federal Institute for Environmental Science and Technology (EAWAG) whose scientists have been promoting SODIS in recent years in more than 30 countries (http://www.sodis.ch/Text2002/T-Projects.htm). This already makes SODIS an important application for drinking water treatment, with even more potential for adoption in the future.

Nevertheless, different scientific and technical issues are still under research. The objective of the recent research on SODIS is to overcome the limitations of this technique such as: (i) the length of time required for inactivation; for example in cloudy days, 2 consecutive days of exposure are recommended; (ii) the volume of water generated at a time during SODIS is very small, a maximum of 3 L per bottle; (iii) several pathogens (especially resistant spores and viruses) remain untested; (iv) when turbidity of water is very high (>100 NTU) exposure times become longer and disinfection can not always be guarantied for all waterborne pathogens. The recent research project SODISWATER (http://www.rcsi.ie/sodis/), funded by the European Commission (FP6), tries to demonstrate that solar disinfection of real water can be an effective and acceptable intervention against waterborne disease for vulnerable communities in developing countries without reliable access to safe water, or in the immediate aftermath of natural or man-made disasters. One of the main scientific objectives of this project is to assess the SODIS disinfection process under real conditions (solar radiation in different seasons, real contaminated water, ambient temperature, etc.) and use of the SODIS technique to generate a larger output of water. Different untested water pathogens have been tested under real conditions [259]. Studies of the various factors on SODIS disinfection have been completed. Such factors include treated volume (tens of liters), solar irradiance, water quality, turbidity, and enhancing technologies (solar CPC, thermal effect, photocatalysts addition, etc.) [249,262].

5.6. Water disinfection with TiO_2 photocatalysis

Since 1985, the field of TiO_2 disinfection research has been growing faster and faster. Literature to 1998 is summarized in the detailed review by Blake et al., including medical applications [263]. From 1985 to date, more than 160 peer-reviewed articles have been published only in the field of TiO_2-assisted water disinfection for a wide range of microorganisms. The first reports on the potential of TiO_2 for disinfection was by Matsunaga et al. in 1985. These authors showed inactivation of the Gram-positive bacteria *Lactobacillus acidophilus*, the Gram-negative bacteria *E. coli*, the yeast *Saccharomyces cerevisiae* and the algae *Chlorella vulgaris* after 120 min of incubation with irradiated TiO_2/Pt

powders. Inactivation from 10^3 CFU/mL to the detection limit was reported, except for the algae, which after 120 min still showed 55% survival. Due to the differences in cell wall properties of the microorganisms tested and independent tests with coenzyme A, the authors attributed disinfection to photochemical oxidation of the intracellular coenzyme [264]. This initial publication was later extended by the same group to application of TiO_2 powder immobilized on acetylcellulose membranes in a continuous sterilization system [265].

5.6.1. Mechanisms of photocatalytic disinfection process

Later publications investigated the exact bactericidal mechanism of TiO_2 photocatalysis. The cell wall is thought to be the first site of attack by the reactive hydroxyl radicals. "Rapid" leakage of potassium ions from the bacteria parallel to the decrease in cell viability was reported by Saito et al. [266]. Maness reported results that can be explained by peroxidation of the polyunsaturated phospholipid component of the cell membrane leading to a loss of essential cell functions, e.g., respiratory activity, and in the end, to cell death [267].

In the following years, several publications reported cell wall disruption and leakage of contents after UV/TiO_2 disinfection treatment [268,269]. *E. coli* photokilling was followed by attenuated total reflection Fourier transform infrared spectroscopy (ATR-FTIR) and atomic force microscopy (AFM). These techniques allowed the determination of the formation of peroxidation products due to photocatalysis of *E. coli* cells, thereby providing even stronger evidence that the changes in the *E. coli* cell wall membranes are precursor events leading to bacterial lysis. A recent publication on this subject studies the adsorption of *E. coli* K 12 cells onto TiO_2 particles (1 g/L) over 60 min of illumination in sodium phosphate solutions. In this article, the rate of adsorption of bacteria onto TiO_2 is reported to be positively correlated with the bactericidal effect of TiO_2. Flow cytometry confirmed that bacterial adsorption could be consistently associated with a reduction or complete loss of *E. coli* membrane integrity [270].

From the first studies to date, there seems to be a consensus in the mechanism of destruction of bacteria by photocatalysis. The first target of the oxidative radicals is the surface of the external membrane of the cell wall. Initially damage takes place on the lipopolysaccharides layer of the external cell wall and on the peptidoglycan layer. Next the peroxidation of the lipid membrane (the radicals oxidize to fatty acids), the oxidation of the proteins' membrane (amino acids) and of polysaccharides take place.

5.6.2. TiO_2-photocatalysis' capability for water disinfection

Ireland et al. reported on disinfection of pure cultures of *E. coli* with anatase crystalline TiO_2 in a flow-through water reactor. Their work already had the foresight to use TiO_2 for drinking water disinfection. They used dechlorinated tap water and surface water samples to evaluate its disinfection capability, and reported rapid cell death for both pure cultures and members of the indigenous flora of natural water samples [271]. This forward-looking approach probably made their work one of those with the most impact and citations in TiO_2 disinfection.

Over the course of time, work with better and better disinfection yields have been published, reporting a four-order decrease in *E. coli* concentration in TiO_2 suspensions exposed to sunlight for 23 min in a batch reactor [272]. Pham et al. reported a 95% reduction of *B. pumilus* spores after exposure to UV light (λ = 365 nm) in the presence of suspended TiO_2 in water [273]. Also the inactivation of several common bacteria (*Serratia marcescens*, *E. coli*, and *Streptococcus aureus*) with UV-C lamps or sunlight was reported in less than 10 min in the presence of TiO_2 powder [274,275].

Little by little, TiO_2 disinfection research went from basic laboratory studies to the first trials with real disinfection applications. In 2000, Herrera Melian et al. reported on TiO_2-assisted disinfection of urban waste water. Two microbial groups, total coliforms and *Streptococcus faecalis*, were disinfected employing both an UV-C-lamp and solar light. This publication was also one of the first to report difficulties with TiO_2 disinfection applied to real water, finding very little difference between TiO_2-photocatalysis and direct solar or UV-C-lamp light irradiation at natural sample pH (7.8), while at pH 5 the presence of TiO_2 notably increased the relative inactivation rate [192]. On the other hand Rincón and Pulgarin did not find any modification in the inactivation rate of *E. coli* in distilled water due to changes in initial pH between 4.0 and 9.0 in the absence or presence of TiO_2-P25 under simulated sunlight illumination [276].

Herrera Melian et al. also published the first mention of a positive effect of TiO_2 disinfection after a long residence time of 2 days, when compared to bare UV or solar irradiation [192]. This issue of improved effect after long time dark periods (probably due to better disinfection yield at the beginning) is discussed in many publications. Of course TiO_2 loses activity in the darkness but authors refer to the absence of bacterial growth. Wist et al. reported the lack of a residual effect due to strong bacteria growth (also named 're-growth') in treated water from the Cauca River (Cali, Colombia) after 24 h as a disadvantage of TiO_2 disinfection of *E. coli* [277]. However, Rincón and Pulgarin reported a light-intensity dependent "residual disinfecting effect" in the presence of TiO_2 (400 or 1000 W/m^2) compared to solar-only disinfection of *E. coli* K12 and bacteria consortia, and did not observe re-growth within the 60 h following treatment with TiO_2 [278]. Microorganisms that are very resistant to UV-A irradiation like *Enterobacter cloacae* have been successfully inactivated by TiO_2 photocatalysis [279]. The authors further report the successful inactivation of various Gram-negative strains of bacilli with differing photosensitivity, such as *E. coli*, *P. aeruginosa* and *S. typhimurium*.

Recent TiO_2 disinfection research focuses more on disinfection applied to more resistant microorganisms. Seven et al. successfully inactivated *E. coli*, *P. aeruginosa*, and *Staphylococcus aureus*, within 40 min and of *S. cerevisiae*, *C. albicans*, within 120 min in the presence of TiO_2, ZnO and Sahara desert sand under lamp irradiation. The very low catalyst concentration they used for the TiO_2 slurry is worth notice: 0.01 g/L. This paper also reports that the only filamentous fungus tested, *Aspergillus niger*, was resistant to the treatment described [280]. Lonnen et al. confirm inactivation of *C. albicans* by TiO_2 photocatalysis and report a 5.5 log decrease in *F. solani* after 4 h of simulated sunlight (20 W/m^2, 300–400 nm UV Xenon lamp). They were the first group to publish such high inactivation rates with a fungal test organism, and especially, with supported TiO_2 [255].

A recent contribution demonstrated the potential of titanium dioxide to inactivate prions in a heterogeneous photocatalytic process. In vitro tests were followed by a bioassay with the scrapie strain 263 K in Syrian hamsters. The results indicated that titanium dioxide photocatalytic treatment of scrapie-infected brain homogenates reduces infectivity titres significantly [281]. The same group demonstrated also the capability of the photo-Fenton reaction to degrade prion proteins. They showed that the photo-Fenton reagent efficiently degrades not only recombinant prion proteins, but also the total protein amount from brain preparations of naturally or experimentally infected species and PrP scrapie contained in sheep scrapie brain homogenates [282].

5.6.3. Effect of catalyst

When suspensions of bacteria or other microorganisms in water are in the presence of titanium dioxide in the dark a small decrease in the concentration of colonies can be observed due to possible

agglomeration of the catalyst with bacteria cells and the subsequent sedimentation. Although solar light or simulated solar light has a bactericidal effect, the addition of TiO_2 in the presence of radiation inactivates microorganisms faster than in the absence of catalyst. Most research on photocatalytic disinfection, like in photocatalytic water decontamination, has been done with the commercial TiO_2 Degussa-P25 photocatalyst. Nevertheless, some works have been carried out with pure anatase and doped titanium dioxide.

The configuration of the catalyst in the reactor can significantly alter in the disinfection result. Typically there are two ways to use the TiO_2 for water treatment purposes, (i) as aqueous suspensions of TiO_2 particles which is usually called *slurry*, and (ii) as immobilised TiO_2 over an inert matrix that has to be resistant to the photocatalytic process, the hydrodynamic pressure in the photo-reactor, etc.

The choice of the catalyst preparation depends, among others factors, on the final application. If the system is designed for drinking water purification for human consumption, the use of TiO_2 in suspension, as a part of a routine intervention for improving the potability of water at house-hold level (point-of-use water treatment) is not feasible. The photocatalyst particles would have to be removed after solar exposure and before consumption.

In general, photocatalytic processes for removal of organic contaminants using suspensions of TiO_2 present higher efficiency rates than the processes with immobilised catalyst; this is due to the fact that catalyst suspensions offer higher active catalyst surface than fixed catalysts. Although the same result could be expected for disinfection of bacteria and viruses and some times this tendency is confirmed [283], it is not always true. This can be explained by the adsorption kinetics and substrate-catalyst which may occur before photogeneration of oxidising species. This concern is very different in the case of organics since bacteria (and other microorganisms) cells are very "big" substrates—orders of magnitude larger than size of particles of catalyst. Many contributions in this field study the design and use of different immobilised photo-catalysts with the aim of finding the best efficiency for the process because fixed catalysts are not as efficient as suspended particles.

During photocatalytic disinfection processes, initial inactivation rate increases when catalyst concentration rises (if suspensions are used) up to a certain value ("optimal catalyst concentration"), then disinfection rate remains constant (or it decays) due to the light screening effect. In the lower range of catalyst concentrations, a significant increase in the activity is observed when increasing the amount of TiO_2, due to the correlation between the bacterial inactivation efficiency and the generation of ROS [284]. For higher concentrations of catalyst, the activity reaches a maximum and then decrease, due to the screening effect that outer layers of catalysts suspension offer to the inner layers in the photo-reactor. Therefore, the generation of ROS is controlled not by the catalyst concentration, but by the incident radiation flux. This effect depends not only of the nature of TiO_2 particles but also on the light intensity and initial bacteria concentration. Consequently, the optimal catalyst concentration depends on the irradiation system and the photoreactor geometry. Several scientific contributions investigated the optimal catalyst concentration; there exist very different results which depend mainly on the photoreactor design and on the light intensity. Obviously, the amount of energy received and its distribution inside the photo-reactor depends on the optical path length of the exposed part of the reactor, on the transmission properties of the materials used, on irradiance, and on the optical behaviour of the solar collectors.

Many different results have been reported by various authors with respect to the optimum catalyst concentration. When using a solar photo-reactor with CPC technology, the optimal catalyst concentration of TiO_2 P25 is 50 mg/L [Fernández et al. [285]], which is similar to that found by Block et al. also with solar radiation: 100 mg/L [274].

5.6.4. Experiences with immobilized catalysts

The biggest problem with TiO_2 slurry disinfection was soon recognized to be the need for posttreatment TiO_2 recovery. Contrary to small concentrations of chlorine, TiO_2 powder cannot be left in drinking water due to inacceptance and insufficiently assessed health risks. Therefore, much research was done to yield efficient catalysts on supports that would keep the TiO_2 out of the treated water. Unfortunately, in photocatalytic disinfection, almost all immobilized TiO_2 either had very limited yields or involved technical effort leading to high cost. It was even reported that immobilization of TiO_2 produces lower disinfection activity compared to slurry systems [283,285].

One of the earliest reports on this topic was published in 1997 for a TiO_2 film reactor and a combination of UV light and an electric field to disinfect water containing *Clostridium perfringens* spores and *E. coli* [286]. In 2002, Curtis et al. reported damage to the pathogen *C. parvum*, responsible for many human diseases. They disinfected *C. parvum* oocysts in electric-field-enhanced photo-oxidation using immobilized titanium dioxide. In simple Petri dish reactors employing two forms of immobilized titanium catalyst (sol–gel and thermal-film), the increase in *Cryptosporidium* oocyst permeability was assessed by propidium iodide exclusion. The results showed that oocyst permeability increased approximately 27% with the thermal-film, and was even less effect with the sol–gel film [287]. Much better inactivation results for *C. parvum* were achieved by Méndez-Hermida et al. with TiO_2 fixed on flexible plastic inserts in 1.5 mL bottles under natural sunlight [260].

To improve efficiency of the immobilized photo-catalysts, some work has been done in electric-field to promote photoelectrocatalytic disinfection. For example, TiO_2 powder can be immobilized electrophoreticaly on electrodes. When electric fields were applied to TiO_2, *E. coli* K12 disinfection rates were reported to increase by 40% using Degussa P25 electrodes and by 80% using Aldrich electrodes [288]. A similar publication by Christensen et al., reported the photoelectrocatalytic and photocatalytic disinfection of *E. coli* suspensions by titanium dioxide in a sparked photo electrochemical reactor with "thermal" electrodes (oxidation of titanium metal mesh) and "sol–gel" electrodes (depositing and then heating a layer of titania gel on titanium mesh). The authors reported that the photoelectrochemical system with "thermal" electrodes was more efficient than their photocatalytic system with TiO_2 slurry [289].

Another way to increase the efficiency of TiO_2 coatings is to modify their chemical composition by doping with other elements, e.g., iron, silver, copper [290]. Yu et al., for example, took advantage of the diffusion of iron atoms through TiO_2 dipcoatings placed on stainless steel. Due to this diffusion of Fe^{3+} and Fe^{2+} ions from stainless steel substrate into TiO_2 films during high-temperature calcinations, the iron behaves as a dopant and the results show significantly better activity than those coatings on glass. In addition, this TiO_2 film seemed to show photo-induced hydrophilicity and so could be used for the sterilization of *Bacillus pumilus* [291].

In one of the most important publications on the use of TiO_2 nanoparticles in disinfection, in 2005, Yu et al. even reported positive results for doping with non-metals. The authors found that sulphur-doped TiO_2 nanoparticles showed strong visible-light-induced activity that effectively kills *Micrococcus lylae*, a common Gram-positive bacterium, within 1 h on S-doped TiO_2 under visible light irradiation [292]. In the last few years, nanotechnology (manipulates nanoscale matter 1–100 nm) has itself become a field

in TiO_2 photocatalysis for disinfection and water treatment in general.

Gumy et al. tested the photocatalytic activity of different types of commercial TiO_2 catalyst (Degussa P-25, Millennium PC-100 and PC-500, Tayca AMT-100 and AMT-600) in suspension or coated on a fibrous web in laboratory decontamination and disinfection experiments. They found good disinfection capacities for all tested catalysts in suspension [283].

5.6.5. Effect of chemical parameters

The nature of the salt, and hence the type of ions, present in the water during disinfection process has an important influence on the kinetics and on the final disinfection result, similar to the decontamination of organics in water using photocatalysis. The inhibiting effect of different electrolytes is well known in photocatalysis, with phosphates being the species with the highest detrimental effect on the efficiency of the process. Phosphates avoid the adsorption of amino acids over TiO_2 particles; carbonates and other ionic species can react with hydroxyl radicals so that they compete with the microorganisms and reduce the efficiency of the photocatalyst.

On the other hand, the use of distilled water for suspensions of bacteria can be a limiting factor for the viability of the bacteria and other microorganisms since, although this avoids interferences between ions and organics compounds and the photocatalytic process, this is a stressful environment for microorganisms [293]. Actually, the lack of a certain ions weakens the bacteria cell wall due the loss of calcium and magnesium ions from its surface. Then, the cell wall becomes fragile and has difficulties to resist the differences of osmotic pressure between the aqueous phase and the inner part of the cell. This finally makes the cells more sensitive to attack by the disinfectant. The physiological stage of cultures (type of growth, strain, exponential or stationary growth phase) also influences disinfection results not only in the presence of TiO_2 but also with solar radiation only [294].

Besides demonstrating the susceptibility of very resistant microorganisms, the TiO_2 disinfection treatment process has been chemically characterized and optimized for engineering. The work of Rincón and Pulgarin should be specially mentioned for their complete and very detailed characterization of physico-chemical factors influencing the photocatalytic TiO_2 disinfection process for *E. coli* and other bacteria. Among other factors, the influence of different types of bacteria consortia, water sources, TiO_2 catalyst type, slurry TiO_2 compared to supported catalyst, UV-light dose, etc., can be found in their work [295–299].

In the work of Alrousan et al. [300] immobilized nanoparticle TiO_2 films were used to inactivate *E. coli* in surface water samples and in distilled water. The presence of nitrate and sulphate anions spiked into distilled water resulted in a decrease in the rate of photocatalytic disinfection. The presence of humic acid, at the concentration found in the surface water, was found to have a more pronounced affect, significantly decreasing the rate of disinfection.

5.6.6. Solar radiation

The choice of the source of light and the reactor's configuration can strongly affect the final disinfection results. The spectral distribution of the source of photons affects very much the inactivation result. For example, if a lamp irradiates partially within the UV-C range, the bactericidal effect is very fast, even in the absence of catalyst. Apart from the spectral distribution, the irradiance (i.e., the radiant energy per unit of time and of cross surface) is a very important parameter. Experiments performed with lamps of light flux between 100 and 2000 $\mu E/m^2$ s yielded total inactivation of *E. coli* within 120–7 min [263].

The irradiation mode in the photo-reactor has also a high influence on the disinfection behaviour. When light exposure is continuous (without temporal interruptions) the bactericidal effect of the process is faster and more efficient than when the light is applied intermittently [285,296]. Some contributions suggest that this effect can be due to bacterial dark-repair mechanisms which allow bacteria to re-activate after treatment [296,301]. This fact can also be attributed to the partial damage produced by the radiation which can not totally inactivate all colonies of bacteria present in the water. It is also known that some damaged cells by UV radiation (not completely died or destroyed) can recover viability by means of two DNA repair mechanisms. One of them is the so-called "photo-reactivation" or "photo-repairing", it exists in cells exposed to radiation of 300–500 nm. The other one is a repair mechanism based on excision (re-synthesis and post-replication of cells).

Light intensity has a determinant role in the disinfection process. Disinfection results of a bacterial suspension exposed to UV-A radiation of 25 W/m^2 (average irradiance) during 2 h are different than those found when the same water is exposed to 50 W/m^2 of UV-A during 1 h. Comparison of experiments in different seasons, early and later in the day, and under cloudy and sunny conditions, leads us to conclude that solar photocatalytic disinfection of *E. coli*, *F. solani*, and *F. antophilum* does not depend proportionally on solar UV irradiance (solar UV intensity) as long as enough photons have been received for disinfection. The minimum UV energy necessary to reach complete inactivation depends on the microorganism and the reactor configuration [301].

Rincón and Pulgarin designed the first method of assessing the bactericidal inactivation rate in solar photocatalytic processes for drinking water [297]. They demonstrated that the solar UV dose necessary to reach target disinfection levels can not be the only indicator of system efficiency, and proposed a new parameter called, "effective disinfection time" (EDT), defined as the treatment time necessary to avoid bacterial regrowth after 24 (or 48 h) in the dark after phototreatment. They published a detailed study about the specific effect of residence time of water in the illuminated part of the solar disinfection system, light intensity and the time of day (morning or afternoon) exposed to solar radiation, and not only the total photon dose.

5.6.7. Disinfection kinetics

The photocatalytic inactivation rate as a function of the initial bacterial concentration obeys to a first order kinetics. This has been already proven with total coliforms, spores, etc. The range of concentration of microorganisms for which the first order kinetics is valid strongly depends on the microorganism itself. Usually, for concentrations between 10^3 and 10^{10} CFU/mL the rate of deactivation does not depend on the initial concentration [263].

Due to the complex mechanism of the disinfection processes, the kinetic analysis of the photocatalytic bacterial inactivation has been usually carried out using empirical equations. That is the case of the disinfection model reported in the literature by Chick and Watson [241,302]:

$$Log\left(\frac{N}{N_0}\right) = -kc^n t \tag{5.5}$$

where N_0 is the initial microorganism population (CFU per milliliter), N is the remaining population at time t, k is the disinfection kinetic constant, c is the concentration of the disinfecting agent at time t, and n the reaction order. In photocatalytic processes, the concentration of the disinfecting agent could be considered to be constant with time, the general expression of the Chick–Watson equation is reduced to [303]:

$$Log\left(\frac{N}{N_0}\right) = -k't \tag{5.6}$$

For solar processes the Chick–Watson's law modified to our experimental conditions, where time is replaced by the amount of solar UVA energy received during the experiments per unit of volume (Q_{UV}) enabling further comparison with results obtained in other solar reactors [304]:

$$Log\left(\frac{N}{N_0}\right) = -k'' Q_{UV} \tag{5.7}$$

$$Q_{UV,n} = Q_{UV,n-1} + (t_n - t_{n-1}) UV_{G,n} \frac{A_r}{V_t} \tag{5.8}$$

where t_n is the exposure time (s); $UV_{G,n}$ the global UV irradiance averaged during exposure time (W/m^2); V_t the total reactor volume (L); and A_r illuminated reactor surface (m^2).

In many cases, the reaction presents an initial delay at the beginning due to the existence of a lag stage in the inactivation of the bacteria, and then the disinfection rate remains constant from the beginning of the reaction and decrease after a period of treatment, when the concentration of microorganism is very low ('shoulder shape' of the curve) [276]. Other authors have found that the disinfection rate remains constant from the beginning of the reaction showing a deceleration after a long period of treatment ('tail shape' of the curve) [276]. Then different modifications of the Chick–Watson expression could be applied to reproduce either the existence of a shoulder at the beginning of the reaction or a tail at the end. However, this model is only valid for the description of the log-linear region of the curve, since the application of the model requires a constant disinfection rate during the whole process.

Another empirical model is described by the Hom equation and its modifications, which could describe the existence of shoulder, linear and tail regions during the photocatalytic process using the following three-parameter equation [305]:

$$Log\left(\frac{N}{N_0}\right) = -\left(\frac{m}{nk'}\right) k C_0^n \left[1 - \exp\left(\frac{-nk't}{m}\right)\right]^m \tag{5.9}$$

where k is the inactivation rate constant (reciprocal time units), k' is the first-order decay constant (reciprocal time units), and m and n are model parameters of the modified Hom model.

5.6.8. Effect of surface interactions

The relative sizes of the microorganisms and the catalyst most commonly used in photocatalysis, TiO_2 P25 made by Degussa (Germany), can give an idea of how the process occurs. The relative location of particles and microorganisms, their surface electric charge (negative cellular membrane and surface of TiO_2 charged as a function of pH), as well as their mean particle size will be key parameters in a possible approach, the subsequent adsorption and eventual penetration of oxide particles through the cellular wall and finally the photocatalytic process.

Gumy et al. clarify the behaviour of bacterial (*E. coli*) inactivation efficiency as a function of isoelectric points (IEP) of different types of TiO_2 powders. These catalysts had specific surface areas varying from 9 to 335 m^2/g and isoelectric points from 3 to 7. They showed that TiO_2 Degussa P-25 consisting of an anatase-rutile powder inactivated *E. coli* with high kinetics that did not vary with the initial pH of the suspension. This was not the case for the other TiO_2 samples used in this study. The IEP could be correlated with the photocatalytic efficiency of the commercial samples for most of TiO_2 powders investigated. The lower the IEP of the TiO_2, the lower the bacterial inactivation activity was found. These authors showed that the clusters of TiO_2 Degussa P-25 are only in partial contact with *E. coli* K-12 (diameter 1 mm) by electron microscopy [283].

The cell wall is more and more accepted as the first target of TiO_2 disinfection [48]. In the case of *Fusarium* the interaction between spores and the catalyst is very strong. But it can be observed that instead of fungi adsorbing onto TiO_2 particles, it is actually the TiO_2 particles that adsorb onto the fungal spores [256] (Fig. 33).

5.7. Fenton and photo-Fenton processes in water disinfection

The problem with using Fenton-like processes in water disinfection and water treatment in general is the competition for $^{\bullet}OH$ radicals between the contaminant and the ligands, which maintain the iron in solution. Once the organic ligands are oxidized, the iron is no longer held in solution at neutral or near neutral pH. The need for low pH for reactions has also been a strong criticism of Fenton processes in disinfection. At pH around 3, most microorganisms are no longer viable without the need of further treatment.

The only recent work about photo-Fenton treatment for disinfection was published by Rincón and Pulgarin for *E. coli* [298]. The authors used real water from Lemans Lake in Switzerland, concentrations of 10 ppm iron from iron salts and 10 ppm H_2O_2 at neutral pH. Their paper reports positive disinfection results, although they do not monitor the iron or H_2O_2 concentrations. It is therefore difficult to know how much iron remains in solution at oxygenated and neutral pH conditions and in what manner this iron is capable of catalyzing the Fenton reaction.

5.7.1. Intracellular iron control and oxidative stress

In the normal metabolism of aerobic cells, H_2O_2 is one of the metabolites originating from the catalyzed reduction of oxygen to water during cell respiration [306]. According to the Fenton reaction, H_2O_2 and iron released inside the cells can cause damage to cell functions *in vivo* and *in vitro* by catalyzing the production of reactive oxygen radicals [307]. The importance of the presence of iron to the initiation of lipid peroxidation was also shown by Minotti and Aust [308].

Even if iron is a potentially dangerous element for living organisms, it is still vital to cell structure, which is why aerobic cells have developed methods to control their intracellular iron

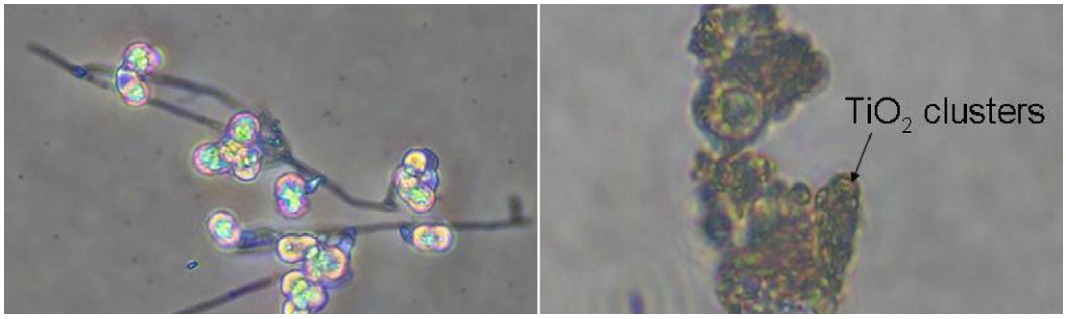

Fig. 33. Chlamydospores of *Fusarium solani* before (left) and after 6 h of photocatalytic treatment.

levels [309]. In mammals, iron is stored in macromolecules as ferritin. From these molecules, iron can be recovered as required by the cell. The amount and form in which iron is present in cells has been discussed in many scientific papers reviewed in a recent publication of Kakhlon and Cabantchik [310]. In 1976, Jacobs proposed the cellular labile iron pool (LIP). This LIP is a model for cell iron in its different forms not captured in the storage molecules. It was operationally defined as a cell chelatable iron pool that may be a mixture of both, iron II and iron III. The more iron is chelatable, the more available it becomes for Fenton reactions, and therefore, cell damage [308]. The control of the intracellular iron concentration is very complex and now seems to be easily disrupted by oxidative stress. Pourzand et al. reported that UV-A irradiation of skin cells can change intracellular iron levels, leading to immediate release of labile iron, possibly from ferritin in human skin fibroplasts [311]. How and why oxidative stress changes intracellular free iron levels in prokaryotic and eukaryotic cells and where iron is released from, have been issues in a great number of important scientific contributions.

Recently, more and more publications explain increased iron in cells after oxidative stress (e.g., induced by UV-A challenge) by reactions between ROS and iron-sulfur clusters of iron-regulating proteins like Fur or aconitase. ROS attacks on oxidative-stress-sensitive proteins can directly liberate an iron atom from the cluster or indirectly increase the iron levels, causing changes in transcriptional iron regulation [312].

5.7.2. The lethal synergy of H_2O_2 and near-UV light

The lethal synergy of H_2O_2 and near-UV light was first reported by Anathaswamy et al., for phage T7 [313]. The same group published a follow-up paper in 1980 on the combined lethality of H_2O_2 and near UV radiation for *E. coli* K12 [314]. They attribute the increased lethality to augmented oxidative stress from the creation of a new chromophore, a photoproduct originating from irradiation of L-tryptophan. They explained that the new L-tryptophan photoproduct was toxic to recombinationless (rec) mutants of *Salmonella typhimurium* and of *E. coli*.

There is practically no further literature on the lethal synergy of H_2O_2 and artificial UV-A or natural sunlight. One of the few papers citing the work of Hartman and Eisenstark was published by Rincón and Pulgarin. They report increased *E. coli* inactivation under solar radiation in the presence of H_2O_2, but this increased H_2O_2 inactivation is only a blank test for photo-Fenton experiments with *E. coli* disinfection. Rincón and Pulgarin also used the interpretation of Eisenstark as the explanation for the increased bacterial inactivation observed [298].

To date, the lethal synergy has never been discussed in the context of the Fenton reaction after iron up-regulation following UV-A-induced ROS attacks up to the contribution of Sichel et al. [315]. This work reports results on inactivation of fungal cells in distilled and well water using H_2O_2 at very low concentrations and sunlight. The synergistic effect of hydrogen peroxide and solar photons is attributed to the generation of $^{\bullet}OH$ radicals from H_2O_2 after the Fenton reaction. As radical production in combination with sunlight and iron is closely connected to skin cancer, and therefore, the medical field, the topic is of great interest [316].

The solar light in the photo-Fenton process contributes to redox cycling of Fe^{3+}–Fe^{2+} in the presence of H_2O_2 and at acid pH. But the literature on intracellular iron control only proves that increased iron concentrations exist in near UV-irradiated cells, not that the intracellular iron is further reduced from Fe^{3+} to Fe^{2+} by sunlight. But the influence of the photo-Fenton process on fungal inactivation is not excluded. The pioneer work of Sichel et al. reports the existence of a lethal synergy of hydrogen peroxide and near-UV radiation to fungal spores in water, leading to a good opportunity for water disinfection for water reuse in agricultural applications [315].

5.8. Solar CPC reactors for water disinfection

In the solar disinfection field it is interesting to point out the idea developed by Caslake et al., which was for drinking water application in remote locations of developing countries. They used a solar disinfection system based on a PVC circuit covered by an acrylic layer transparent to the UV range. The system worked without catalyst and it was used for disinfection of contaminated river water in Peru. In spite of high turbidity found, they obtained 4 log reduction for total coliforms [246].

Vidal et al. [317] published the first pilot plant study about TiO_2 solar photocatalysis for water disinfection. These authors constructed a new low-cost CPC prototype to better use the solar radiation for water disinfection objectives. This solar photo-reactor has 4.5 m^2 of CPC aperture and it was tilted at local latitude to maximize the available solar radiation for long exposure periods (few hours). In this combined flow-through and batch reactor system, the fluid stops circulating when the desired disinfection level is reached. The results obtained for *E. coli* and *Enterococcus faecalis* (initial concentration $\sim 10^2$–10^4 CFU/mL), with TiO_2 suspensions (0.5 g/L), showed a 5-log decrease after 30 min of solar irradiation (where the average solar UV value was around 25 W/m^2). The authors reported an economic analysis of this technology for future application not only to solar photocatalytic disinfection, but also to decontamination of organic pollutants.

Very recent work has studied improvement of solar disinfection using supported TiO_2 on resistant flexible materials, like cylinders, pills, balls, mesh, etc. One example is TiO_2 deposited on glass fibre inserted in a tubular photoreactor in a CPC solar collector [285]. The authors demonstrated that the CPC solar photoreactor is efficient for *E. coli* inactivation by solar photocatalysis with TiO_2 slurries and supported TiO_2 with treatment periods of 30–60 min. They also showed that the total photocatalytic deactivation of *E. coli* suspensions resulted from the combined effect of sunlight and the oxidant species generated in the TiO_2. However, while sunlight deactivated *E. coli* suspensions, bacteria regrowth was detected if TiO_2 was not present. Nevertheless, the CPC (solar) photoreactor used was efficient enough to persevere with photocatalytic applications for drinking water disinfection.

McLoughlin et al. [318] studied the use of three types of static solar collectors for the disinfection of water containing *Escherichia coli*. They demonstrated that three lab-scale solar photo-reactors with aluminium reflectors consisting of compound parabolic, parabolic and V-groove profiles all enhance the effect of the natural solar radiation, although the CPC is more efficient than the parabolic or V-groove profiles. They also proved that low concentrations of titanium dioxide on a rod inserted in the reactors moderately enhance the overall disinfection performance in the compound parabolic reactor. Solar disinfection using low cost compound parabolic collectors was analyzed in depth in another study by McLoughlin et al. [319], using solar radiation and *E. coli* as the target microorganism. The results proved that bacterial deactivation rates using sunlight alone can be enhanced by low concentrations of titanium dioxide suspended in the water. Their results were unclear, however, when they used a standardized UV-dose threshold. As a result, they suggest another disinfection mechanism in the reactor configuration, both a synergistic effect between UV light and the mechanical stress of recirculation, or, a stroboscopic shock effect in which bacteria are intermittently exposed to light and dark in the reactor.

Very recent research work for concrete applications in the field of solar photocatalytic water treatment has also been sponsored by the European Commission's International Cooperation (INCO)

Program in two different projects. Both projects aimed at developing a cost-effective technology based on solar photocatalysis for water decontamination and disinfection in rural areas of developing countries. As a final research step, both projects developed solar reactors to decontaminate and disinfect small volumes of water. The target was drinking water treatment in households and small communities and the research work was carried out with *E. coli* and humic acids. Also within these projects, real field tests were carried out with these prototype photoreactors installed in Argentina, Egypt, Mexico, Morocco, Peru, and Tunisia [48]. In 2007, results published reported the successful operation of the prototypes under real conditions [320].

When exposed to sunlight, the classical SODIS reactor bottles are only illuminated on the upper side so that a large fraction of the available radiation cannot reach the water. In order to increase the radiation reaching the bottles, there have been several attempts to concentrate solar radiation using reflecting surfaces. Kehoe et al. found experimentally that the disinfection rate constants could increase two fold using aluminium foil attached to the back of the bottles [252]. Rijal and Fujioka [321] used wall reflectors and observed improved efficiencies which they attributed solely to the increase in water temperature of the system. Martín Domínguez et al. found that reflective solar boxes could reduce the disinfection time to 3–4 h [322]. Although these works achieved some degree of enhancement by the use of the reflectors, none of them analyzed which is the best concentrating optics to enhance the radiation reaching the bottles in SODIS. That is the case of the recent contribution of Navntoft et al. [262]. It was focused on the use of CPC mirrors to enhance the SODIS process. These authors report improved solar disinfection results for suspensions of *Escherichia coli* in well-water using compound parabolic collector (CPC). They showed to enhance the efficiency of solar disinfection (SODIS) for batch reactors under real, solar radiation (cloudy and cloudless) conditions. On sunny days, the CPC system yielded a more than 5-log unit reduction in bacterial population, i.e., the bacterial concentration decreased from 10^6 CFU/mL to below the detection limit 1 h sooner than the system fitted with no CPC. On cloudy days, only systems fitted with CPC achieved complete inactivation [262].

The SODIS process depends mainly on the UV-A wavelengths present in sunlight. Solar UV-A as received at sea level, is composed of roughly similar portions of both direct and diffuse electromagnetic radiation. On sunny days, the solar UV-A spectrum is composed of ~60% direct and ~40% diffuse solar radiation. Due to the diffuse nature of the UV-A and the cylindrical shape of the bottles, the use of concentrating systems based on non-imaging optics with low concentrating factor has a clear potential compared to imaging optics-based systems. Other reflecting systems tested in previous works have a varying concentration during the day because they are essentially image forming systems and depend on the angle of incidence of the sun on the reflector. Meanwhile the concentrators based on non-imaging optics, called compound parabolic concentrators (CPC), have the major advantage that the concentration factor remains constant for all values of sun zenith angle within the acceptance angle limit. Therefore, this technological enhancement can be used to design future larger scale systems to treat high volumes of water for several households.

5.9. Hydroponic agriculture: potential application for solar photocatalytic disinfection

The agricultural surface devoted to hydroponics culturing increases every year in our country and, particularly, in the south-eastern region (the estimated current surface is 4800 ha), where the horticultural systems reach the highest technical degree. These soil-less culturing systems, using organic or inorganic inert substrates or liquid nutrient solutions (NFT NGS), possess a different environment in the plant root zone that is very different from a traditional pathosystem, as the soil is replaced by those substrates or solutions. Current hydroponic cultures employ substrates based on perlite, rock wool or coconut fibre [323]. Even in semiarid zones with high solar radiation, but scarce water sources, large commercial greenhouse operations making use of soilless cultivation are expanding, because they save water and fertilizer and optimize production.

One of the highest expectations of hydroponics and soilless cultures is that they might serve as an alternative to methyl bromide soil fumigation [324]. Due to the strong environmental impact, this alternative is considered an important opportunity for sustainable agriculture. Another advantage of soilless or hydroponic cultivation is increased productivity, as greenhouse planting densities can be doubled. The hydroponic solution (nutrient-rich water) is usually pumped to the plants by regulated drip irrigation systems. Wastewater from the roots is recaptured, disinfected, and reused. This practice not only helps reduce environmental waste and contamination, but conserves fresh irrigation water and controls nutrients.

Recirculation of the nutrient solution in such cultures provides obvious advantages as far as environmental and economical criteria is concerned (water and fertilizer saving). Nevertheless, problems arise by accumulation of phytopathogens (microorganisms and plant root exudates) due to continual recirculation, and are far from solved. Therefore, the most developed countries such as The Netherlands or Sweden are already investigating innovative and efficient methods to achieve an optimum control in those types of horticultural growing systems. Such control involves necessarily an efficient disinfection of the nutrient solution and a precise and in situ monitoring of the key species.

The vast majority of relevant pathogens in soil-less cultures belong to the order of oomycetes and is characterized by their asexual free-swimming spores called zoospores. This particular feature makes them a high risk to a culturing medium based on water recirculation. As far as non-zoosporangia fungal pathogens are concerned (common dwellers of irrigation piping), two genders of important genus are found in the Spanish south-east area: *Fusarium oxysporum* (in different special forms that affect horticulture) and *Verticillium dahliae*.

Among the most important and general diseases of such cultures, several species of Pythium in cucumber and bean are found. These species kill the plants in the highest production season. Tomatoes growing in Granada province, particularly those of the cherry type, are often affected by the agents *P. parasitica alpidium bornovanus*, melon necrotic spot virus (MNSV) and more recently, *Fusarium oxysporum* f.sp. *radiciscucumerium*, a microorganism that causes loses above 14% of sick plants in cucumber cultures on perlite. The damage originated by these microorganisms increases its severity when recirculation hydroponic cultures are employed.

These pathogenic microorganisms are difficult to control once they have entered the agricultural system. Various chemical fungicides (ethridiazol, furalaxyl, methalaxyl, benomyl, copper oxalate or oxyquinoline sulfate) have been tested for pathogen control but have turned out to be phytotoxic in soil-less cultures. Chlorine, a universal disinfectant, has provided disparate results and often shows phytotoxicity. The application of surfactants for controlling *Alpidium bornovanus* and incorporation of 5–7% sodium hypochlorite in the irrigation water, have demonstrated limited success. Non-chemical methods of pathogen control in hydroponic cultures do not offer a solution nowadays to keep productions high, yet culture disinfecting methods must be replaced at any moment.

Growers sterilize the recycled nutrient water by heating it to about 90 °C (194 °F). Substrates are sterilized for reuse with steam [239]. Even though power consumption is high with such heat sterilization systems, they are widely used. 90 °C is high enough to inactivate many of the microorganisms, but complete sterilization would require even higher power (121 °C and 1 bar overpressure for 15 min) applied to small volumes of water [325].

Sterilization of these liquid-nutrient solutions in hydroponic plantations is especially delicate, as soilless cultures develop a pathogenic environment in their plant root zone that is very different from traditional agriculture. Unfortunately, it can be said that the transition from soil to soilless cultures has not led to the disappearance of soil-borne diseases, but in the appearance of more water-borne diseases [229]. In this sense, phytopathogenic fungi are especially resistant pathogens, which spread easily in traditional plantations and even more quickly through pumped nutrient solutions.

Various disinfecting agents have been tested for pathogen control, but as in the case of recirculating nutrient solutions, they have often turned out to be phytotoxic or hazardous to health or environment. Even chlorine and hydrogen peroxide soon show phytotoxicity [230]. As disinfection in soilless cultivation is especially sensitive to strong disinfecting agents, this nutrient solution is a good target for solar photocatalytic disinfection, which not only disinfects without introducing hazardous substances into the environment, but also becomes inactive in the dark root zones of the plants. Disinfection of water containing phytopathogenic agents by the use of solar photocatalysis with TiO_2 and probably other AOPs can be an alternative method for disinfecting nutrient solutions without using environmentally hazardous substances.

Therefore, it is essential to evaluate different alternatives to ensure an adequate control of such phytopathogen agents. These alternatives should focus on minimizing production cost and to be friendly to the environment. In this regard we find the possible new application of renewable energies, namely the solar radiation. After promising results on photocatalytic disinfection of water contaminated with phytopathogens [256,293,315], it seems clear that photochemical systems activated with sunlight for the treatment of the nutrient solution in hydroponic cultures have a potential application. They would enable a dual disinfecting action on the one hand, the pasteurizing effect of increasing water temperature due to the action of the solar thermal energy on the collector; on the other, the effect of highly reactive oxygen species (hydroxyl radical, $^{\bullet}OH$). Even, the economical viability of the use of additives is not very clear. This issue together with the increasing requirements of quality of human consumption product (like agricultural ones) support the idea of using chemical-free systems to control pathogens in agriculture. The European Union has reduced the number of allowed phyto-sanitary compounds from 400 to 90.

6. Future prospects and challenges

Solar TiO_2 photocatalysis could be applicable to different organic hazardous contaminants, such as pesticides, solvents, detergents and a variety of industrial chemicals, which are capable of substantial contamination of the environment due to their toxicity and persistency. Nevertheless, the process efficiency can be considered linearly dependent on the energy flux but only 5% of the whole solar spectrum is available for TiO_2 band gap. A realistic assumption of solar collector efficiency of 75% and 1% for the catalyst means 0.04% original solar photons are efficiently used in the process. From the standpoint of solar collecting technology, this is a rather inefficient process even considering for a high added-value application. Solar AOPs have the advantage over other AOPs of using sunlight and having as its main characteristic that it is an environmentally friendly technology. TiO_2 is a cheap photostable catalyst, and the process may run at ambient temperature and pressure. Additionally the oxidant, molecular oxygen (O_2) is the mildest. Therefore, in principle, the process involves a mild catalyst working under mild conditions with mild oxidants. However, as concentration and number of contaminants increase, the process becomes more complicated and challenging problems such as slow kinetics, low photoefficiency and unpredictable mechanisms need to be solved. It is clear that naked TiO_2 needs extra help to undertake practical applications and this may cause it to lose some of the charm of its mild operation. Therefore, there is a need to find new catalysts able to work with band gaps which better overlap the solar spectrum and no "cheap" solution to be used in wastewater treatment has yet been developed.

Contaminant treatment, in its strictest meaning, is the complete mineralization of the contaminants, but, photocatalytic processes only make sense for hazardous non-biodegradable pollutants. When feasible, biological treatment is the cheapest treatment and also the most compatible with the environment. Therefore, biologically recalcitrant compounds could be treated with photocatalytic technologies until biodegradability is achieved, later transferring the water to a conventional biological plant. Such a combination reduces treatment time and optimizes the overall economics, since the solar detoxification system can be significantly smaller. Therefore, the use of AOPs as a pretreatment step can be justified if the intermediates resulting from the reaction are readily degraded by microorganisms. The feasibility of such a photocatalytic-biological process has been already demonstrated at large scale.

Toxicity testing of the photocatalytically treated wastewater is therefore necessary, particularly when incomplete degradation is planned. Recently, the use of acute toxicity bioassays has meant an important improvement in the evaluation of AOPs because of their reproducibility, adequate format for quick analysis, short analysis time, as well as well-defined analytical protocols. Numerous bioassay procedures are now available, however, if we consider that toxicity is a biological response, the values obtained by a single toxicity assay can be an insufficient measure of the adverse biological impact. Consequently, a battery of assays is recommended to be applied to assess toxicity adequately, and careful selection is essential. A great confidence in the detoxification assessment is achieved, when two or more different bioassays representatives of different taxonomic groups point in the same direction.

Photo-Fenton, either solar or lamp-driven, has the potential of becoming widely applied, especially for wastewaters with medium pollution concentrations (TOC from tens of milligrams per liter up to around one gram per liter). At higher contaminant concentrations the process itself is feasible but would not work in its optimal concentration range causing high oxidant reagent costs if high COD abatements are necessary. Several aspects, which in part are currently under development, may also greatly contribute to market introduction upon achieving maturity: (i) catalysts based on immobilized iron; (ii) additives which enhance the process performance, either regarding kinetics or pH operation range; (iii) optimization of photoreactors taking into account the processes specific requirements; (iv) ways to minimize hydrogen peroxide consumption, which is the main cost factor regarding consumables. Revolutionary advances may be the developments of: (i) new catalysts, which may enhance pH operation range, reduce reagent consumption, viable wavelength range, catalyst separation; (ii) new integrated processes, e.g., photo-Fenton process integrated with membrane distillation, sonication or hydraulic cavitation; (iii) new oxidants, i.e., the replacement of hydrogen peroxide as an added reagent (approaches may include the in situ generation of the oxidant or a real replacement by a different electron acceptor).

Little by little, TiO_2 disinfection research went from basic laboratory studies to the first trials with real disinfection applications. Microorganisms that are very resistant to UV-A irradiation have been successfully inactivated by TiO_2 photocatalysis and therefore recent TiO_2 disinfection research focuses more on disinfection applied to more resistant microorganisms. The irradiation way on the photo-reactor has a high influence on the disinfection behaviour. When light exposure is made continuously (without temporal interruptions) the disinfection effect of the process is more fast and efficient than when the light is applied intermittently. The minimum UV energy necessary to reach complete inactivation depends on the microorganism and the reactor configuration. Therefore, there are aspects that are essential to generate a technology as: (i) optimization of photoreactors taking into account the processes specific requirements; (ii) development of viable process schemes (batch, continuous, semi-continuous); (iii) development of process control strategies; (iv) the influence of process parameters; (v) assessment of the influence of the water chemical parameters, (vi) find out applications different to potable water disinfection (as a chemical-free system to control pathogens in agriculture).

The current lack of data for comparison of solar photocatalysis with other technologies definitely presents an obstacle towards an industrial application. One issue would be to give sound examples of techno-economic studies. Another aspect should be the assessment of the environmental impact in its broadest sense. One excellent tool is the application of technologies such as life cycle analysis. Several such studies were performed comparing different technologies [326–328]. These studies confirm that solar photocatalysis is a promising technology compared to other investigated technologies, showing the least impact in most of the investigated categories.

Finally, to lead to industry application it will be critical that the photocatalytic processes can be developed up to a stage, where the process:

- Is cost-efficient compared to other processes.
- Is sustainable.
- Is robust, i.e., small to moderate changes to the wastewater stream do not affect the plant's efficiency and operability strongly.
- Is predictable, i.e., process design and up-scaling can be done reliably.
- Is easy to implement, i.e., suppliers and engineering companies can start marketing the process without huge initial investment costs, which could only be recovered by high turnovers.
- Is easy to operate and maintain, operation error must not lead to "catastrophic events".
- Poses low risk for staff (occupational health and safety).
- Is safe regarding the environment (minimize risks of leakage, discharge of not sufficiently treated effluent).
- Gives additional benefit to the industry applying the process (e.g., giving the company the image of being "green").

Acknowledgements

The authors wish to thank the European Commission for financial support for the INNOWATECH project under the Sixth Framework Programme, under the "Global Change and Ecosystems Programme" (Contract No. 036882) and SODISWATER project, under the "Confirming the International Role of Community Research for Development Programme" (Contract No. 031650). The authors also wish to thank the Spanish Ministry of Science and Innovation under the Consolider-Ingenio 2010 programme (Project CSD2006-00044 TRAGUA; http://www.consolider-tragua.com)

References

[1] S. Suárez, M. Carballa, F. Omil, J.M. Lema, Rev. Environ. Sci. Biotechnol. 7 (2008) 125.
[2] S.D. Richardson, Anal. Chem. 80 (2008) 4373.
[3] T. Wintgens, F. Salehi, R. Hochstrat, T. Melin, Water Sci. Technol. 57 (2008) 99.
[4] P.R. Gogate, A.B. Pandit, Adv. Environ. Res. 8 (2004) 501.
[5] M. Pera-Titus, V. García-Molina, M.A. Baños, J. Giménez, S. Esplugas, Appl. Catal. B: Environ. 47 (2004) 219.
[6] M.A. Shannon, P.W. Bohn, M. Elimelech, J.G. Georgiadis, B.J. Mariñas, A.M. Mayes, Nature 452 (2008) 301.
[7] C. Comninellis, A. Kapalka, S. Malato, S.A. Parsons, I. Poulios, D. Mantzavinos, J. Chem. Technol. Biotechnol. 83 (2008) 769.
[8] A. Fujishima, T.N. Rao, D.A. Tryk, J. Photochem. Photobiol. C: Photochem. Rev. 1 (2000) 1.
[9] H. Gerischer, Electrochim. Acta 35 (1990) 1677.
[10] J.A. Byrne, B.R. Eggins, J. Electroanal. Chem. 457 (1998) 61.
[11] N. Serpone, G. Sauvé, R. Koch, H. Tahiri, P. Pichat, P. Piccini, E. Pelizzetti, H. Hidaka, J. Photochem. Photobiol. A: Chem. 94 (1996) 191.
[12] J. Cunningham, J. Sedlak, Catal. Today 29 (1996) 309.
[13] D. Monllor-Satoca, R. Gómez, M. González-Hidalgo, P. Salvador, Catal. Today 129 (2007) 247.
[14] C. Minero, Catal. Today 54 (1999) 205.
[15] C. Minero, E. Pelizzetti, S. Malato, J. Blanco, Sol. Energy 56 (1996) 421.
[16] A.E. Cassano, O.E. Alfano, Catal. Today 58 (2000) 167.
[17] M.L. Satuf, R.J. Brandi, A.E. Cassano, O.M. Alfano, Catal. Today 129 (2007) 110.
[18] J. Blanco, S. Malato, Solar Detoxification, UNESCO Publishing, France, 2003.
[19] J.R. Bolton, K.G. Bircher, W. Tumas, C.A. Tolman, Pure Appl. Chem. 73 (2001) 627.
[20] J.M. Herrmann, Top. Catal. 14 (2005) 48.
[21] S. Malato, J. Blanco, A. Campos, J. Cáceres, C. Guillard, J.M. Herrmann, A.R. Fernández-Alba, Appl. Catal. B: Environ. 42 (2003) 349.
[22] C. Kormann, D.W. Bahnemann, M.R. Hoffmann, Environ. Sci. Technol. 25 (1991) 494.
[23] J. Blanco, S. Malato, J. de las Nieves, P. Fernández, Method of sedimentation of colloidal semiconductor particles, European patent application EP-1-101-737-A1, European Patent Office bulletin 21 (2001).
[24] S. Malato, J. Gimenez, C. Richter, D. Curco, J. Blanco, Water Sci. Technol. 35 (1997) 157.
[25] C.S. Turchi, D.F. Ollis, J. Catal. 122 (1990) 178.
[26] H. Gerischer, Electrochim. Acta 40 (1995) 1277.
[27] S.T. Martin, A.T. Lee, M.R. Hoffmann, Environ. Sci. Technol. 29 (1995) 2567.
[28] J.M. Herrmann, Catal. Today 53 (1999) 115.
[29] J. Blanco, S. Malato, P. Fernández, A. Vidal, A. Morales, P. Trincado, J.C. de Oliveira, C. Minero, M. Musci, C. Casalle, M. Brunotte, S. Tratzky, N. Dischinger, K.H. Funken, C. Sattler, M. Vincent, M. Collares-Pereira, J.F. Mendes, C.M. Rangel, Sol. Energy 67 (2000) 317.
[30] J. Blanco-Galvez, P. Fernández-Ibáñez, S. Malato-Rodríguez, Sol. Energy Eng. 129 (2007) 4.
[31] R.E. Bird, R.L. Hulstrom, L.J. Lewis, Sol. Energy 30 (1983) 563.
[32] D.Y. Goswami, K.W. Böer, Adv. Sol. Energy Am. Sol. Energy Soc. (1995) 165.
[33] D. Bahnemann, Sol. Energy 77 (2004) 445.
[34] J.A. Ajona, A. Vidal, Sol. Energy 68 (2000) 109.
[35] W.T. Welford, R. Winston, The Optics of Non-imaging Concentrators Light and Solar Energy, Academic Press Inc., New York, 1978.
[36] R.L. Pozzo, M.A. Baltanás, A.E. Cassano, Catal. Today 39 (1997) 219.
[37] S. Anandan, M. Yoon, J. Photochem. Photobiol. C: Photochem. Rev. 4 (2003) 5.
[38] Y. Chen, D.D. Dionysiou, Appl. Catal. B: Environ. 69 (2006) 24.
[39] C.M. Sayes, R. Wahi, P.A. Kurian, Y. Liu, J.L. West, K.D. Ausman, D.B. Warheit, V.L. Colvin, Toxicol. Sci. 92 (2006) 174.
[40] G. Oberdörster, V. Stone, K. Donaldson, Nanotoxicology 1 (2007) 2.
[41] V. Augugliano, M. Litter, L. Palmisano, J. Soria, J. Photochem. Photobiol. C: Photochem. Rev. 7 (2007) 123.
[42] D.F. Ollis, Ann. N.Y. Acad. Sci. 984 (2003) 65.
[43] S. Mozia, M. Tomaszewska, A.W. Morawski, Catal. Today 129 (2007) 3.
[44] M. Petrović, S. Gonzalez, D. Barceló, Trends Anal. Chem. 22 (2003) 685.
[45] M. Klavarioti, D. Mantzavinos, D. Kassinos, Environ. Int. 35 (2009) 402.
[46] P. Calza, E. Pelizzetti, C. Minero, J. Appl. Electrochem. 35 (2005) 665.
[47] I.K. Konstantinou, T.A. Albanis, Appl. Catal. B: Environ. 49 (2004) 1.
[48] S. Malato, J. Blanco, D.C. Alarcón, M.I. Maldonado, P. Fernández, W. Gernjak, Catal. Today 122 (2007) 137.
[49] I.K. Konstantinou, T.A. Albanis, Appl. Catal. B: Environ. 42 (2003) 319.
[50] H.D. Burrows, L. Canle, M. Santaballa, J.A. Steenken, J. Photochem. Photobiol. B: Biol. 67 (2002) 71.
[51] J.M. Herrmann, Ch. Guillard, M. Arguello, A. Agüera, A. Tejedor, L. Piedra, A. Fernández-Alba, Catal. Today 54 (1999) 353.
[52] I.K. Konstantinou, V.A. Sakkas, T.A. Albanis, Appl. Catal. B: Environ. 34 (2001) 227.
[53] A. Agüera, M. Mezcua, D. Hernando, S. Malato, J. Cáceres, A. Fernández-Alba, Int. J. Environ. Anal. Chem. 84 (2004) 149.
[54] T.E. Doll, H. Frimmel, Water Res. 38 (2004) 955.
[55] L.A. Pérez-Estrada, S. Malato, W. Gernjak, A. Agüera, E.M. Thurman, I. Ferrer, A.R. Fernández-Alba, Environ. Sci. Technol. 39 (2005) 8300.
[56] L.A. Pérez-Estrada, S. Malato, A. Agüera, A.R. Fernández-Alba, Catal. Today 129 (2007) 207.
[57] D.A. Lambropoulou, M.D. Hernando, I.K. Konstantinou, E.M. Thurman, I. Ferrer, T.A. Albanis, A.R. Fernández-Alba, J. Chromatogr. A 1183 (2008) 38.

[58] C. Medana, P. Calza, F. Carbone, E. Pelizzetti, H. Hidaka, C. Baiocchi, Rapid Commun. Mass Spectrom. 22 (2008) 301.
[59] J. Radjenovic, C. Sirtori, M. Petrovic, D. Barcelo, S. Malato, Appl. Catal. B: Environ. 89 (2009) 265.
[60] C. Sirtori, A. Zapata, S. Malato, W. Gernjak, A.R. Fernández-Alba, A. Agüera, Photochem. Photobiol. Sci. 8 (2009) 644.
[61] M. Petrovic, D. Barceló, Trends Anal. Chem. 26 (2007) 486.
[62] M.C. Hennion, J. Chromatogr. A 856 (1999) 3.
[63] N. Fontanals, R.M. Marcé, F. Borrull, J. Chromatogr. A 1152 (2007) 14.
[64] M. Davoren, A.M. Fogarty, Environ. Ecotoxicol. Environ. Safety 59 (2004) 116.
[65] M. Lapertot, S. Ebrahimi, I. Oller, M.I. Maldonado, W. Gernjak, S. Malato, C. Pulgarín, Ecotoxicol. Environ. Safety 69 (2008) 546.
[66] D.Y. Goswami, J. Sol. Energy: Trans. ASME 119 (1997) 101.
[67] S. Malato, J. Blanco, A. Vidal, C. Richter, Appl. Catal. B: Environ. 37 (2002) 1.
[68] L. Bousselmi, S.U. Geissen, H. Schroeder, Water Sci. Technol. 49 (2004) 331.
[69] I. Oller, S. Malato, J.A. Sánchez-Pérez, M.I. Maldonado, W. Gernjak, L. Pérez-Estrada, J.A. Muñoz, C. Ramos, C. Pulgarín, Ind. Eng. Chem. Res. 46 (2007) 7467.
[70] S. Malato, J. Blanco, M.I. Maldonado, P. Fernández-Ibáñez, A. Campos, Appl. Catal. B: Environ. 28 (2000) 163.
[71] K. Harada, T. Hisanaga, K. Tanaka, Water Res. 24 (1990) 1415.
[72] M. Poulios, A. Kositzi, Kouras, J. Photochem. Photobiol. A: Chem. 115 (1998) 175.
[73] I.R. Bellobono, A. Carrara, B. Barni, A. Gazzotti, J. Photochem. Photobiol. A: Chem. 84 (1994) 83.
[74] K. Hofstadler, R. Bauer, S. Novalic, G. Heisler, Environ. Sci. Technol. 28 (1994) 670.
[75] P. Neta, V. Madhavan, H. Zemel, R.W. Fessenden, J. Am. Chem. Soc. 99 (1977) 163.
[76] G.R. Peyton, Mar. Chem. 41 (1993) 91.
[77] G.P. Anipsitakis, D.D. Dionysiou, M.A. Gonzalez, Environ. Sci. Technol. 40 (2006) 1000.
[78] L. Venkatasubramanian, P. Dharmalingam, P. Maruthamuthu, Int. J. Chem. Kinet. 22 (1990) 69.
[79] J. Madhavan, B. Muthuraaman, S. Murugesan, S. Anandan, P. Maruthamuthu, Sol. Energy Mater. Sol. Cells 90 (2006) 1875.
[80] G.P. Anipsitakis, D.D. Dionysiou, Appl. Catal. B: Environ. 54 (2000) 155.
[81] G.P. Anipsitakis, T.P. Tufano, D.D. Dionysiou, Water Res. 42 (2008) 2899.
[82] S. Malato, J. Blanco, C. Richter, B. Braun, M.I. Maldonado, Appl. Catal. B: Environ. 17 (1998) 347.
[83] M. Ni, M.K.H. Leung, D.Y.C. Leung, K. Sumathy, Renew. Sust. Energy Rev. 11 (2007) 401.
[84] M.I. Litter, Appl. Catal. B: Environ. 23 (1999) 89.
[85] A. Fujishima, X. Zhang, D.A. Tryk, Surf. Sci. Reports 63 (2008) 515.
[86] P. Cheng, M. Gu, Y. Jin, Prog. Chem. 17 (2005) 8.
[87] D. Chatterjee, S. Dasgupta, J. Photochem. Photobiol. C: Photochem. Rev. 6 (2005) 186.
[88] A. Zaleska, Recent Patents on Engineering 2 (2008) 157.
[89] R. Asahi, T. Morikawa, T. Ohwaki, K. Aoki, Y. Taga, Science 293 (2001) 269.
[90] H. Irie, Y. Watanabe, K. Hashimoto, J. Phys. Chem. B 5 (2003) 483.
[91] T. Ihara, M. Miyoshi, Y. Triyama, O. Marsumato, S. Sugihara, Appl. Catal. B 42 (2003) 403.
[92] Z. Zhao, Q. Liu, J. Phys. D: Appl. Phys. 41 (2008) 1.
[93] J.A. Rengifo-Herrera, E. Mielczarski, J. Mielczarski, N.C. Castillo, J. Kiwi, C. Pulgarin, Appl. Catal. B: Environ. 84 (2008) 448.
[94] Z. Wang, W. Cai, X. Hong, X. Zhao, F. Xu, C. Cai, Appl. Catal. B: Environ. 57 (2005) 223.
[95] R.A. Doong, C.H. Chen, R.A. Maithreepala, S.M. Chang, Water Res. 35 (2001) 2873.
[96] V. Keller, F. Garin, Catal. Commun. 4 (2003) 377.
[97] M. Anpo, M. Takeuchi, J. Catal. 216 (2003) 505.
[98] H. Yamashita, M. Harada, J. Misaka, M. Takeuchi, B. Neppolian, M. Anpo, Catal. Today 84 (2003) 191.
[99] H. Yamashita, M. Harada, J. Misaka, M. Takeuchi, K. Ikeue, M. Anpo, J. Photochem. Photobiol. A: Chem. 148 (2002) 257.
[100] M. Kitano, M. Matsuoka, M. Ueshima, M. Anpo, Appl. Catal. A: Gen. 325 (2007) 1.
[101] M. Takeuchi, H. Yamashita, M. Matsuoka, M. Anpo, T. Hirao, N. Itoh, Catal. Lett. 67 (2000) 135.
[102] M. Anpo, Pure Appl. Chem. 72 (2000) 1787.
[103] R. Argazzi, N.Y.M. Iha, H. Zabri, F. Odobel, C.A. Bignozzi, Coord. Chem. Rev. 248 (2004) 1299.
[104] A.S. Polo, M.K. Itokazu, N.Y.M. Iha, Coord. Chem. Rev. 248 (2004) 1343.
[105] L. Guangming, Z. Jincai, New J. Chem. 24 (2000) 411.
[106] F. Zhang, J. Zhao, T. Shen, H. Hidaka, E. Pelizzetti, N. Serpone, Appl. Catal. B: Environ. 15 (1998) 147.
[107] F. Zhang, J. Zhao, L. Zang, T. Shen, H. Hidaka, E. Pelizzetti, N. Serpone, J. Mol. Catal. A: Chem. 120 (1997) 173.
[108] J. Zhao, T. Wu, K. Wu, K. Oikawa, H. Hidaka, N. Serpone, Environ. Sci. Technol. 32 (1998) 2394.
[109] I. Martini, J.H. Hodak, G.V. Hartland, J. Phys. Chem. B 102 (1998) 607.
[110] J.M. Rehm, G.L. Mclendon, Y. Nagasawa, K. Yoshihara, J. Moser, M. Gratzel, J. Phys. Chem. 100 (1996) 9577.
[111] A.K. Jana, J. Photochem. Photobiol. A: Chem. 132 (2000) 1.
[112] J.Y. Hu, S. Wang, W.J. Ng, S.L. Ong, Water Res. 33 (1999) 2587.
[113] L. Sanchez, J. Peral, X. Domenech, Appl. Catal. B: Environ. 19 (1998) 59.
[114] S. Wang, F. Shiraishi, K. Nakano, Chem. Eng. J. 87 (2002) 261.
[115] T.E. Agustina, H.M. Ang, V.K. Vareek, J. Photochem. Photobiol. C: Photochem. Rev. 6 (2005) 264.
[116] F.J. Beltrán, Ozone Reaction Kinetics for Water and Wastewater Systems, Lewis Publ CRC Press, Boca raton, FL, 2003.
[117] P. Kopf, E. Gilbert, S.H. Eberle, J. Photochem. Photobiol. A 136 (2000) 163.
[118] J. Weiss, Trans. Faraday Soc. 31 (1935) 668.
[119] M.J. Farré, M.I. Franch, S. Malato, J. Ayllon, J. Peral, X. Domenech, Chemosphere 58 (2005) 1127.
[120] M. Addamo, V. Augugliaro, E.G. Lopez, V. Loddo, G. Marci, L. Palmisano, Catal. Today 107/108 (2005) 612.
[121] F.J. Beltrán, F.J. Rivas, O. Gimeno, J. Chem. Technol. Biotechnol. 80 (2005) 973.
[122] I.A. Balcioglu, G. Nicola, B. Miray, J. Photochem. Photobiol. A 135 (2000) 229.
[123] C. Flox, J.A. Garrido, R.M. Rodríguez, P.L. Cabot, F. Centellas, C. Arias, E. Brillas, Catal. Today 129 (2007) 29.
[124] J.M. Peralta-Hernández, Y. Meas-Vong, F.J. Rodríguez, T.W. Chapman, M.I. Maldonado, L.A. Godínez, Water Res. 40 (2006) 1754.
[125] M.R. Hoffmann, I. Hua, R. Höchemer, Ultrason. Sonochem. 3 (1996) S163.
[126] C. Pétrier, D. Casadonte, in: T.J. Mason, A. Thiehm (Eds.), Advances in Sonochemistry: Ultrasound in Environmental Protection, vol. 6, JAI Press Inc., Stamford, 2001, p. 91.
[127] H. Okuno, B. Yim, Y. Mizukoshi, Y. Nagata, Y. Maeda, Ultrason. Sonochem. 7 (2000) 261.
[128] T.J. Mason, C. Pétrier, in: S. Parson (Ed.), Advanced Oxidation Process for Water and Wastewater Treatment, IWA Publishing, London, 2004, p. 185.
[129] J. Peller, O. Wiest, P.V. Kamat, J. Phys. Chem. A 105 (2001) 3176.
[130] P. Théron, P. Pichat, C. Guillard, C. Pétrier, T. Chopin, Phys. Chem. Chem. Phys. 1 (1999) 4663.
[131] C. Berberidou, I. Poulios, N.P. Xekoukoulotakis, D. Mantzavinos, Appl. Catal. B: Environ. 74 (2007) 63.
[132] N. Stock, J. Peller, K. Vinodgopal, P.V. Kamat, Environ. Sci. Technol. 34 (2000) 1747.
[133] R.A. Torres, J.I. Nieto, E. Combet, C. Pétrier, C. Pulgarin, Appl. Catal. B: Environ. 80 (2008) 168.
[134] O. Legrini, E. Oliveros, A.M. Braun, Chem. Rev. 93 (1993) 671.
[135] H. Suty, C. De Traversay, M. Cost, Water Sci. Technol. 49 (2004) 227.
[136] E. Neyens, J. Baeyens, J. Hazard. Mater. B98 (2003) 33.
[137] F. Haber, J. Weiss, Proc. Roy. Soc. A 134 (1934) 332.
[138] C. Walling, Chem. Res. 8 (1975) 125.
[139] S.H. Bossman, E. Oliveros, S. Göb, S. Siegwart, E.P. Dahlen, L. Payawan Jr., M. Straub, M. Worner, A.M. Braun, J. Phys. Chem. 102 (1998) 5542.
[140] J.J. Pignatello, D. Liu, P. Huston, Environ. Sci. Technol. 33 (1999) 1832.
[141] J.J. Pignatello, E. Oliveros, A. MacKay, Crit. Rev. Environ. Sci. Technol. 36 (2006) 1.
[142] R.G. Zepp, B.C. Faust, J. Hoigné, Environ. Sci. Technol. 26 (1992) 313.
[143] H. Fallmann, T. Krutzler, R. Bauer, S. Malato, J. Blanco, Catal. Today 54 (1999) 309.
[144] P.L. Huston, J.J. Pignatello, Water Res. 33 (1999) 1238.
[145] W. Gernjak, T. Krutzler, A. Glaser, S. Malato, J. Cáceres, R. Bauer, A.R. Fernández-Alba, Chemosphere 50 (2003) 71.
[146] F. Herrera, C. Pulgarin, V. Nadtochenko, J. Kiwi, Appl. Catal. B: Environ. 17 (1998) 141.
[147] I. Arslan-Alaton, F. Gurses, J. Photochem. Photobiol. A: Chem. 165 (2004) 165.
[148] A.G. Trovo, S.A. Santos Melo, R.F. Pupo Nogueira, J. Photochem. Photobiol. A: Chem. 198 (2008) 215.
[149] W. Gernjak, M.I. Maldonado, S. Malato, J. Cáceres, T. Krutzler, A. Glaser, R. Bauer, Sol. Energy 77 (2004) 567.
[150] W. Gernjak, T. Krutzler, R. Bauer, S. Malato, J. Sol. Energy: Trans. ASME 129 (2007) 53.
[151] M.E. Sigman, A.C. Buchanan, J. Adv. Oxid. Technol. 2 (1997) 415.
[152] J. De Laat, G. Le Truong, B. Legube, Chemosphere 55 (2004) 715.
[153] W. Feng, D. Nansheng, Chemosphere 41 (2000) 1137.
[154] A. Bozzi, T. Yuranova, P. Lais, J. Kiwi, Water Res. 39 (2005) 1441.
[155] F. Martínez, G. Calleja, J.A. Melero, R. Molina, Appl. Catal. B: Environ. 60 (2005) 185.
[156] L. Pérez-Estrada, M.I. Maldonado, W. Gernjak, A. Agüera, A.R. Fernández-Alba, M.M. Ballesteros, S. Malato, Catal. Today 101 (2005) 219.
[157] Y. Sun, J.J. Pignatello, J. Agric. Food Chem. 40 (1992) 322.
[158] R.F.P. Nogueira, M.R.A. Silva, A.G. Trovo, Sol. Energy 79 (2005) 384.
[159] S. Malato, J. Blanco, M.I. Maldonado, P. Fernández, D. Alarcon, M. Collares, J. Farinha, J. Correia, Sol. Energy 77 (2004) 513.
[160] G. Sagawe, A. Lehnard, M. Lubber, G. Rochendorf, D. Bahnemann, Helv. Chim. Acta 84 (2001) 3742.
[161] V. Sarria, S. Parra, N. Adler, P. Péringer, N. Benitez, C. Pulgarin, Catal. Today 76 (2002) 301.
[162] V. Sarria, M. Deront, P. Péringer, C. Pulgarín, Appl. Catal. B: Environ. 40 (2003) 231.
[163] D. Mantzavinos, E. Psillakis, J. Chem. Technol. Biotechnol. 79 (2004) 431.
[164] P.R. Gogate, A.B. Pandit, Adv. Environ. Res. 8 (2004) 553.
[165] P.N. Hawker, M.V. Twigg, in: P.B. King (Ed.), Encyclopedia of Inorganic Chemistry, Wiley, Chichester, 1994, p. 1698.
[166] C.M. Flynn Jr., Chem. Rev. 84 (1984) 31.
[167] H. Krýsová, J. Jirkovský, J. Krýsa, G. Mailhot, M. Bolte, Appl. Catal. B: Environ. 40 (2003) 1.
[168] P. Mazellier, B. Sulzberger, Environ. Sci. Technol. 35 (2001) 3314.
[169] B. Sulzberger, H. Laubscher, G. Karametaxas, in: G.R. Helz, R.G. Zepp, D.G. Crosby (Eds.), Aquatic and Surface Photochemistry, Lewis Publishers, Boca Raton, 1994, p. 53.
[170] H.J.H. Fenton, J. Chem. Soc. 65 (1894) 899.
[171] A.Y. Sychev, V.G. Isak, Chem. Rev. 64 (1995) 1105.
[172] H. Gallard, J. De Laat, B. Legube, Water Res. 33 (1999) 2929.
[173] C. von Sonntag, P. Dowideit, X. Fang, R. Mertens, X. Pan, M.N. Schuchmann, H.P. Schuchmann, Water Sci. Technol. 35 (1997) 9.
[174] R. Chen, J.J. Pignatello, Environ. Sci. Technol. 31 (1997) 2399.

[175] V. Kavitha, K. Palanivelu, Chemosphere 55 (2004) 1235.
[176] J. Kiwi, A. Lopez, V. Nadtochenko, Environ. Sci. Technol. 34 (2000) 2162.
[177] J.J. Pignatello, Environ. Sci. Technol. 26 (1992) 944.
[178] A. Safarzadeh-Amiri, J.R. Bolton, S.R. Carter, J. Adv. Oxid. Technol. 1 (1996) 18.
[179] Y. Sun, J.J. Pignatello, J. Agric. Food Chem. 41 (1993) 308.
[180] A.I. Ononye, A.R. McIntosh, J.R. Bolton, J. Phys. Chem. 90 (1986) 6266.
[181] B.C. Faust, J. Hoigne, Atmos. Environ. 24 (1990) 79.
[182] M.R.A. Silva, A.G. Trovó, R.F.P. Nogueira, J. Photochem. Photobiol. A: Chem. 191 (2007) 187.
[183] W. Gernjak, M. Fuerhacker, P. Fernández-Ibañez, J. Blanco, S. Malato, Appl. Catal. B: Environ. 64 (2006) 121.
[184] T. Krutzler, H. Fallmann, P. Maletzky, R. Bauer, S. Malato, J. Blanco, Catal. Today 54 (1999) 321.
[185] V. Sarria, S. Kenfack, O. Guillod, C. Pulgarin, J. Photochem. Photobiol. A: Chem. 159 (2003) 89.
[186] S. Göb, E. Oliveros, S.H. Bossmann, A.M. Braun, C.A.O. Nascimento, R. Guardani, Water Sci. Technol. 44 (2001) 339.
[187] E. Oliveros, O. Legrini, M. Hohl, T. Müller, A.M. Braun, Chem. Eng. Proc. 36 (1997) 397.
[188] F. Torrades, M. Pérez, H.D. Mansilla, J. Peral, Chemosphere 53 (2003) 1211.
[189] A. Safarzadeh-Amiri, J.R. Bolton, S.R. Carter, Sol. Energy 56 (1996) 439.
[190] D. Gumy, P. Fernández-Ibañez, S. Malato, C. Pulgarín, O. Enea, Kiwi, Catal. Today 101 (2005) 375.
[191] F.A. Al Momani, A.T. Shawaqfeh, M.S. Shawaqfeh, Sol. Energy 81 (2007) 1213.
[192] J.A. Herrera Melián, J.M. Doña Rodríguez, A. Vieira Suárez, E. Tello Rendón, C. Valdés do Campo, J. Arana, J. Pérez Peña, Chemosphere 41 (2000) 323.
[193] M. Hincapié, M.I. Maldonado, I. Oller, W. Gernjak, J.A. Sánchez-Pérez, M.M. Ballesteros, S. Malato, Catal. Today 101 (2005) 203.
[194] S. Malato, J. Blanco, M.I. Maldonado, P. Fernández, W. Gernjak, I. Oller, Chemosphere 58 (2005) 391.
[195] I. Oller, W. Gernjak, M.I. Maldonado, L.A. Pérez-Estrada, J.A. Sánchez-Pérez, S. Malato, J. Hazard. Mater. B 138 (2006) 507.
[196] J. Bacardit, J. Stötzner, E. Chamarro, S. Esplugas, Ind. Eng. Chem. Proc. 46 (2007) 7615.
[197] I. Oller, S. Malato, J.A. Sánchez-Pérez, M.I. Maldonado, W. Gernjak, L.A. Pérez-Estrada, Water Sci. Technol. 55 (2007) 230.
[198] A. Machulek Jr., J.E.F. Moráes, C. Vautier-Gongo, C.A. Silverio, L.C. Friedrich, C.A.O. Nascimiento, M. González, F.H. Quina, Environ. Sci. Technol. 41 (2007) 8459.
[199] J. Bacardit, I. Oller, M.I. Maldonado, E. Chamarro, S. Malato, S. Esplugas, J. Adv. Oxid. Technol. 10 (2007) 219.
[200] B. Utset, J. Garcia, J. Casado, X. Domenech, Chemosphere 41 (2000) 1187.
[201] P. Wyness, J.F. Klausner, D.Y. Goswami, J. Sol. Energy: Trans. ASME 116 (1994) 2.
[202] M. Well, R.H.G. Dillert, D.W. Bahnemann, V.W. Benz, M.A. Mueller, J. Sol. Energy: Trans. ASME 119 (1997) 114.
[203] P. Wyness, J.F. Klausner, D.Y. Goswami, J. Sol. Energy: Trans. ASME 116 (1994) 8.
[204] G.H. Rossetti, E.D. Albizzati, O.M. Alfano, Sol. Energy 77 (2004) 461.
[205] Standard tables for terrestrial solar spectral irradiance at air mass 1.5 for a 37 tilted surface, ASTM - American Society for Testing and Materials, 1987, E892-87.
[206] J.D. Álvarez, W. Gernjak, S. Malato, M. Berenguel, M. Fuerhacker, L.J. Yebra, J. Sol. Energy: Trans. ASME 129 (2007) 37.
[207] J. Beltrán-Heredia, J. Torregrosa, J.R. Dominguez, J.A. Peres, Chemosphere 42 (2001) 351.
[208] C. Domínguez, J. García, M.A. Pedraz, A. Torres, M.A. Galán, Catal. Today 40 (1998) 85.
[209] J. Marugán, M.J. Lopez-Muñoz, W. Gernjak, S. Malato, Ind. Eng. Chem. Res. 45 (2006) 8900.
[210] J. Marugán, J. Aguado, W. Gernjak, S. Malato, Catal. Today 129 (2007) 59.
[211] H. Měšťánková, G. Mailhot, J. Jirkovský, J. Krýsa, M. Bolte, Appl. Catal. B: Environ. 57 (2005) 257.
[212] E. Guinea, C. Arias, P.L. Cabot, J.A. Garrido, R.M. Rodríguez, F. Centellas, E. Brillas, Water Res. 42 (2008) 499.
[213] R. Molinari, P. Argurio, T. Poerio, F. Bonaddio, Sep. Sci. Technol. 42 (2007) 1597.
[214] G. Yardin, S. Chiron, Chemosphere 62 (2006) 1395.
[215] European Commission, Implementation of Council Directive 91/27/EEC of 21 May 1991 concerning urban waste water treatment, as amended by Commission Directive 98/15/EC of 27 February 1998, Commission of the European Communities, Brussels, 2004.
[216] A. Zapata, I. Oller, R. Gallay, C. Pulgarín, M.I. Maldonado, S. Malato, W. Gernjak, J. Adv. Oxid. Technol. 11 (2008) 261.
[217] U. Pagga, Chemosphere 35 (1997) 2953.
[218] P. Reuschenbach, U. Pagga, U. Strotmann, Water Res. 37 (2003) 1571.
[219] M.M. Ballesteros Martín, J.A. Sánchez Pérez, J.L. Casas López, I. Oller, S. Malato Rodríguez, Water Res. 43 (2009) 784.
[220] M. Farré, D. Barceló, Trends Anal. Chem. 22 (2003) 299.
[221] A.M. Amat, A. Arques, A. García-Ripoll, L. Santos-Juanes, R. Vicente, I. Oller, M.I. Maldonado, S. Malato, Water Res. 43 (2009) 784.
[222] J.P. Scott, D.F. Ollis, Environ. Prog. 14 (1995) 88.
[223] I. Oller, P. Fernández-Ibañez, M.I. Maldonado, L. Pérez-Estrada, W. Gernjak, C. Pulgarín, P. Passarinho, S. Malato, Res. Chem. Intermed. 33 (2007) 407.
[224] S. Malato, J. Blanco, M.I. Maldonado, I. Oller, W. Gernjak, L.A. Pérez-Estrada, J. Hazard. Mater. 146 (2007) 440.
[225] WHO, Economic and health effects of increasing coverage of low cost household drinking-water supply and sanitation interventions to countries off-track to meet MDG target 10, 2007.
[226] WHO, Guidelines for drinking-water quality first addendum to third edition 1 recommendations. WHO Library Cataloguing-in-Publication Data, 2006.
[227] FAO, AQUASTAT, FAO's Information System on Water and Agriculture, NRL 2008. (http://www.fao.org/nr/water/aquastat/main/index.stm).
[228] E.J. Anaissie, R.T. Kuchar, J.H. Rex, A. Francesconi, M. Kasai, F.C. Müller, M. Lozano-Chiu, R.C. Summerbell, M.C. Dignani, S.J. Chanock, T.J. Walsh, Clin. Infect. Dis. 33 (2001) 1871.
[229] W.T. Runia, S. Boonstra, Mededelingen 66 (2001) 73.
[230] J. Coosemans, Acta Hortic. 382 (1995) 263.
[231] C.M. Sharpless, M.A. Page, K.G. Linden, Water Res. 37 (2003) 4730.
[232] C.A. Lawrence, S.S. Block, Disinfection, Sterilization and Preservation, Lea and Febiger, Philadelphia, 1983.
[233] W.A. Rutala, D.J. Weber, Infect. Control Hosp. Epidemiol. 25 (2004) 333.
[234] WHO, International Programme on Chemical Safety (IPCS), Disinfectants and disinfectant by-products, International Program on Chemical Safety (Environmental Health Criteria 216), Geneva, 1999.
[235] W.J. Masschelin, in: R.G. Rice (Ed.), Ultraviolet Light in Water and Wastewater Sanitation, Lewis Publishers, 2002, p. 59.
[236] R. Sadler, A. Seawright, G. Shaw, N. Dennison, D. Connell, W. Barron, P. White, J. Toxicol. Environ. Chem. 87 (2005) 575.
[237] EPA, First Annual 1999 Accomplishments Report EPA's Agency-wide Multimedia Persistent, Bioaccumulative, and Toxic Pollutants Initiative accomplishments Report, EPA 742-R-00-003, 2000. (http://www.epa.gov/pbt).
[238] FRAG-UK, Fungicide resistance. Crown Copyright Central Science Laboratory, 2007. (http://frag.csl.gov.uk/frac_table3.cfm).
[239] EPA, Ozone Layer Depletion - Regulatory Programs. The Phaseout of Methyl Bromide, 2008. (http://www.epa.gov/Ozone/mbr/index.html).
[240] N.R. Ward, R.L. Wolfe, B.H. Olson, Appl. Environ. Microbiol. 48 (1984) 508.
[241] H. Chick, J. Hyg. 8 (1908) 92.
[242] M. Berney, H.U. Weilenmann, A. Simonetti, T. Egli, J. Appl. Microbiol. 101 (2006) 828.
[243] J.C. Hoff, E.W. Akin, Environ. Health Perspect. 69 (1986) 7.
[244] G. Bitton, Wastewater Microbiology, 3rd ed., John Wiley and Sons, New Jersey, 2005, p. 65043.
[245] R.M. Tyrrell, S.M. Keyse, J. Photochem. Photobiol. B: Biol. 4 (1990) 349.
[246] L.F. Caslake, D.J. Connolly, V. Menon, C.M. Duncanson, R. Rojas, A. Tavakoli, J. Appl. Environ. Microbiol. 70 (2004) 1145.
[247] A. Acra, Y. Karahagopian, Z. Raffoul, R. Dajani, The Lancet 2 (1980) 1257.
[248] E. Ubomba-Jaswa, C. Navntoft, M.I. Polo-López, P. Fernández-Ibáñez, K.G. McGuigan, Photochem. Photobiol. Sci 8 (5) (2009) 587.
[249] M. Wegelin, S. Canonica, K. Mechsner, T. Fleischmann, F. Pesaro, A. Metzler, J. Water SRT-Aqua 43 (1994) 154.
[250] T.M. Joyce, K.G. McGuigan, M. Elemore-Meegan, R.M. Conroy, Appl. Environ. Microbiol. 62 (1996) 399.
[251] L.W. Gill, O.A. McLoughlin, J. Sol. Energy Eng. 129 (2007) 111.
[252] S.C. Kehoe, M.R. Barer, L.O. Devlin, K.G. McGuigan, Lett. Appl. Microbiol. 38 (2004) 410.
[253] R.J. Smith, S.C. Kehoe, K.G. McGuigan, M.R. Barer, Lett. Appl. Microbiol. 31 (2000) 284.
[254] K.G. McGuigan, F. Méndez-Hermida, J.A. Castro-Hermida, E. Ares-Mazás, S.C. Kehoe, M. Boyle, C. Sichel, P. Fernández-Ibañez, B.P. Meyer, S. Ramalingham, E.A. Meyer, J. Appl. Microbiol. 101 (2006) 453.
[255] J. Lonnen, S. Kilvington, S.C. Kehoe, F. Al-Touati, K.G. McGuigan, Water Res. 39 (2005) 877.
[256] C. Sichel, M. de Cara, J. Tello, J. Blanco, P. Fernández-Ibáñez, Appl. Catal. B: Environ. 74 (2007) 152.
[257] W. Heaselgrave, N. Patel, S. Kilvington, S.C. Kehoe, K.G. McGuigan, Lett. Appl. Microbiol. 43 (2006) 125.
[258] R.M. Conroy, M. Elmore-Meegan, T. Joyce, K.G. Mcguigan, J. Barnes, Lancet 348 (1996) 1695.
[259] M. Boyle, C. Sichel, P. Fernández-Ibáñez, G.B. Arias-Quiroz, M. Iriarte-Puña, A. Mercado, E. Ubomba-Jaswa, K.G. McGuigan, Appl. Environ. Microbiol. 74 (2008) 2997.
[260] F. Méndez-Hermida, E. Ares-Mazás, K.G. McGuigan, M. Boyle, C. Sichel, P. Fernández-Ibáñez, J. Potochem. Photobiol. B: Biol. 88 (2007) 105.
[261] S.C. Kehoe, T.M. Joyce, P. Ibrahim, J.B. Gillespie, R.A. Shahar, K.G. McGuigan, Water Res. 35 (2001) 1061.
[262] C. Navntoft, E. Ubomba-Jaswa, K.G. McGuigan, P. Fernández-Ibáñez, J. Photochem. Photobiol. B: Biol. 93 (2008) 155.
[263] D.M. Blake, P.C. Maness, Z. Huang, E.J. Wolfrum, J. Huang, Sep. Purif. Methods 28 (1999) 1.
[264] T. Matsunaga, R. Tomoda, T. Nakajima, H. Wake, FEMS Microbiol. Lett. 29 (1985) 211.
[265] T. Matsunaga, R. Tomoda, T. Nakajima, N. Nakamura, T. Komine, Appl. Environ. Microbiol. 54 (1988) 1330.
[266] T. Saito, T. Iwase, J. Horie, T. Morioka, J. Photochem. Photobiol. B: Biol. 14 (1992) 369.
[267] P.C. Mannes, S. Smolinski, D.M. Blake, Z. Huang, E.J. Wolfrung, W.A. Jacoby, Appl. Environ. Microbiol. 65 (1999) 4094.
[268] J. Kiwi, V. Nadtochenco, J. Phys. Chem. B 108 (2004) 17675.
[269] J. Kiwi, V. Nadtochenco, Langmuir 21 (2005) 4631.
[270] G. Gogniat, M. Thyssen, M. Denis, C. Pulgarin, S. Dukan, FEMS Microbiol. Lett. 258 (2006) 18.
[271] J.C. Ireland, P. Klostermann, E.W. Rice, R.M. Clark, Appl. Environ. Microbiol. 59 (1993) 1668.
[272] P. Zhang, R.J. Scrudato, G. Germano, Chemosphere 28 (1994) 607.

[273] H.N. Pham, T. McDowell, E. Wilkins, J. Environ. Sci. Health A: Environ. Sci. Eng. 30 (1995) 627.
[274] S.S. Block, V.P. Seng, D.W. Goswami, J. Sol. Energy Eng. 119 (1997) 85.
[275] M. Bekbölet, Water Sci. Technol. 35 (1997) 95.
[276] A.G. Rincón, C. Pulgarin, Appl. Catal. B: Environ. 51 (2004) 283.
[277] J. Wist, J. Sanabria, C. Dierolf, W. Torres, C. Pulgarin, J. Photochem. Photobiol. A: Chem. 147 (2002) 241.
[278] A.G. Rincón, C. Pulgarin, Appl. Catal. B: Environ. 49 (2004) 99.
[279] J.A. Ibañez, M.I. Litter, R.A. Pizarro, J. Photochem. Photobiol. A: Chem. 157 (2003) 81.
[280] O. Seven, B. Dindar, S. Aydemir, D. Metin, M.A. Ozinel, S. Icli, J. Photochem. Photobiol. A: Chem. 165 (2004) 103.
[281] I. Paspaltsis, K. Kotta, R. Lagoudaki, N. Grigoriadis, I. Poulios, T. Sklaviadis, J. Gen. Virol. 87 (2006) 3125.
[282] I. Paspaltsis, C. Berberidou, I. Poulios, T. Sklaviadis, J. Hosp. Infect. 71 (2009) 149.
[283] D. Gumy, A.G. Rincón, R. Hajdu, C. Pulgarin, Sol. Energy 80 (2006) 1376.
[284] M. Cho, H. Chung, W. Choi, J. Yoon, Water Res. 38 (2004) 1069.
[285] P. Fernández, J. Blanco, C. Sichel, S. Malato, Catal. Today 101 (2005) 345.
[286] I.M. Butterfield, P.A. Christensen Curtis, T.P.J. Gunlazuardi, Water Res. 31 (1997) 675.
[287] T.P. Curtis, G.W. Alker, B.M. Dowling, P.A. Christensen, Water Res. 36 (2002) 2410.
[288] P.S.M. Dunlop, J.A. Byrne, N. Manga, B.R. Eggins, J. Photochem. Photobiol. A: Chem. 148 (2002) 355.
[289] P.A. Christensen, T.P. Curtis, T.A. Egerton, S.A.M. Kosa, J.R. Tinlin, Appl. Catal. B: Environ. 41 (2003) 371.
[290] L. Armelao, D. Barreca, G. Bottaro, A. Gasparotto, C. Maccato, C. Maragno, E. Tondello, U.L. Štangar, M. Bergant, D. Mahne, Nanotechnology 18 (2007) 5709.
[291] J.C. Yu, W. Ho, J. Lin, H. Yip, P.K. Wong, Environ. Sci. Technol. 37 (2003) 2296.
[292] J.C. Yu, W. Ho, J. Yu, H. Yip, K.W. Po, J. Zhao, Environ. Sci. Technol. 39 (2005) 1175.
[293] C. Sichel, J. Blanco, S. Malato, P. Fernández-Ibáñez, J. Photochem. Photobiol. A: Chem. 189 (2007) 239.
[294] M. Berney, H.U. Weilenmann, J. Ihssen, C. Bassin, T. Egli, J. Appl. Environ. Microbiol. 72 (2006) 2586.
[295] A.G. Rincón, C. Pulgarin, N. Adler, P. Peringer, J. Photochem. Photobiol. A: Chem. 139 (2001) 233.
[296] A.G. Rincón, C. Pulgarin, Appl. Catal. B: Environ. 44 (2003) 263.
[297] A.G. Rincón, C. Pulgarin, Sol. Energy 77 (2004) 635.
[298] A.G. Rincón, C. Pulgarin, Appl. Catal. B: Environ. 63 (2005) 222.
[299] A.G. Rincón, C. Pulgarin, Catal. Today 101 (2005) 331.
[300] D.M.A. Alrousan, P.S.M. Dunlop, T.A. McMurray, J.A. Byrne, Water Res. 43 (2009) 47.
[301] C. Sichel, J. Tello, M. de Cara, P. Fernández-Ibáñez, Catal. Today 129 (2007) 152.
[302] H.E. Watson, J. Hyg. 8 (1908) 536.
[303] J. Marugán, R. van Grieken, C. Cordo, C. Cruz, Appl. Catal. B: Environ. 82 (2008) 27.
[304] P. Fernández-Ibáñez, C. Sichel, M.I. Polo-López, M. de Cara-García, J.C. Tello, Catal. Today 144 (2009) 62.
[305] M. Cho, H. Chung, J. Yoon, Appl. Environ. Microbiol. 69 (2003) 2284.
[306] I. Fridovich, Arch. Biochem. Biophys. 247 (1986) 1.
[307] K. Keyer, J.A. Imlay, Biochemistry 93 (1996) 13635.
[308] G. Minotti, S.D. Aust, Chem. Phys. Lipids 44 (1987) 191.
[309] B. Andriopoulos, B. Hegedüsch, J. Mangin, H. Riedel, U. Hebling, J. Wang, K. Pantopoulos, S. Mueller, J. Biol. Chem. 282 (2007) 20301.
[310] O. Kakholon, Z. Cabantchik, Free Radic. Biol. Med. 3 (2002) 1037.
[311] C. Pourzand, R.D. Watkin, .E. Brown, R.M. Tyrrell, Cell Biol. 96 (1999) 6751.
[312] P.J. Kiley, H. Beinert, Curr. Opin. Microbiol. 6 (2003) 181.
[313] H.N. Anathaswamy, A. Eisenstark, J. Photochem. Photobiol. B: Biol. 24 (1977) 439.
[314] P.S. Hartman, A. Eisenstark, Mutat. Res. 72 (1980) 31.
[315] C. Sichel, P. Fernández-Ibáñez, M. de Cara, J. Tello, Water Res. 43 (2009) 1841.
[316] S. Varghese, A. Wu, S. Park, K.R.C. Imlay, J.A. Imlay, Mol. Microbiol. 64 (2007) 822.
[317] A. Vidal, A.I. Díaz, A. El Hraiki, M. Romero, I. Muguruza, F. Senhaji, J. González, Catal. Today 54 (1999) 183.
[318] O.A. McLoughlin, P. Fernández-Ibañez, W. Gernjak, S. Malato Rodríguez, L.W. Gill, Sol. Energy 77 (2004) 625.
[319] O.A. McLoughlin, S.C. Kehoe, K.G. McGuigan, E.F. Duffy, F. Al Touati, W. Gernjak, I. Oller Alberola, S. Malato, L.W. Gill, Sol. Energy 77 (2004) 657.
[320] C. Navntoft, P. Araujo, M.I. Litter, M.C. Apella, D. Fernández, M.E. Puchulu, V.H. Del Margarita, M.A. Blesa, J. Sol. Energy Eng.: Trans. ASME 129 (2007) 127.
[321] G.K. Rijal, R.S. Fujioka, Water Sci. Technol. 48 (2003) 481.
[322] A. Martín Domínguez, M.T. Alarcón Herrera, I.R. Martin Domínguez, A. Gonzalez-Herrera, Sol. Energy 78 (2005) 31.
[323] M. Raviv, Hortic. Technol. 15 (2005) 52.
[324] EPA, Ozone Layer Depletion - Regulatory Programs. 2008. (http://www.epa.gov/Ozone/mbr/casestudies/volume3/hydropn3.html).
[325] Beth Israel Deaconess Medical Center 2004. Biosafety Manual.
[326] I. Mũnoz, J. Peral, A.J. Ayllón, S. Malato, P. Passarinho, X. Doménech, Water Res. 40 (2006) 3533.
[327] I. Mũnoz, J. Peral, A.J. Ayllón, S. Malato, M.J. Martin, J.Y. Perrot, M. Vincent, X. Doménech, Environ. Eng. Sci. 24 (2007) 638.
[328] I. Muñoz, S. Malato, A. Rodríguez, X. Doménech, J. Adv. Oxid. Technol. 11 (2008) 270.